



The Detector Configuration of the ATLAS experiment for Run 3 of the LHC

Clément Camincher (University of Victoria (CA)), Paolo Iengo (INFN)



**University
of Victoria**



ATLAS detector

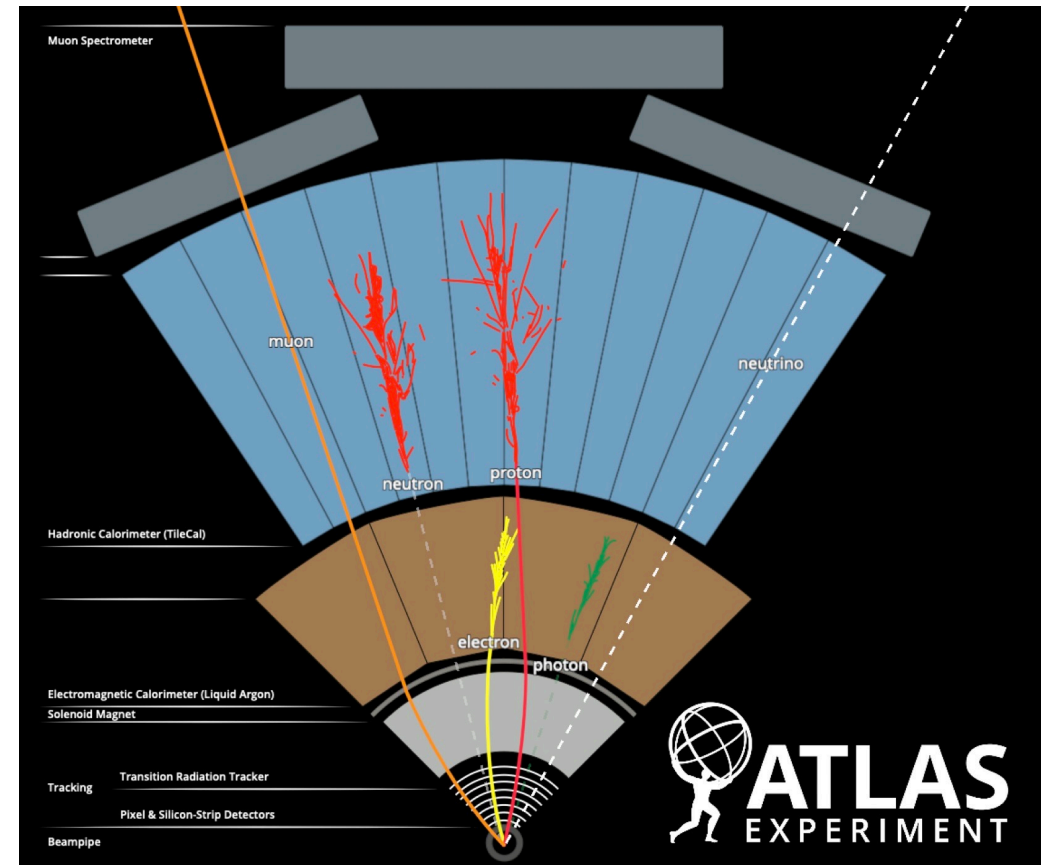
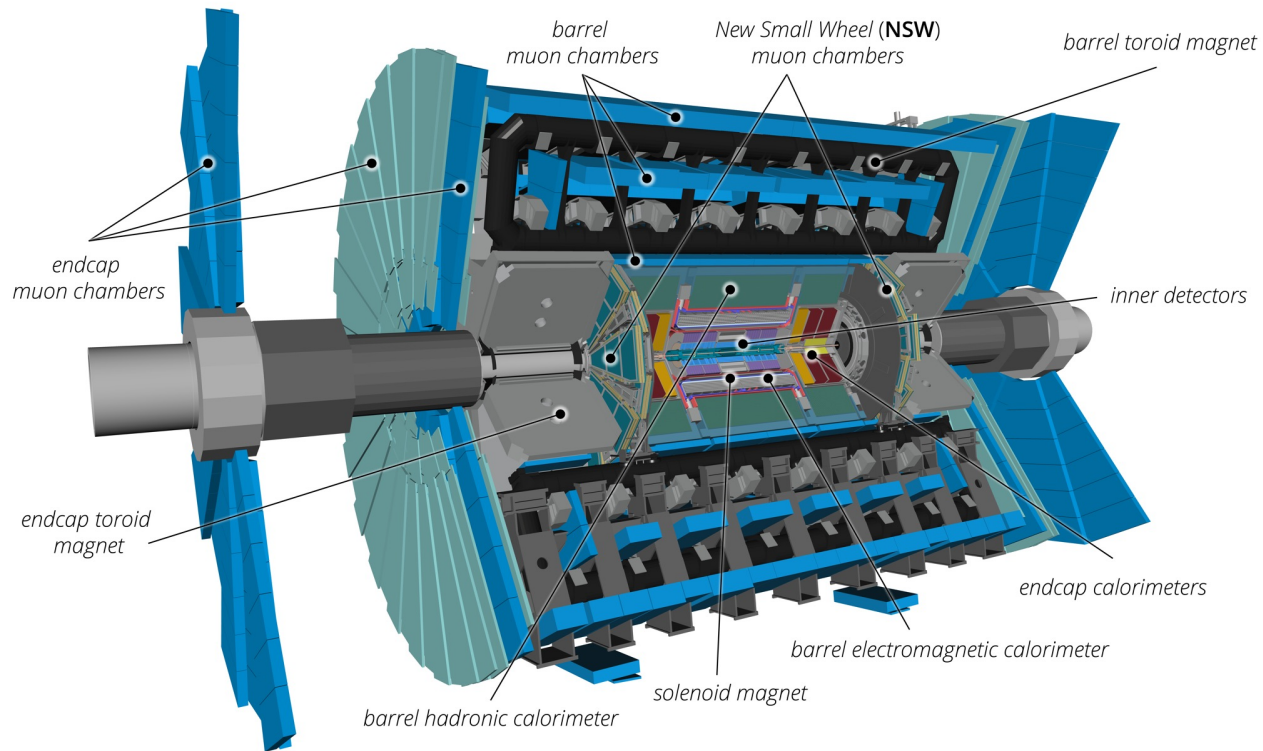
<https://arxiv.org/abs/2305.16623>

Multipurpose detector

Targeting Higgs and beyond standard model physics searches

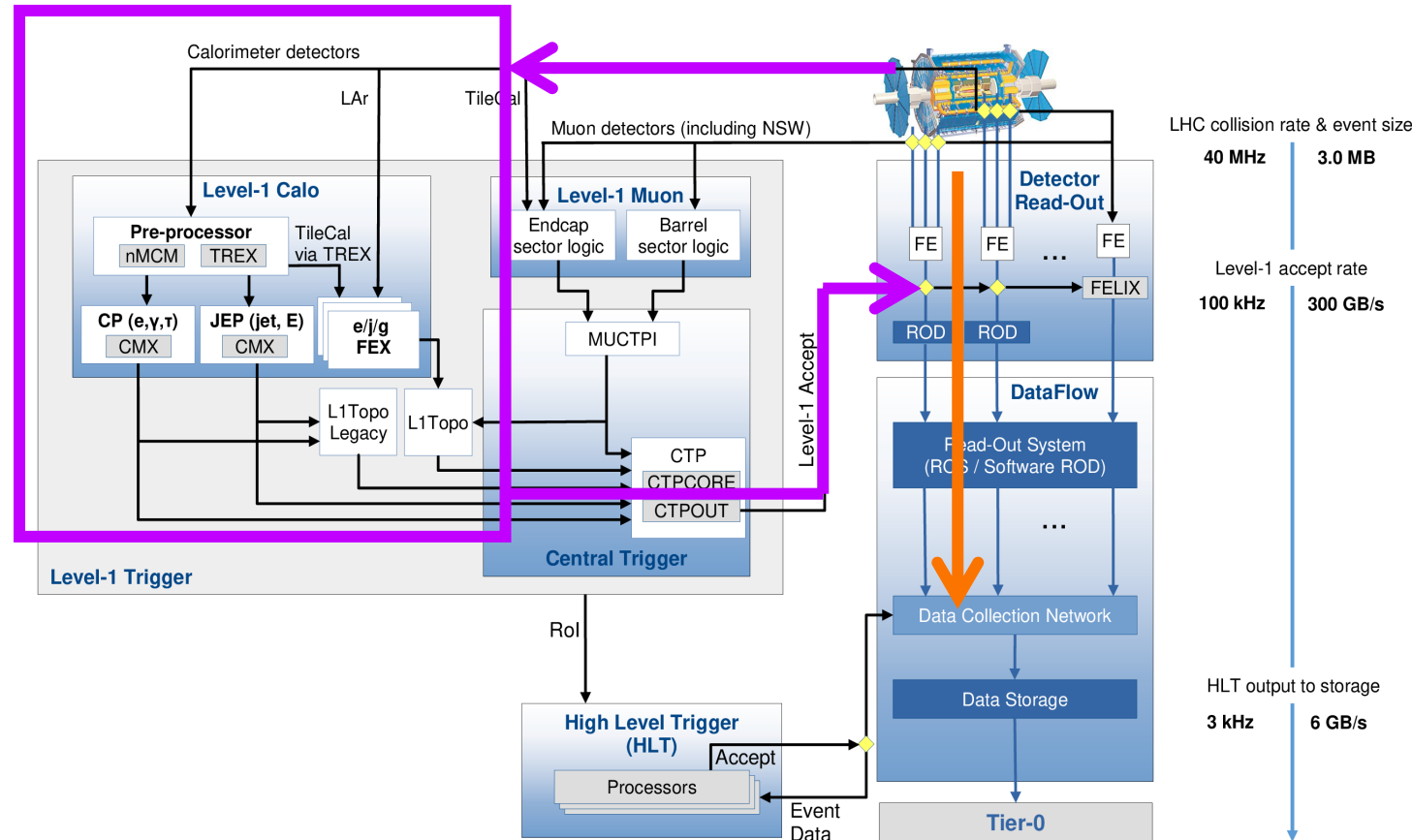
Onion layer detector structure

Inner detector -> Calorimeters -> Muon spectrometer



Trigger and readout architecture

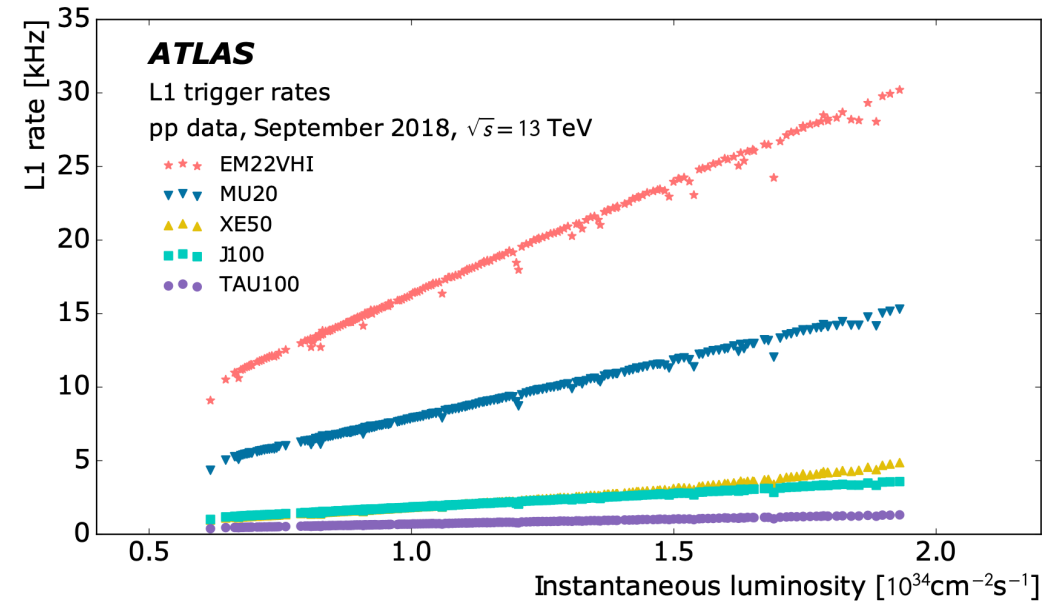
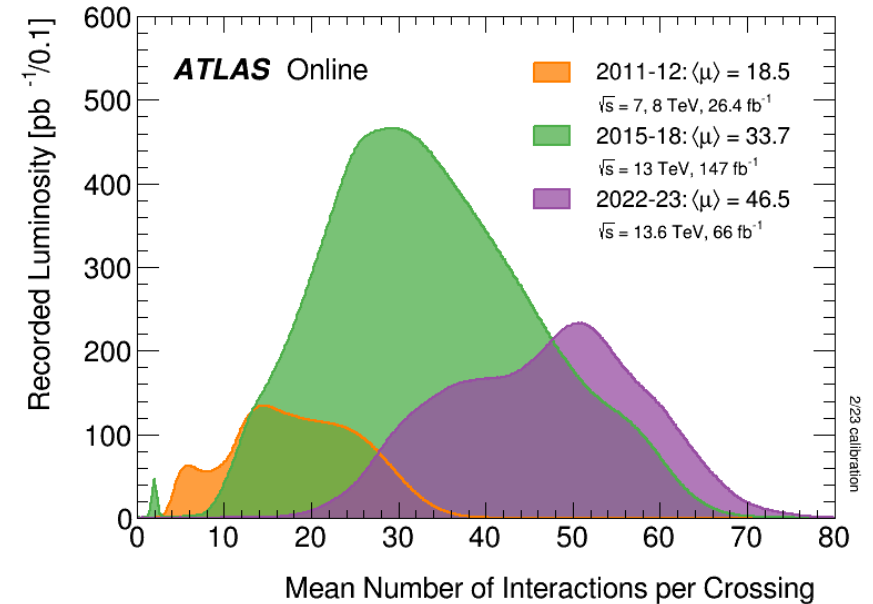
- All collisions events cannot be recorded @ 40 MHz
- ATLAS has 2 levels of trigger for online event selection
 - Level-1 (Hardware trigger)
 - Analyses events @ 40 MHz
 - Send L1 Accept signal @100kHz to readout detector with full precision
 - Made of custom electronics
 - Fixed latency
 - Max latency $2.5 \mu\text{s}$
 - HLT(Software trigger)
 - 100 kHz -> ~ 3 kHz of recorded data



This presentation will focus on the Calorimeter L1 trigger

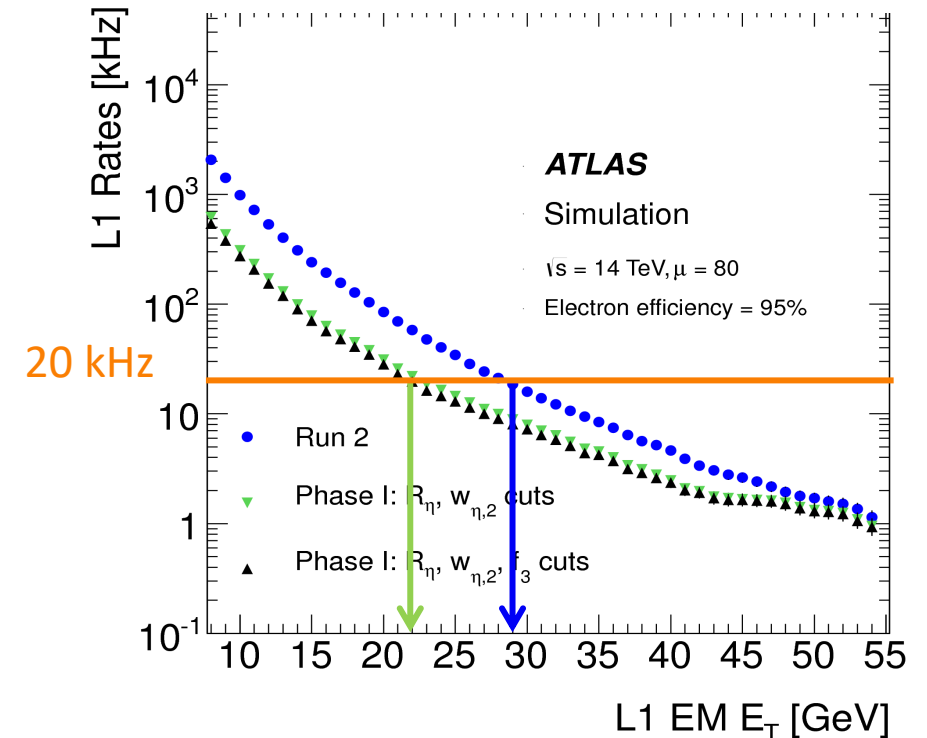
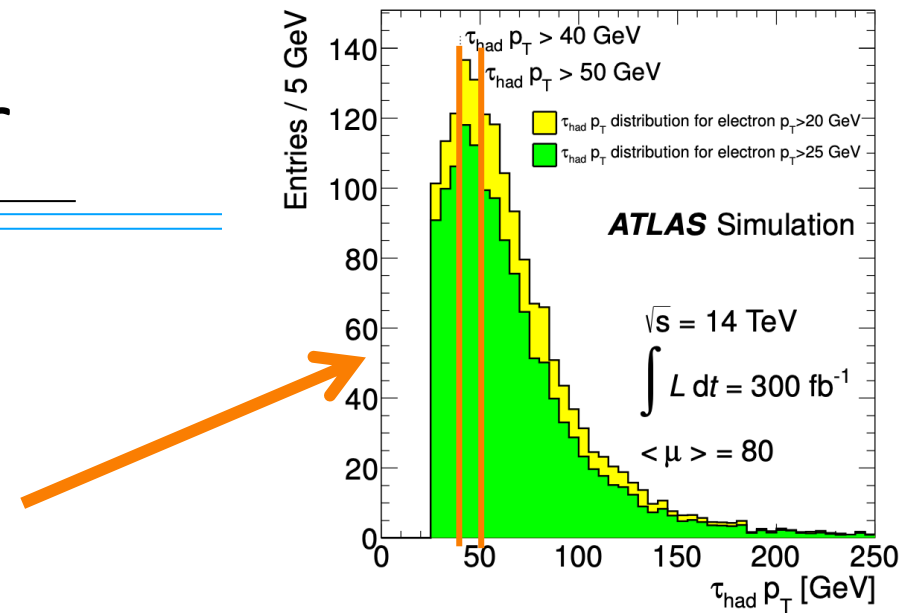
You said more Luminosity ?

- During Run 3 the LHC is expected to run at higher instantaneous luminosity
- Achieved by increasing the number of interactions per bunch crossing
- Higher rate of interesting events 😊
- Higher rate of background 😞
- In addition the increased pile-up makes it more challenging to identify signal events

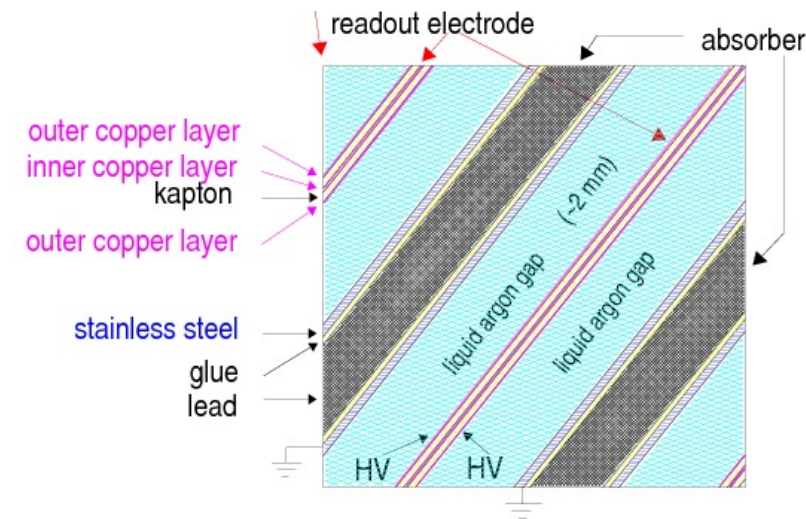
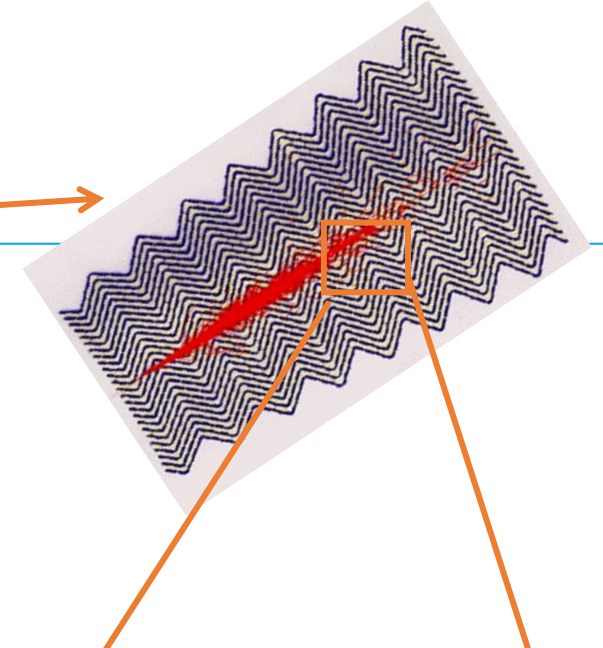
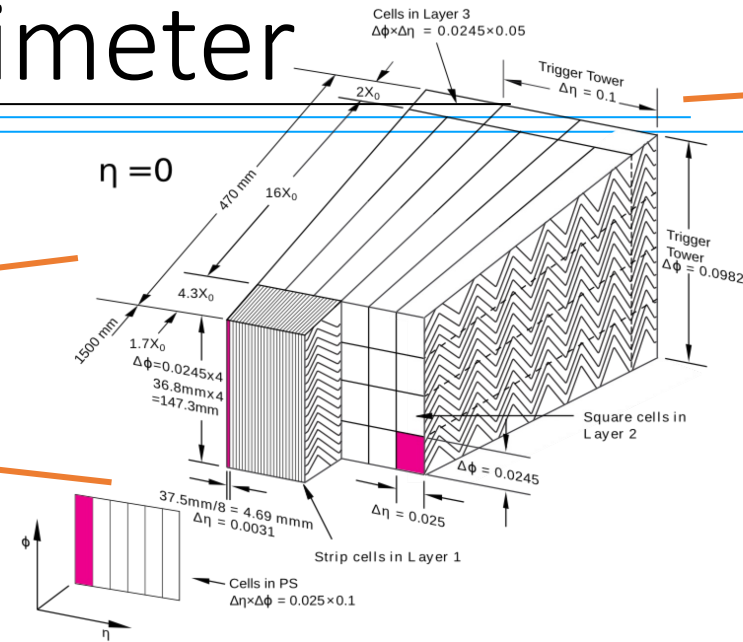
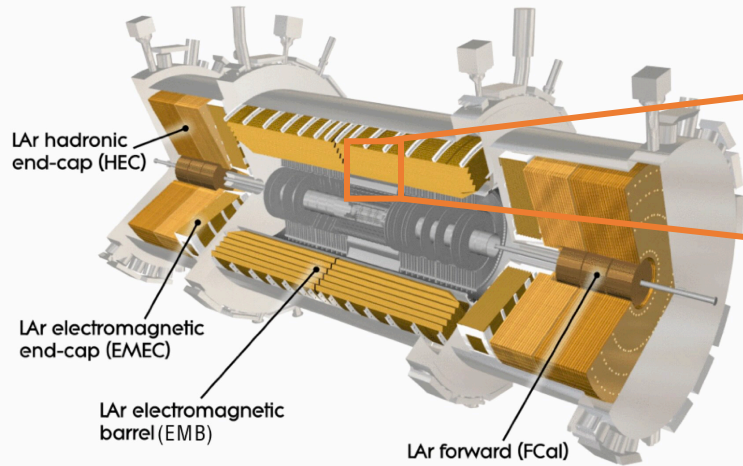


Motivation for a new trigger

- Possible Solutions to cope with increased rates :
 - **Record more** -> The current hardware cannot cope
 - **Tighten selection** -> Can reduce significantly search capabilities when soft leptons are involved
 For instance in $H \rightarrow \tau_{\text{had}} \tau_{\text{lep}}$ channel a change of cut
 - from 20 to 25 GeV on electron p_T
 - from 40 to 50 GeV on τ_{had} $\Rightarrow \sim 37\%$ of signal loss
 - **Do a better selection** -> Require a new trigger system
- In ATLAS Typically 20 kHz @ Level-1 are allocated to electromagnetic trigger
- Here of for $Z \rightarrow ee$ events in Run 3 conditions
 - Run 2 trigger conditions would impose E_T cut at ~ 30 GeV
 - With improved selection can expect to reduce E_T cut down to ~ 22 GeV



Liquid Argon Calorimeter

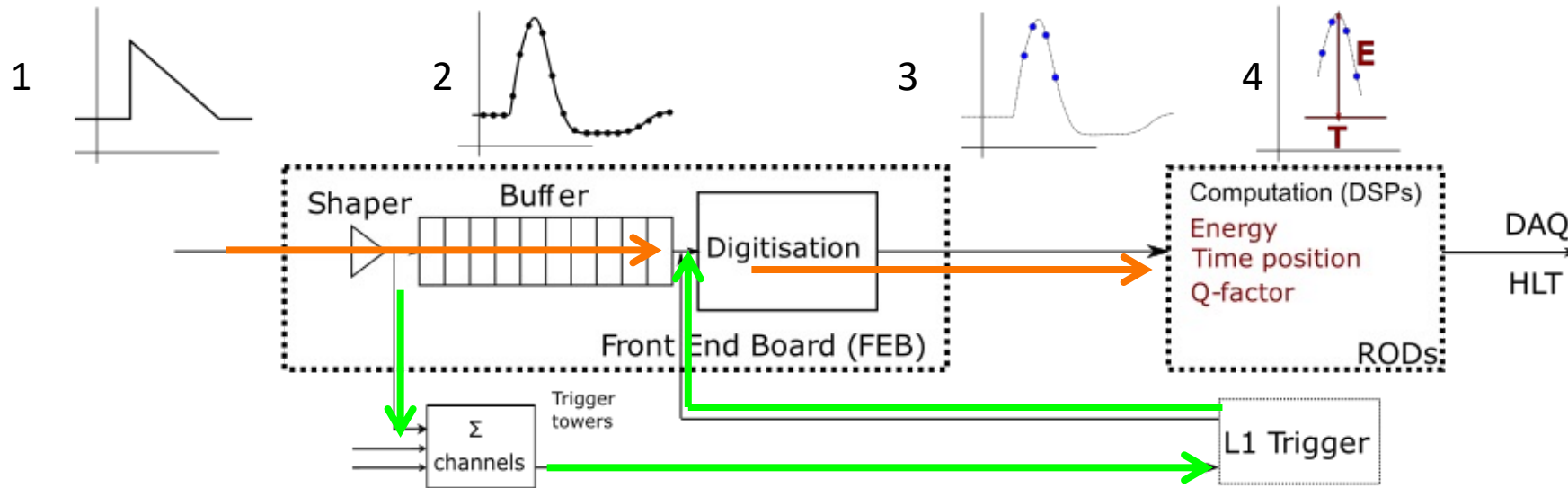


- Lead + liquid argon for electromagnetic calorimetry (Barrel + End-Cap)
- Copper or Tungsten + liquid argon for hadronic calorimetry in forward regions (End-Cap)
- Volume is divided in unit of readout called “cells” (smallest measurable volume)
- Calorimeter measure the deposited energy in each of the cell

- Particles interact with lead and produce electromagnetic shower.
 - Signal is collected via the electrodes within the liquid argon gap

Famous accordion shape for full azimuthal coverage

LAr readout before Phase-I

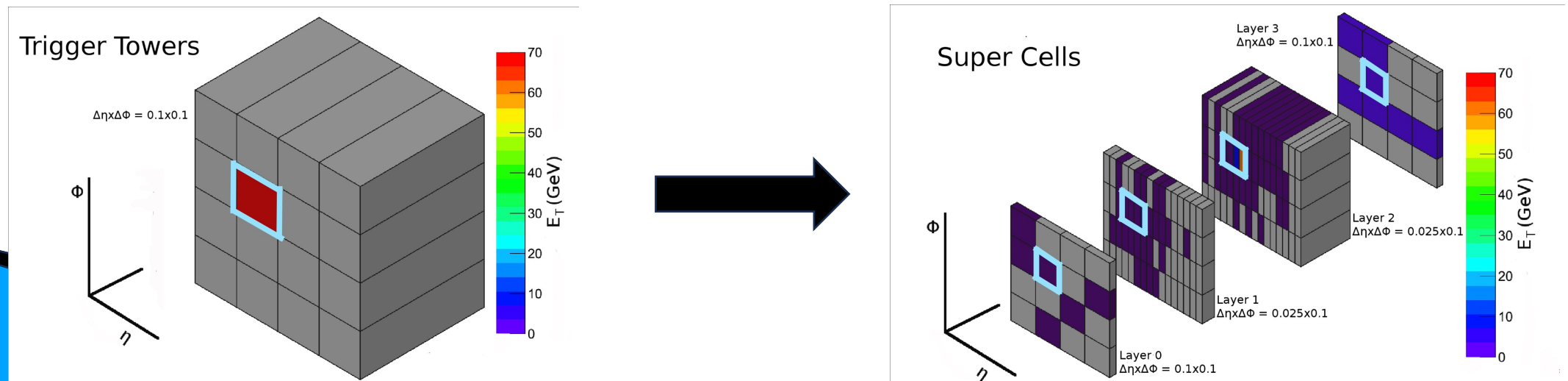


1. Signal is generated as a triangular pulse
2. Shaped to form a bipolar pulse and sampled @ 40 MHz buffered analogically on front-end board
3. Upon L1-Accept 4 samples are digitized and send off-detector
4. Pulse amplitude proportional to deposited energies computed out of the ADC samples using optimal filtering algorithms

- 2 Paths existed during Run 1 and Run 2
- **Precision readout**
 - Record only upon trigger accept
 - Readout of all 182k Cells
 - **Analog trigger path**
 - Sum channel analogically
 - Uses 6000 Trigger Towers

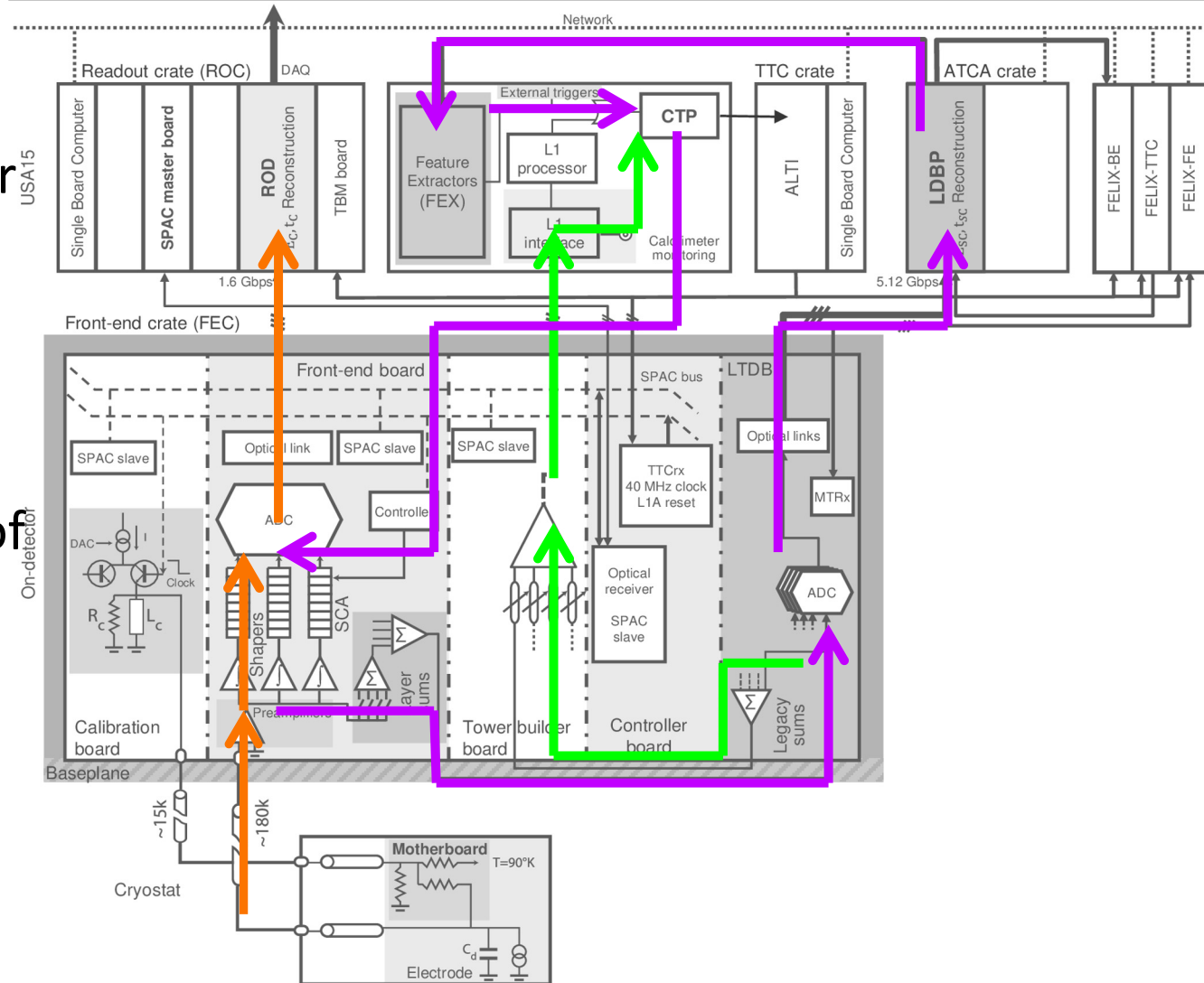
Principle of LAr Phase-I upgrade

- Run 1 and Run 2 trigger used 6k **Trigger Towers** ($\Delta\phi \times \Delta\eta = 0.1 \times 0.1$)
 - Built by analogically summing the signal of up to 64 Cells
- On Phase-I sums are modified to create 34k **Super Cells (SC)**
 - Increase up to 10 times the granularity on Barrel regions
 - Layer information is preserved => allowing for shower shape variable computation
 - Increase the energy measurement precision (from 10b ADCs to 12b ADCs)



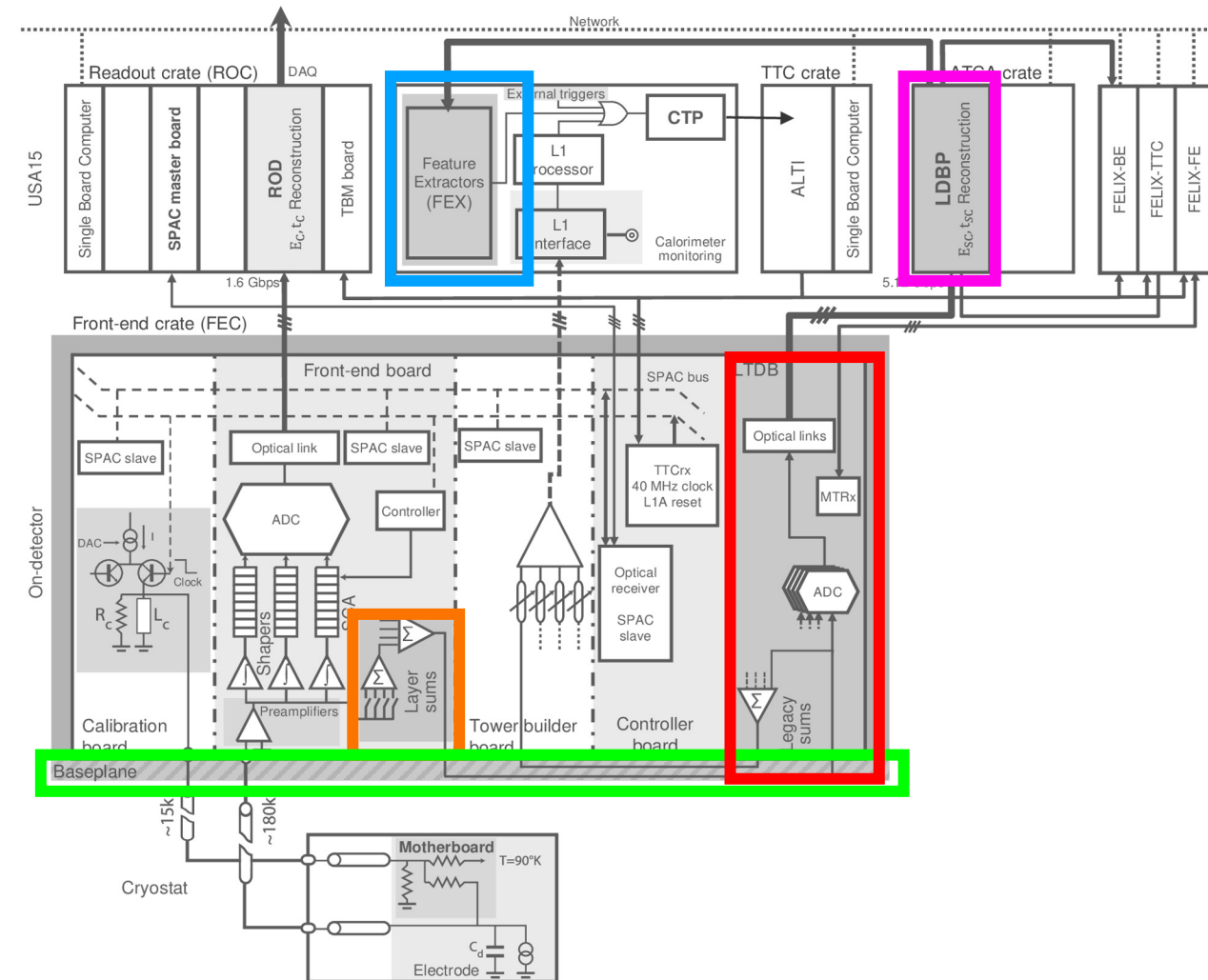
Adding a new readout path

- A new trigger readout path was created
 - From analogue signal to central trigger
 - Still had to comply with the $2.5 \mu\text{s}$ fixed latency of ATLAS
 - Used a new architecture with data digitized @ 40 MHz on detector and stream out to off-detector => Gain of experience in perspective of HL-LHC
- Legacy analogue trigger was preserved as backup



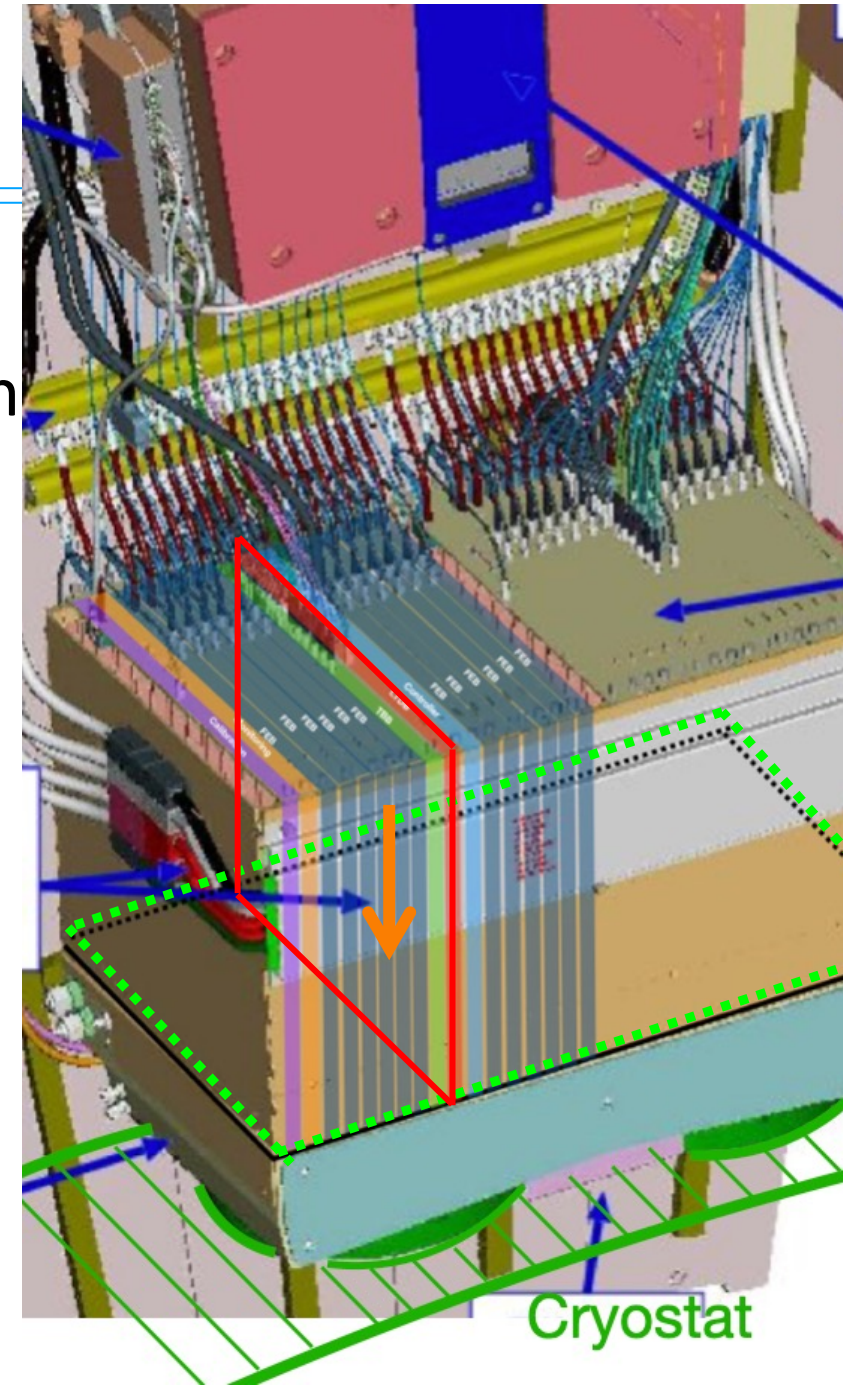
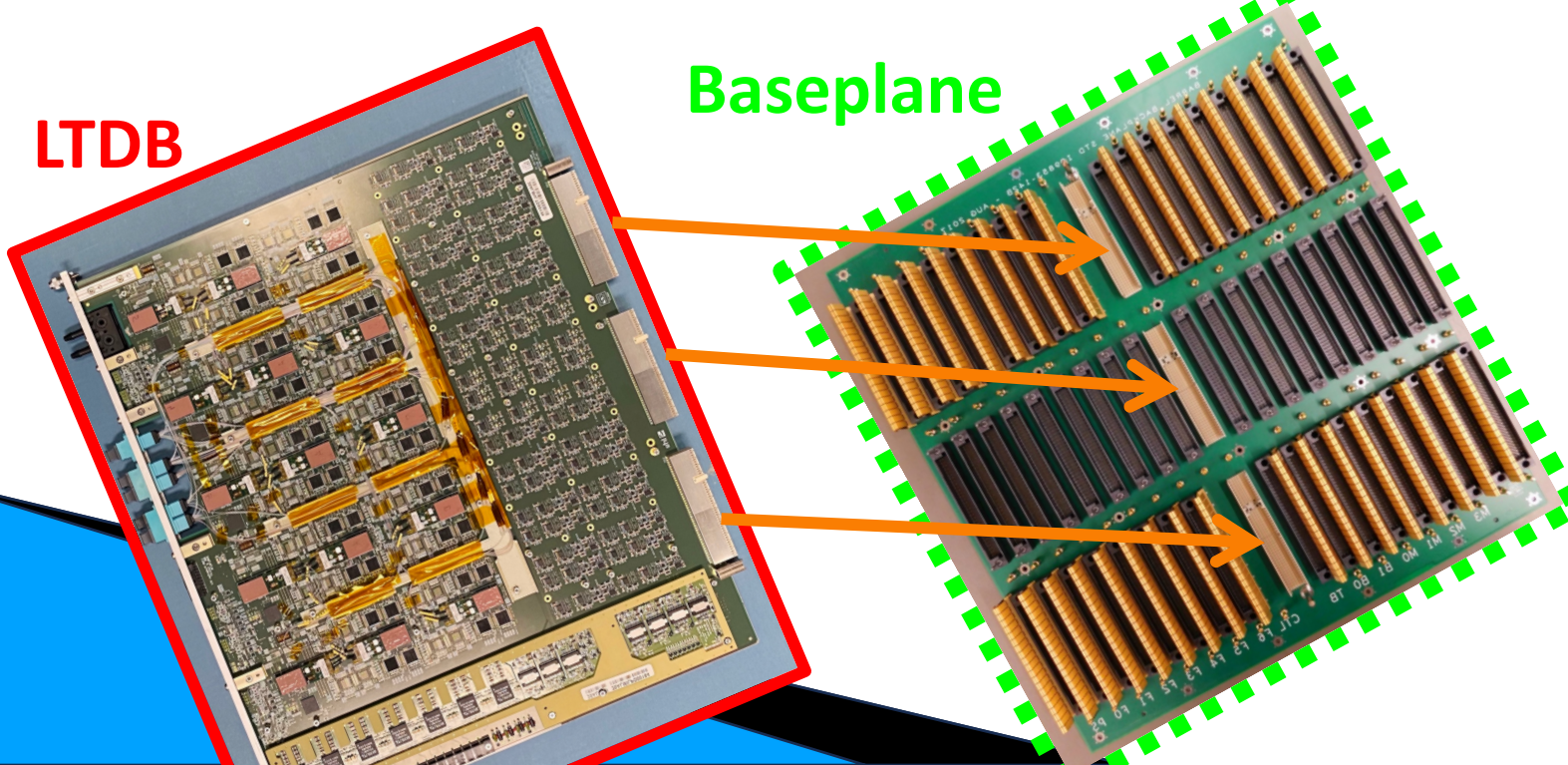
What hardware shall be added ?

- **Layer Sum boards** mezzanine to modify summation of cell signals
- **New Baseplane** to re-route SC signal
- **LAr Trigger Digitizer Board (LTDB)** on-detector to sample and digitize SC signal @ 40 MHz
- **LAr Digital Processing Blade (LDPB)** off-detector to process energies values for each SC
- **Feature Extractor (FEX)** to reconstruct Trigger Objects (TOBs)

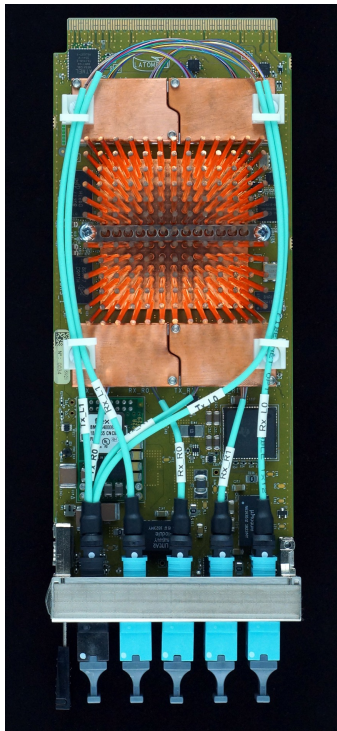


On detector hardware installation

- Front-End electronics sit on 58 crates on detector
- The exchange of 114 baseplanes required extraction of 2000 boards
- Re-install all the legacy boards + 124 new LTDBs

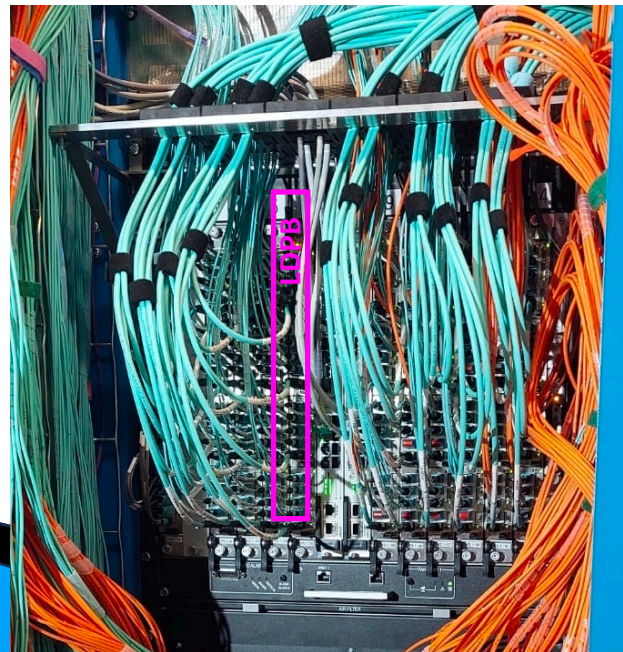
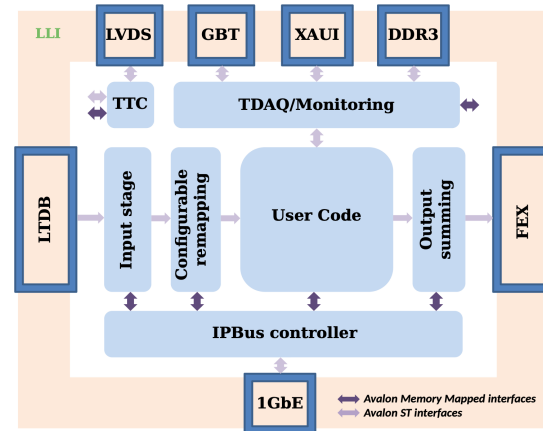


LAr Off-detector installation



A LATOME with the visible FPGA heat sink and optical components

Schematic of LATOME firmware

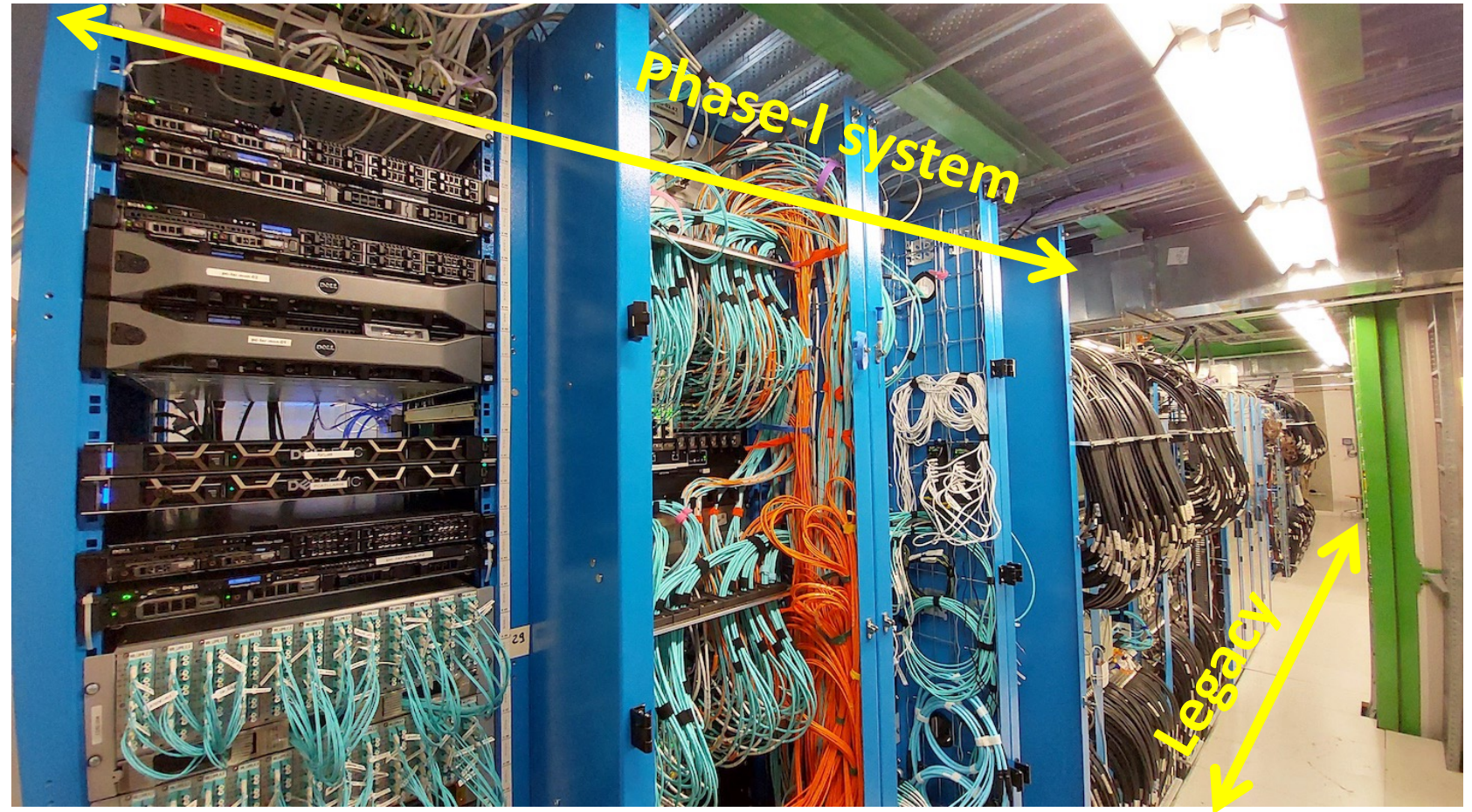


- **LDPB** = 1 Carrier + 4 processing Mezzanines (LATOMEs)
- Firmware on LATOMEs allows to massively parallelise the following steps for up to 320 super cells :
 - Receives ADC samples from LTDBs
 - Calculates E_T and t
 - Assigns E_T to the correct BCID
 - Sums Energies depending on the output FEX
- In total for the whole system
 - 30 LArCarrier (Virtex-7 Xilinx FPGA)
 - 116 LATOMEs (Arria10 Intel FPGA)
 - Input from LTDB -> 25.2 Tb/s
 - Output to FEX -> 41.1 Tb/s

ATCA crate equipped with 40 LATOMEs in 10 LDPBs and fully cabled

Visual Overview

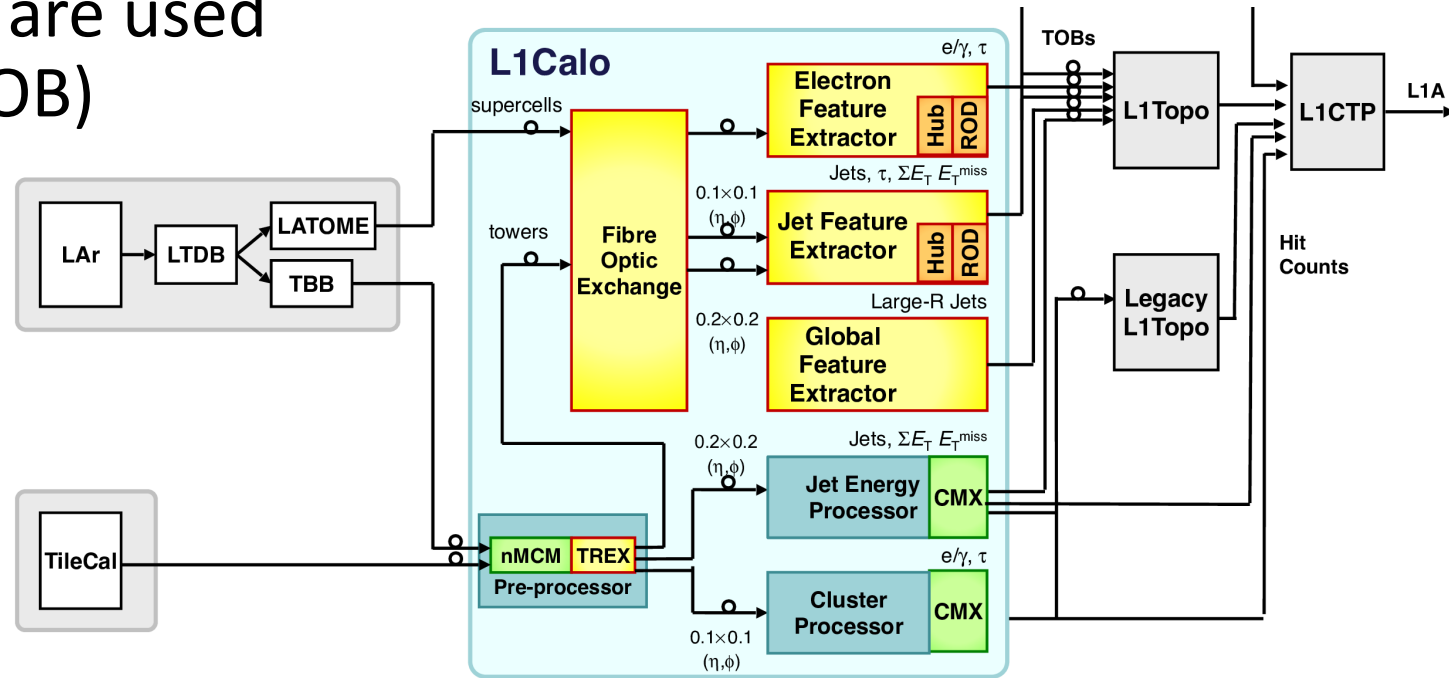
- Limited space required high density system
- However system has approximately 10 times more units of readout than the legacy



Profit significantly of signal digitization on detector
=> Hence the new name of "Digital Trigger"

Feature EXtractor system

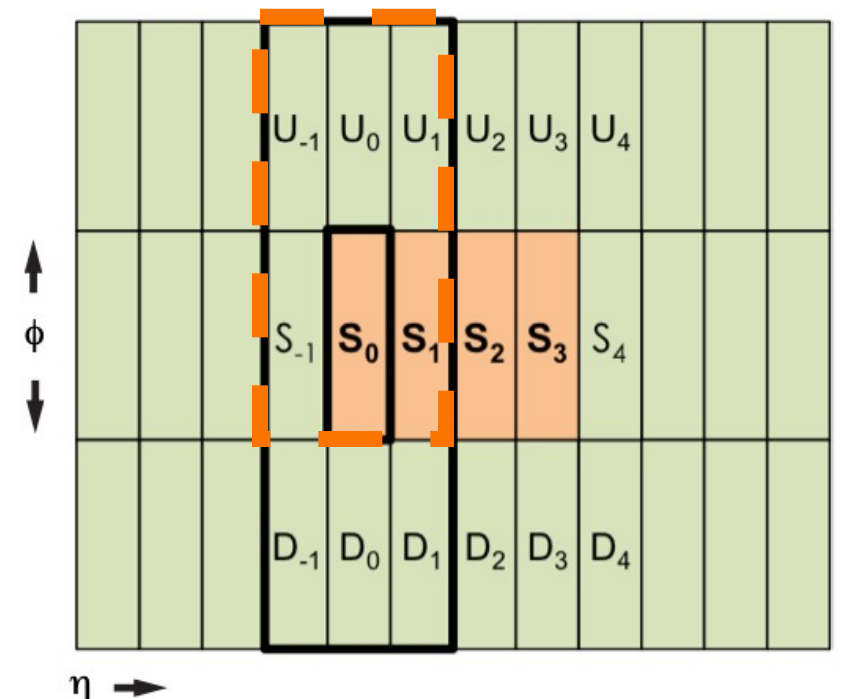
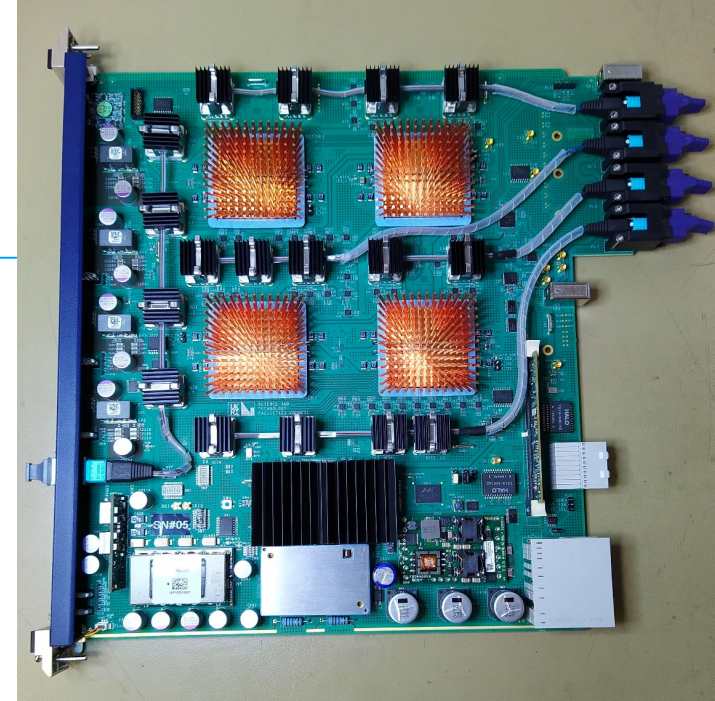
- Downstream to LATOMEs, FEXs are used to reconstruct Trigger object (TOB)
- TOB contains
 - Type of object
 - Position
 - Energy
 - Quality/Isolation
- 3 Types of FEX :
 - 24 “electron FEX” -> e/γ and τ
 - 6 “jet FEX” -> jets, τ and E_T^{miss}
 - 1 “Global FEX” -> Large jets, E_T^{miss} and ΣE_T



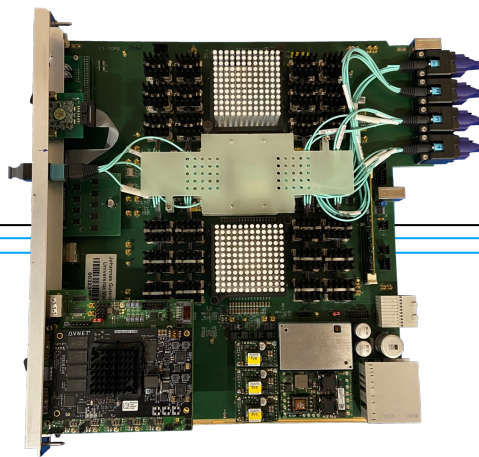
- Additional fiber plan (FOX) to re-route signal from LATOME to the FEXs
- TRES module used to digitize Tile Cal legacy analogue inputs

Example : e/γ algorithms

- 4 FPGA (Virtex-7 Xilinx) / eFEX module
- Building of e/γ TOBs is sliced in $\eta \times \phi$ regions each containing
 - A core of 4 Barrel middle layer super cells + the surrounding cells
- Each FPGA process 32 regions in parallel
- Algorithm :
 - Search for local maximum on the core Super Cells (S_0)
 - Search for neighbouring maximum on surrounding cells (U_0)
 - Define a cluster of 3×2 super cells around (S_0 and U_0)
 - Sum energies on other layer to define an e/γ TOB
 - Apply correction per layer to account for inhomogeneous dead material
- Additional shower shape variables are calculated and included in the TOB quality information



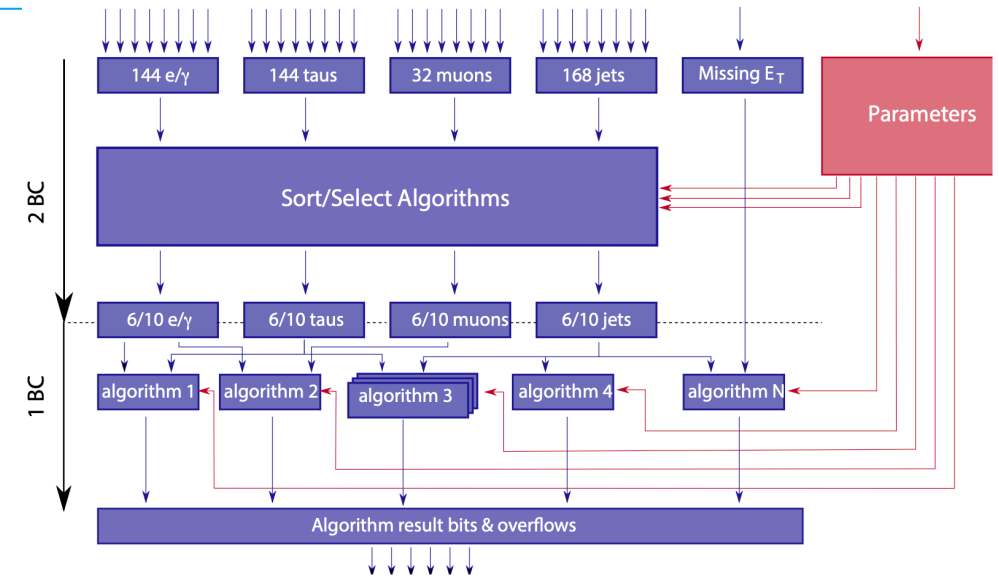
L1Topo



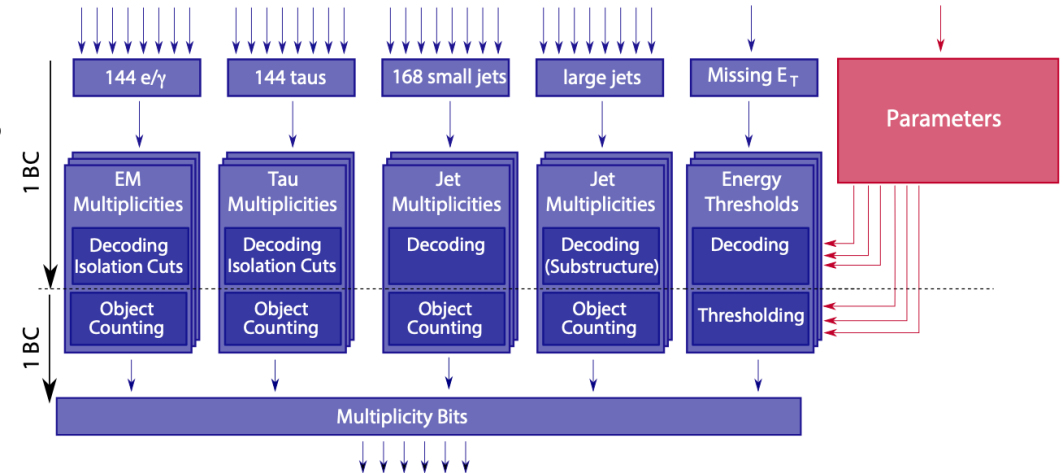
- 2 FPGA/board each running a specific firmware on all TOBs
- Firmware for topological algorithms
 - Gather all TOBs and select the most relevant
 - Apply algorithm based on global variables ($\Delta\phi$, $\Delta\eta$, $M_{inv}\dots$)
- Firmware for multiplicity algorithms
 - Get all the TOB and based on isolation count globally how many are passing the criteria
- Send ~ 1 bit per each of the $O(100)$ algorithms to Central Trigger for final decision

L1Topo board with 2 Ultrascale+ (Xilinx) FPGAs

Architecture of the firmware for topological algorithms

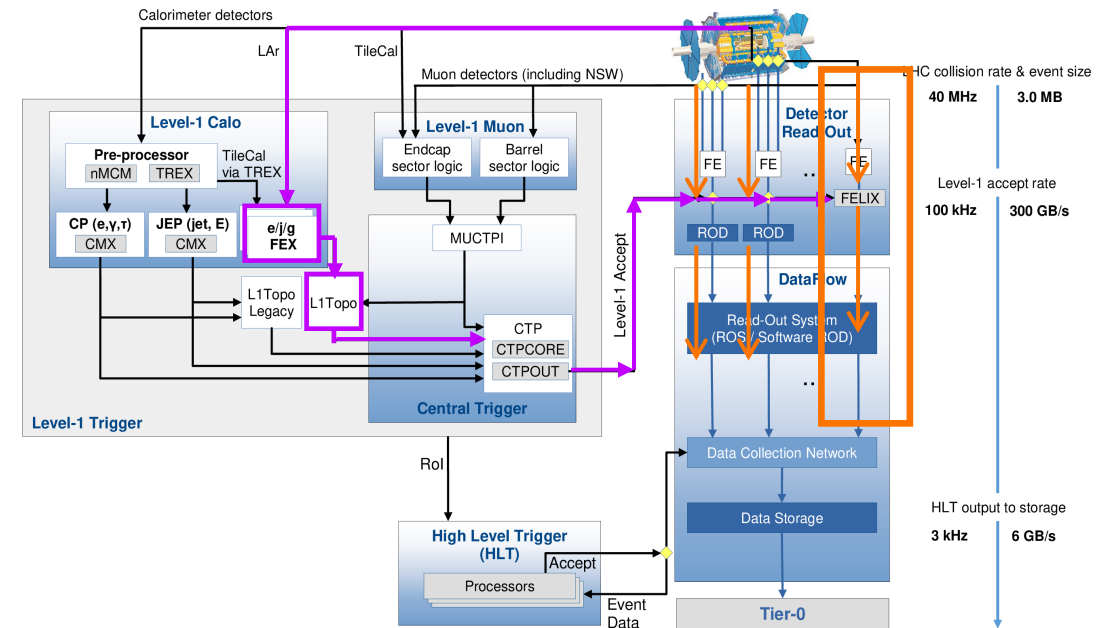
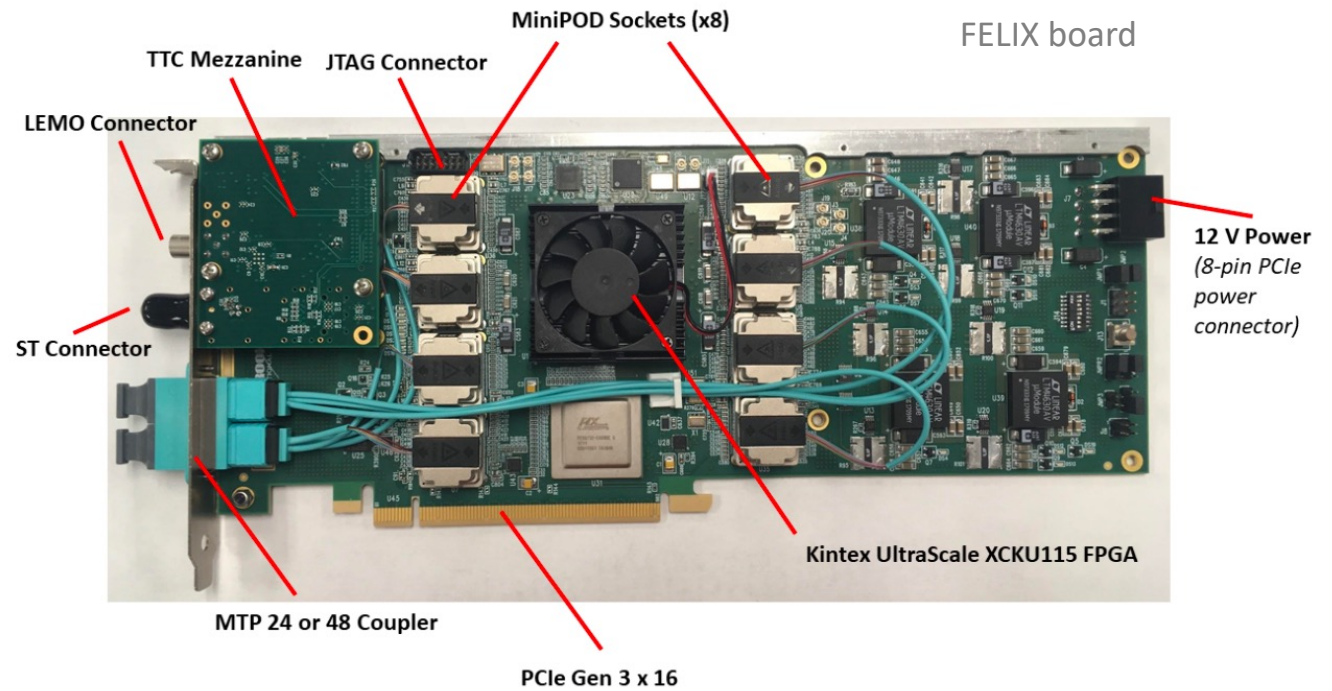


Architecture of the firmware for multiplicity algorithms

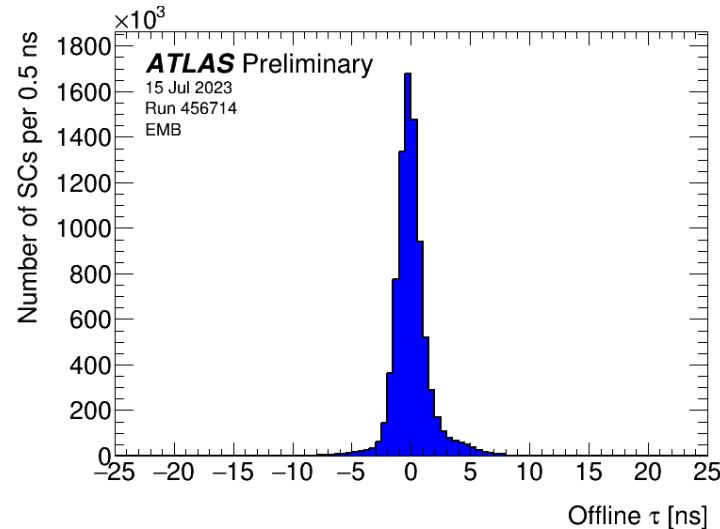
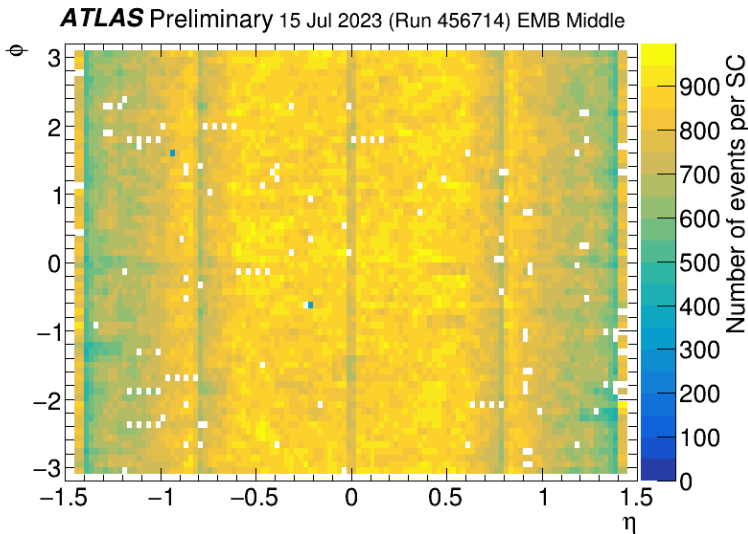
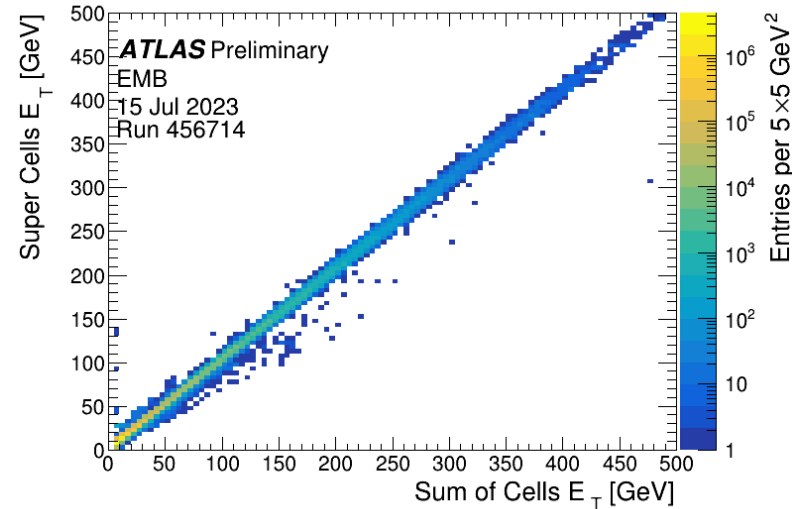
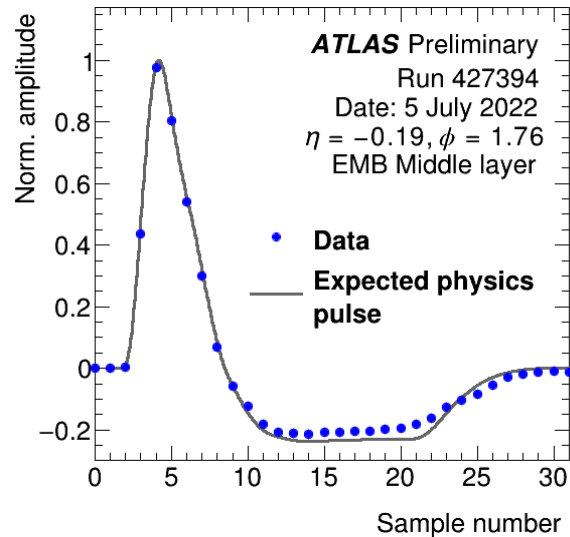


Readout

- New readout also put in place
- On all stage (LAr , L1Calo, L1Topo) information are readout for HLT seeding, performance and monitoring purpose
- Unified architecture based on PCI board (FELIX) had been installed
- Interfaced with the rest of the readout structure
- FELIX are also used to configure the LTDBs and to transmit timed-in (TTC) signals

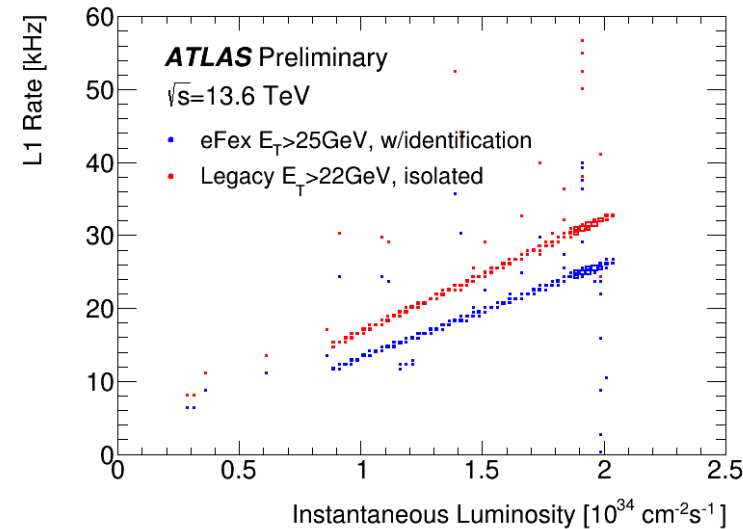
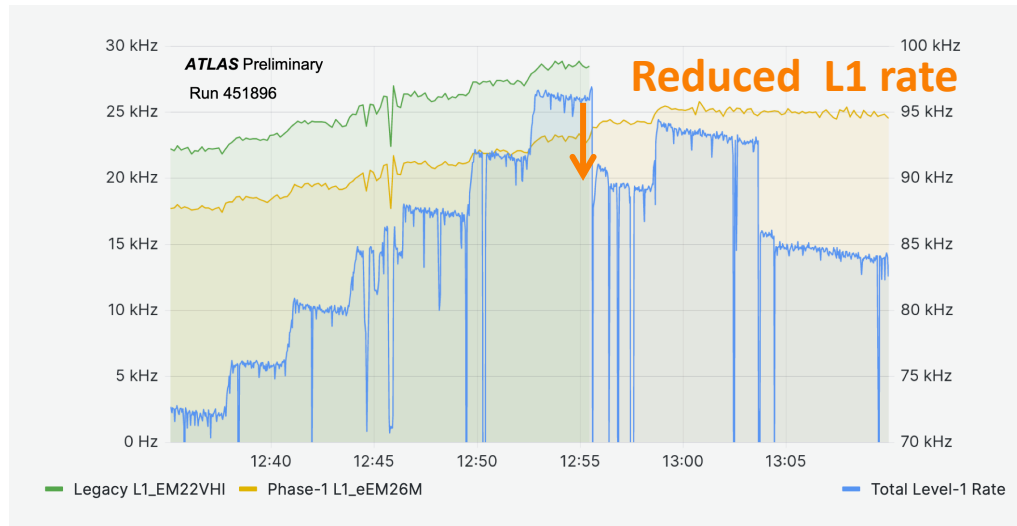


Digital trigger readout performances



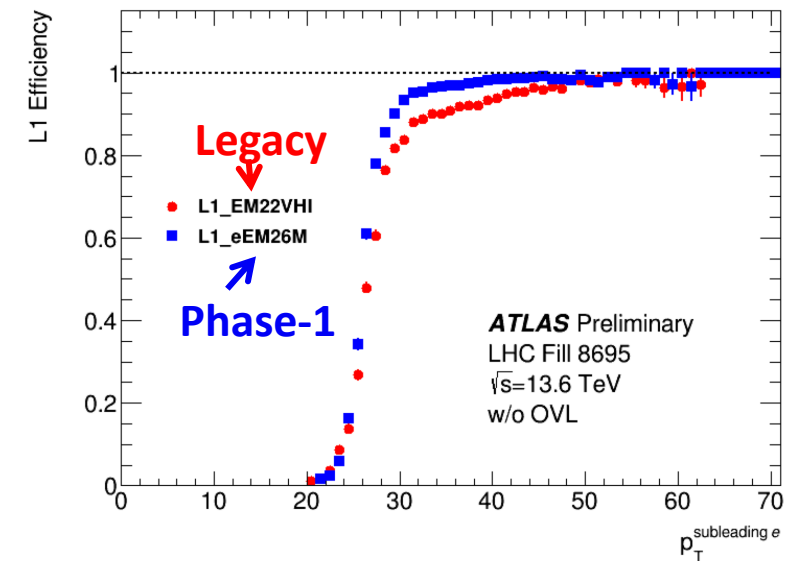
- Pulse shape measured on super cell are matching expected pulse
- Good agreement between reconstructed energies of Super Cell and Sum of corresponding cells in precision readout
- Very good overall coverage
- Timing is well below the 25 ns allowing to identify properly the BCID and avoiding early triggers

Performance of the whole trigger chain



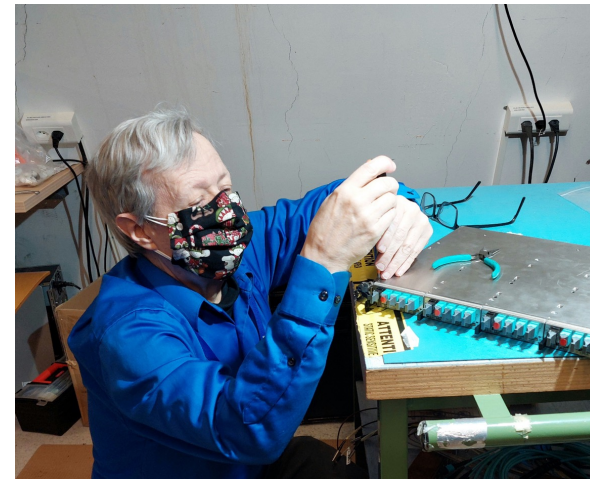
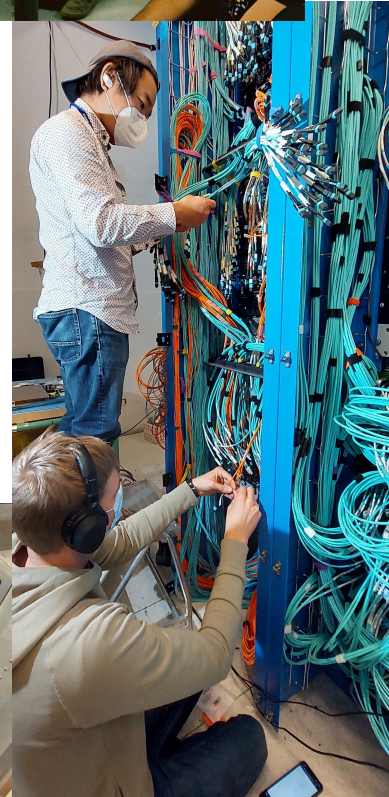
- Sharper efficiency curve on Phase-I based item
- Show better selection of relevant objects at energies just above thresholds

- On comparable trigger items
- See overall rate reduction by ~ 5 kHz when legacy trigger was cut
- The difference of rate saving increase with instantaneous luminosity with a constant ratio
- Expect further rate reduction with other Phase-I calorimeters items and other FEX systems



Conclusion

- Digital Trigger has been installed and is now fully functional
- It was gradually included since 2023 in ATLAS productions triggers and is now used as primary trigger system
- Good performance in terms of coverage and energy reconstruction
- Significant rate reductions (~ 5 kHz) for electromagnetic object while keeping very good signal efficiency
- Continuous improvement during operation time
- Digital Trigger will remain operational for the HL-LHC



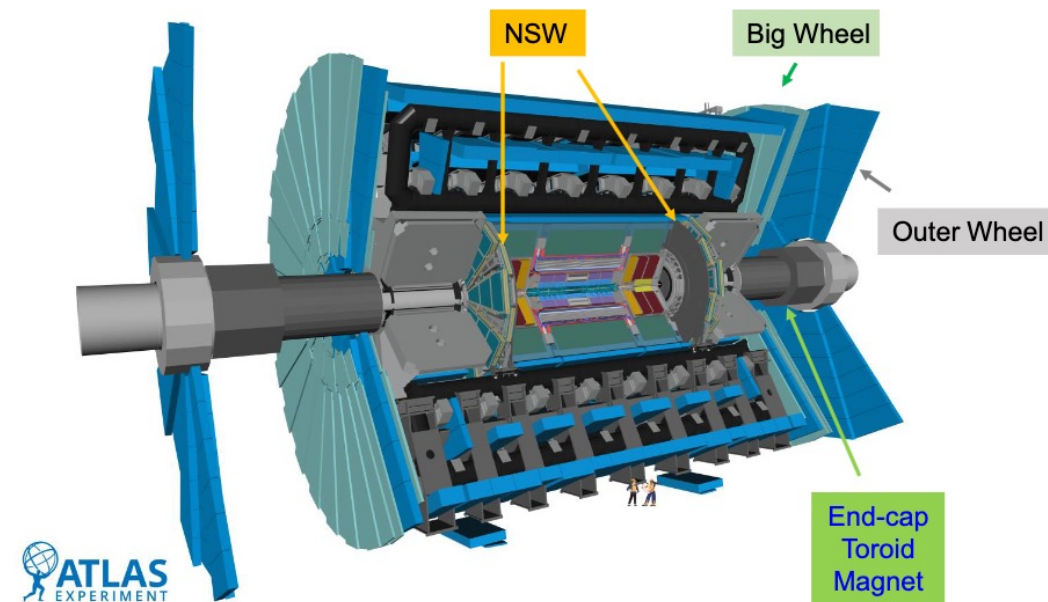
Muon System Phase1 Upgrade

- New Small Wheel



Introduction: NSW

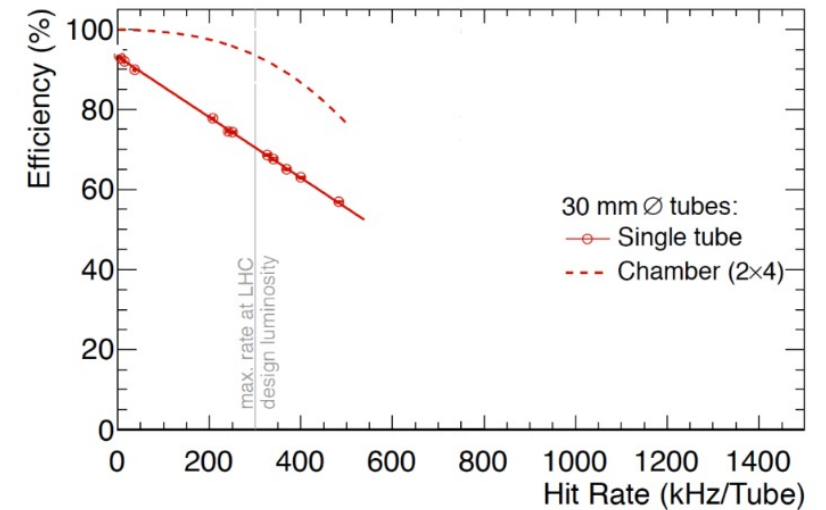
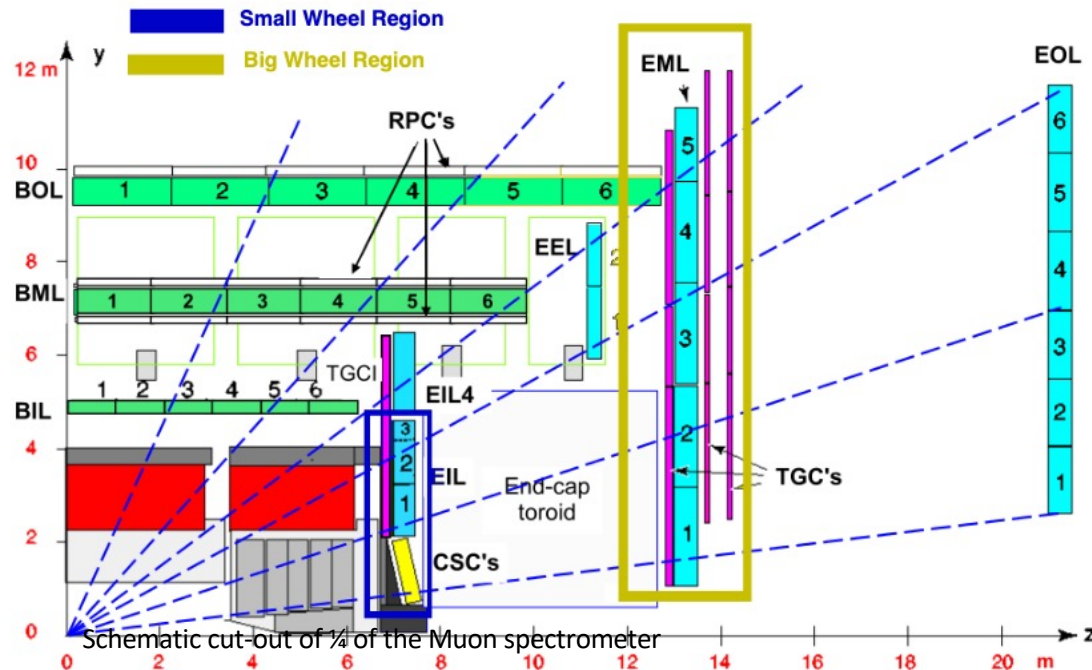
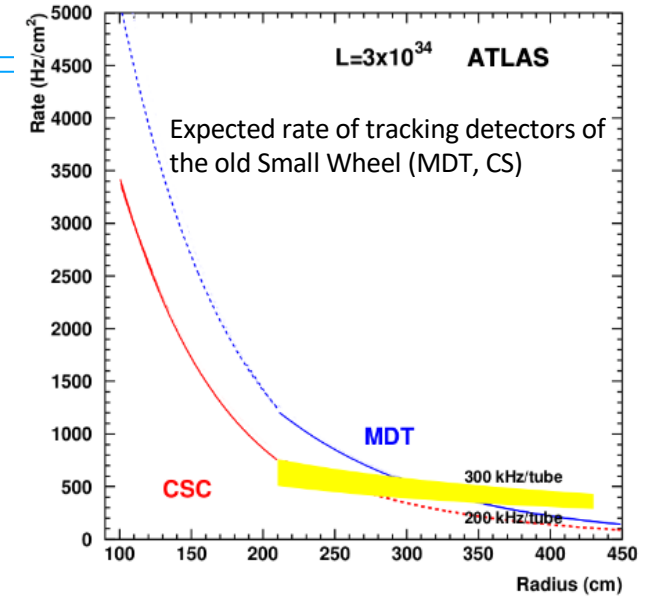
- The New Small Wheel (NSW) is the largest ATLAS Phase1 upgrade project
 - Replacement of the two innermost Muon detector stations of the End-cap regions
 - Main goals:
 - Improve L1 muon trigger rejection capability
 - Maintain good detector performance in high pileup environment for Run3 and beyond



- Diameter: ~10 m diameter, weight: >100 T; not really a 'small' thing

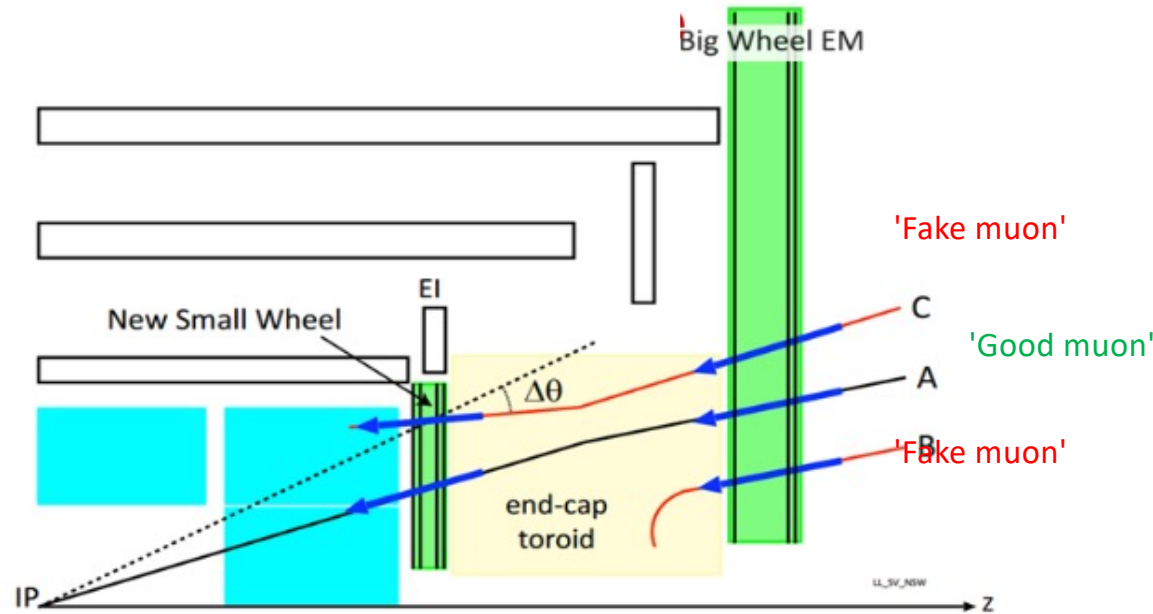
NSW - Motivation

- With luminosity increase in Run3 and beyond the performance of the old Small Wheel detectors (MDT, TGC, CSC) would be affected by rate capability limitations
- Replace the detectors with technologies able to cope higher background, preserving tracking capability in $1.3 < |\eta| < 2.7$:
 - Offline muon construction: 15% pT resolution at ~ 1 TeV/c.
 - 97% segment reconstruction efficiency for muon pT > 10 GeV/c

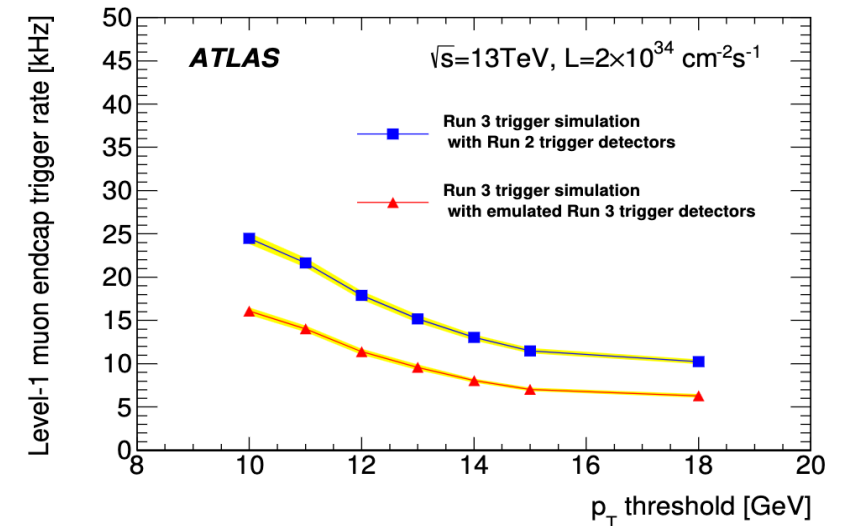
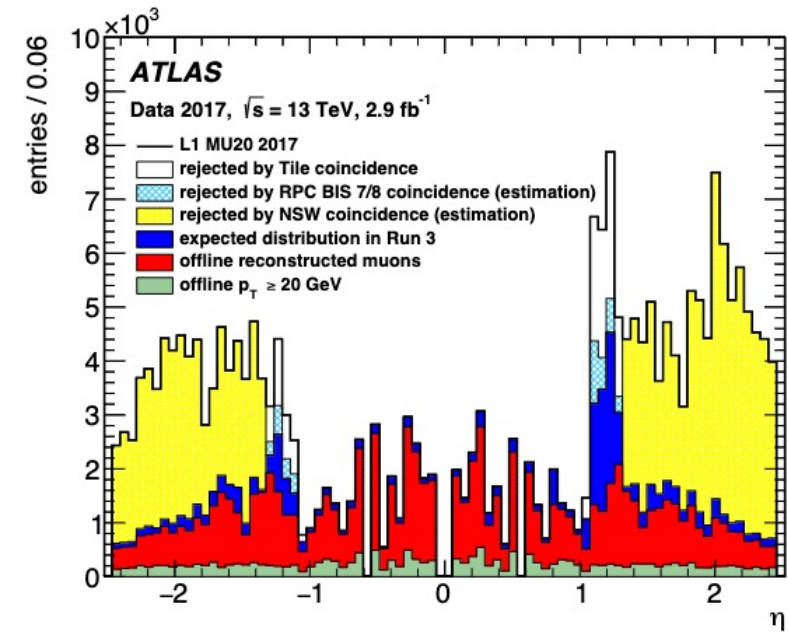


NSW - Motivation

- Large L1 muon fake trigger rates observed in end-cap regions in Run1 and Run2: tolerable at low lumi, not at $2 \times 10^{34} \text{ cm}^{-2}\text{s}^{-1}$
- Trigger coincidence between inner (NSW) and middle (Big Wheel) station drastically reduce the trigger rate from fakes; already with a coarse segment measurement (Phasel1 requirement)
- L1 trigger segments measurements with up to 1 mrad pointing accuracy (Phasel2 requirement) in $1.3 < |\eta| < 2.4$



- NSW can preserve bandwidth for good trigger items



NSW – Detector requirements

- System performance requirements:
 - Offline muon construction: 15% p_T resolution at ~ 1 TeV/c
 - 97% segment reconstruction efficiency for muon $p_T > 10$ GeV/c
 - Trigger capability
 - L1 trigger segments measurements with up to 1 mrad pointing accuracy
- Main requirements for NSW detectors:
 - Space resolution: $O(100)$ μm
 - Good double track separation (few mm)
 - 25 ns BC identification capability
 - Rate capability 20 kHz/cm²
 - Longevity to stand the entire ATLAS lifetime (run at HL-LHC until >2040)
 - Construction of large-size detectors
- Two complementary gaseous detector technologies selected, both able to provide tracking and triggering capabilities
 - Small-strip Thin Gap Chambers (sTGC)
 - MICRO-MEsh Gaseous Structure (Micromegas, MM)



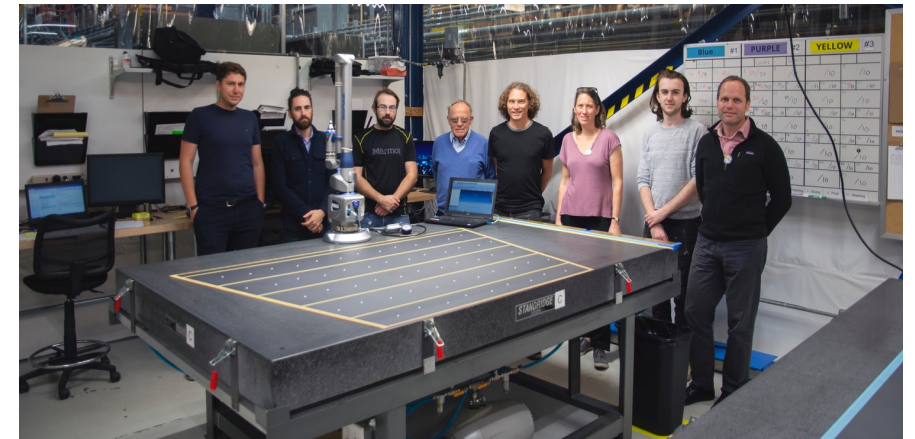
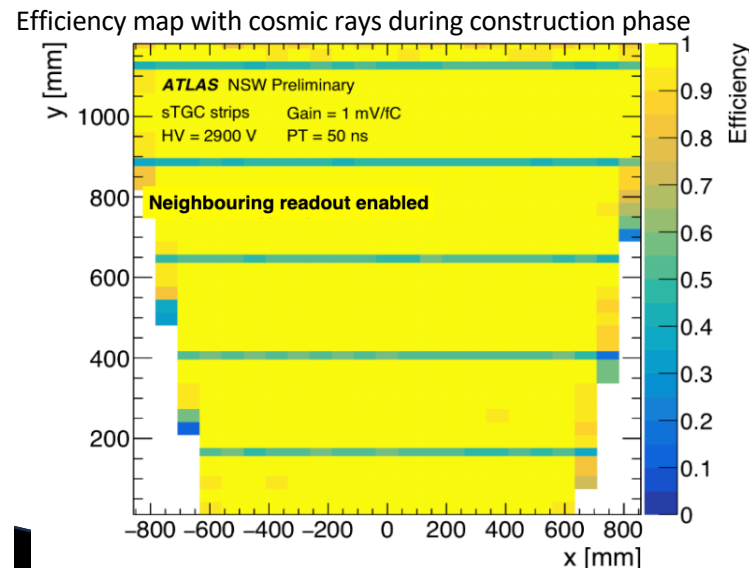
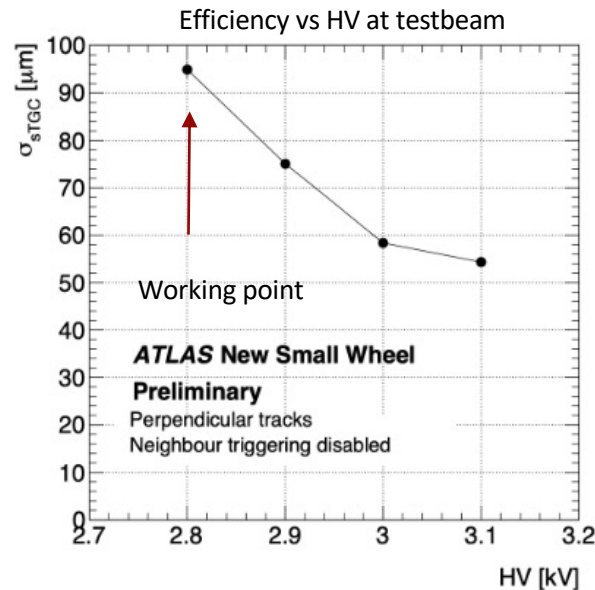
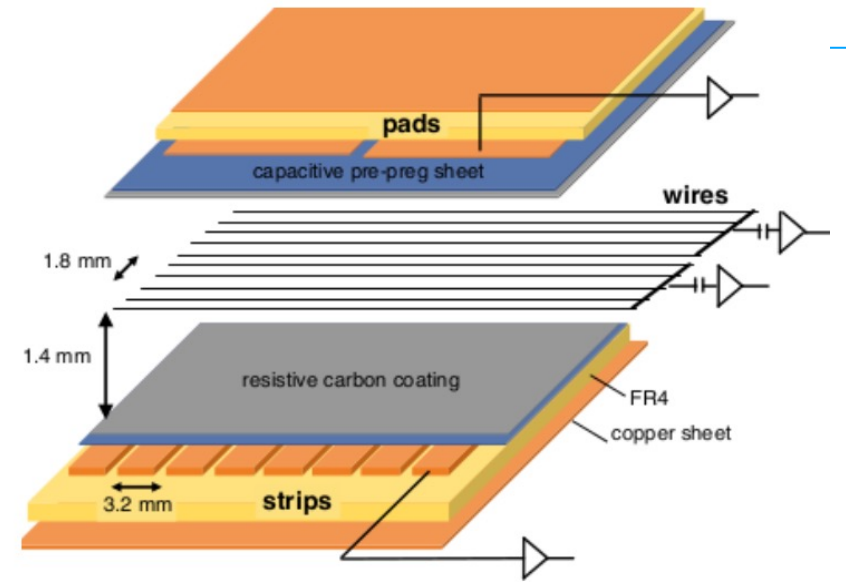
| sTGC | |
|-----------------------|---|
| η coverage | $1.3 < \eta < 2.7$ (2.4 for trigger) |
| Number of quadruplets | 192 |
| Number of gas volumes | 768 |
| Number of channels | 357k |
| Function | Trigger, precision tracking, 2nd coordinate |

| Micromegas | |
|-----------------------|---|
| η coverage | $1.3 < \eta < 2.7$ (2.4 for trigger) |
| Number of quadruplets | 128 |
| Number of gas volumes | 512 |
| Number of channels | 2.05M |
| Function | Precision tracking, trigger, 2nd coordinate |

- NSW alone has 2.3x # of readout channels of the rest of the ATLAS Muon spectrometer --> change of scale for a single system

NSW Detectors: sTGC

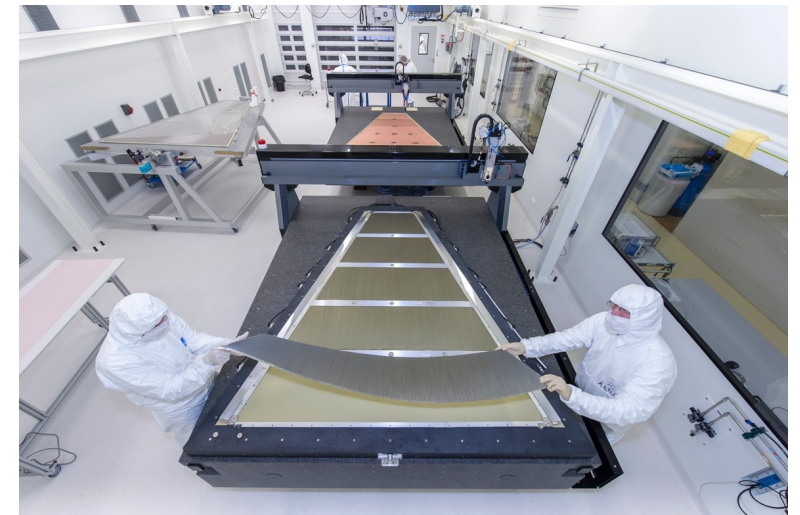
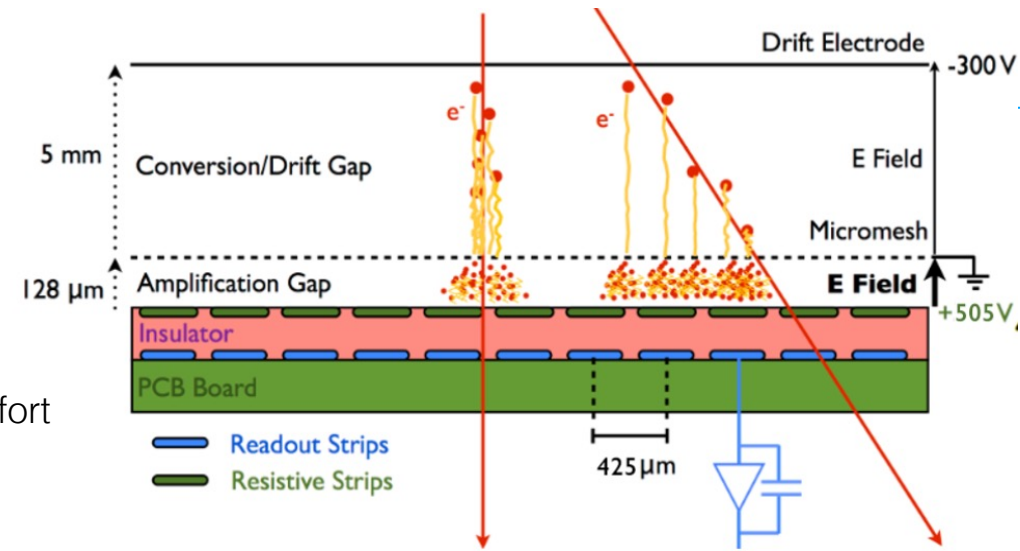
- Multi-wire chambers with resistive cathode and three-fold readout
 - Wires, pads, strips
- Evolution of the well-established TGC technology toward higher rates
 - Lower surface resistivity carbon coating --> faster charge evacuation
 - Smaller strip pitch (3.2 mm)
 - Thin gap --> good time resolution for bunch-crossing identification
 - High radial resolution and rough ϕ resolution from pads
 - Gas mixture: CO₂:n-pentane (55:45)
- Construction sites: Canada, Chile, China, Israel, Russia



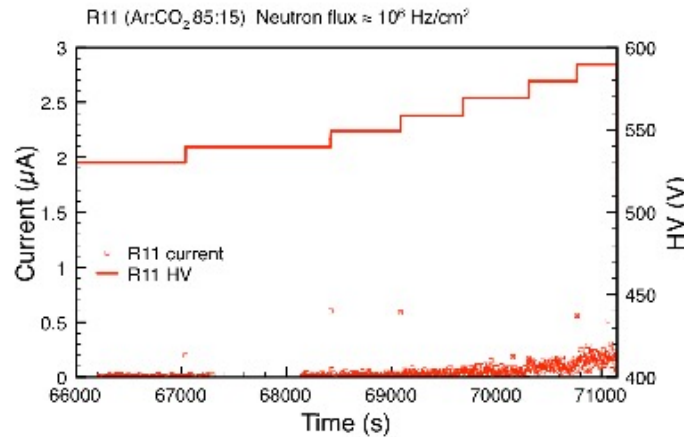
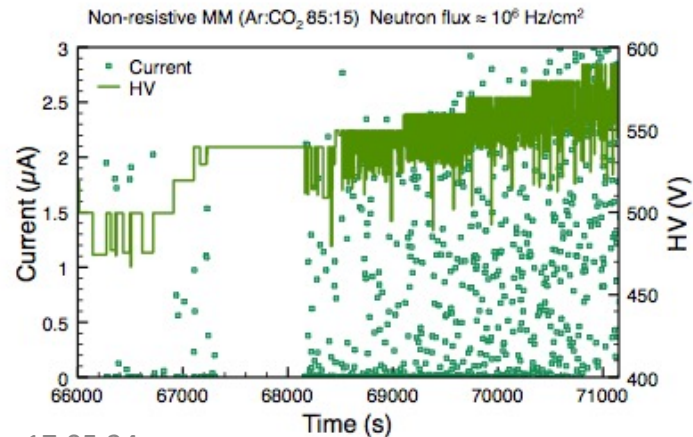
sTGC construction @ TRIUMF (credit: <https://www.triumf.ca/atlas-group/NSW>)

NSW Detectors: Micromegas

- Micro-Pattern Gaseous Detectors (MPGD)
 - Micro-mesh (transparent to electrons) separates ionisation and amplification gaps --> ion tail suppression: high rate capability
 - Drift time ~ 100 ns
 - Strip pitch: 425, 450 μm
- R&D of MM for application to large system at colliders needed a dedicated effort
 - Development of resistive Micromegas for suppression of discharge intensity
 - Industrial mass production of precise large-size MM anode boards
 - Mechanical solutions for large-area MPGD
 - Tracking for inclined tracks
- Construction sites: France, Germany, Italy, CERN/Greece/Russia

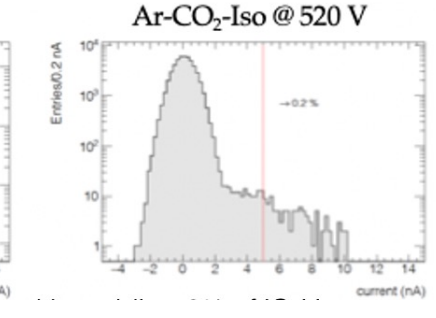
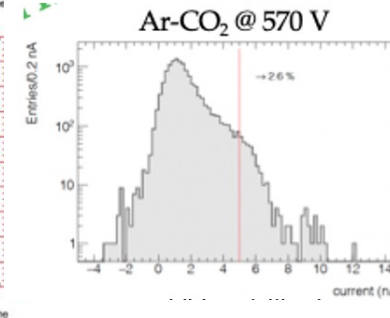
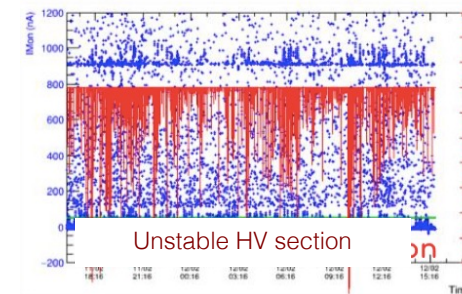
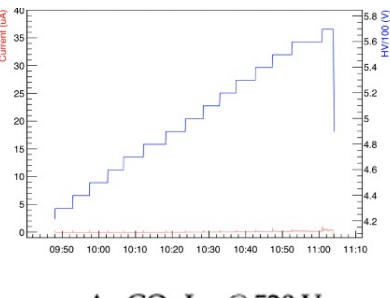
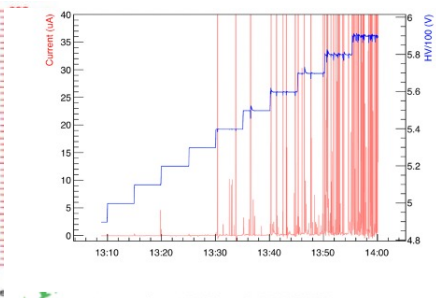
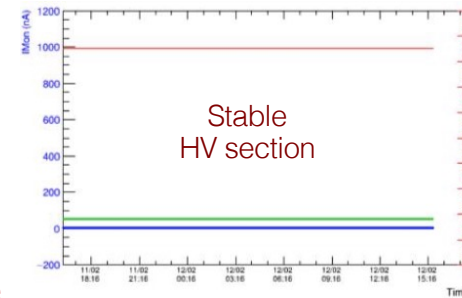
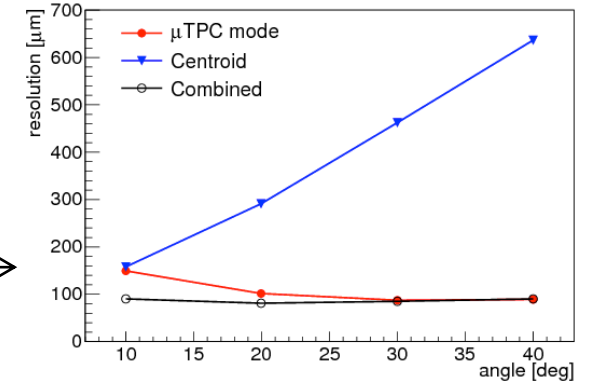
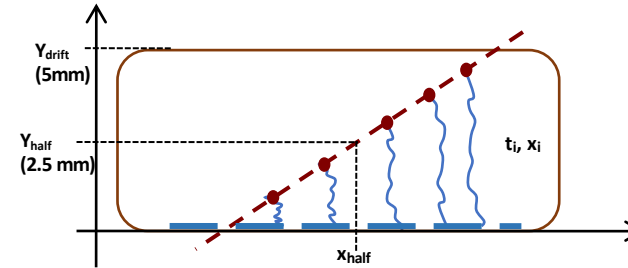


MM construction @ CEA Saclay



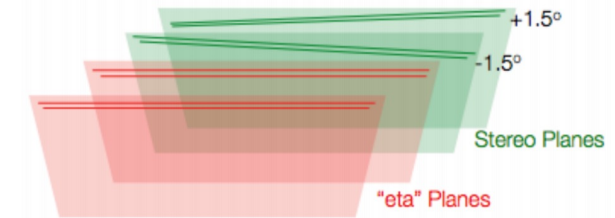
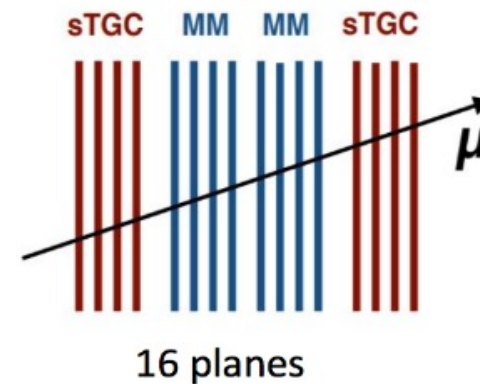
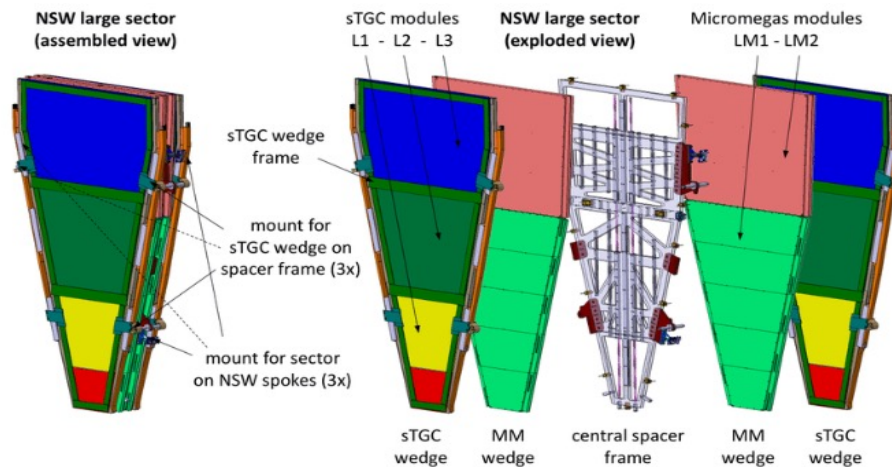
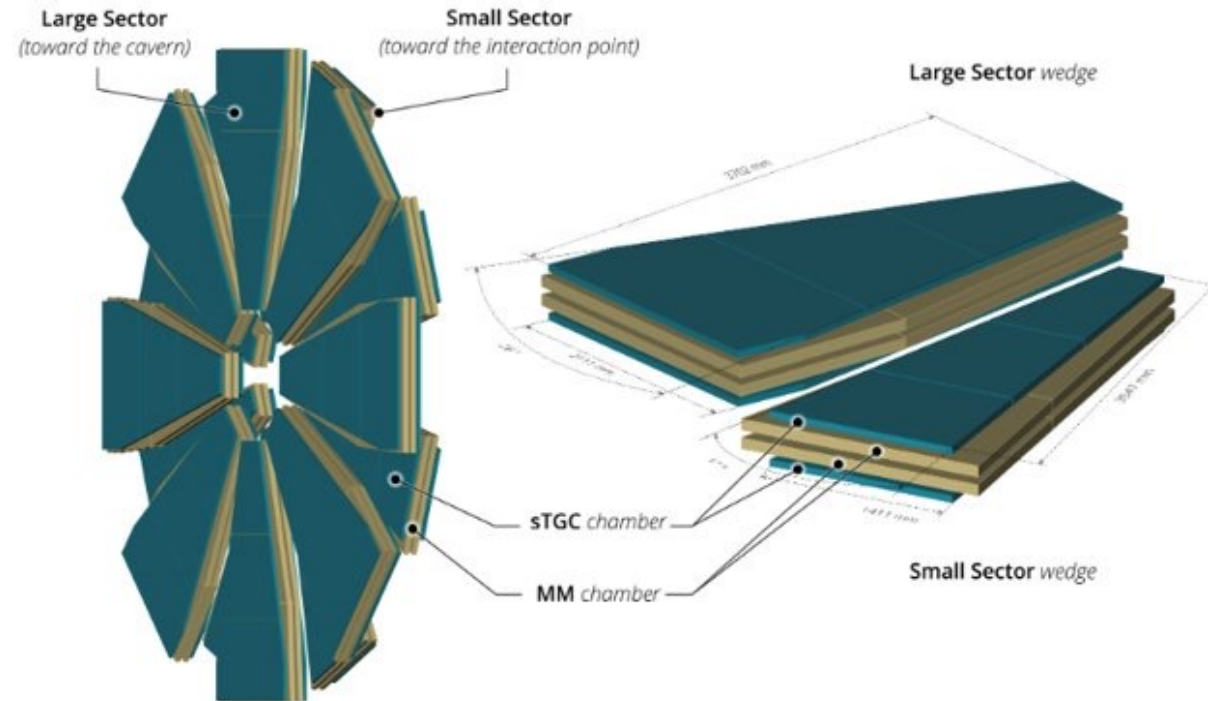
NSW Detectors: Micromegas

- Like in a TPC the time information can be exploited to track charged particles in the 5 mm drift region: the uTPC technique
 - Requires sufficient granularity and time resolution
- 'HV stability crisis' during construction phase: large echo in the community (and beyond)
- Several action taken & solutions implemented
 - Cleaning → establish proper cleaning procedure for anode boards and for mesh
 - Humidity → reduce humidity
 - Correlation with RO board resistivity → Passivation
 - Role of the mesh
 - Original gas mixture Ar:CO₂ 93:7 adopted to use the same gas as CSC/MDT detectors in ATLAS Not an optimal gas for a parallel single-stage amplification structure. Changes to Ar:CO₂:iC₄H₁₀ 93:5:2 → problematic HV sectors reduced to physiological level



NSW layout

- Each wheel consists of 16 Sectors (8 large, 8 small)
 - 1 Sector: assembly of 2 sTGC and 2 MM wedges mounted on a common support
 - 1 sTGC wedge: 3 detectors
 - 1 MM wedge: 2 detectors
 - Each detector (quadruplet) has 4 active layers
- 16 detector layers --> high redundancy
 - Harsh environment
 - Limited accessibility for maintenance
- Active surface for each technology: 1280 m²
Largest MPGD detector system ever built (for MM)



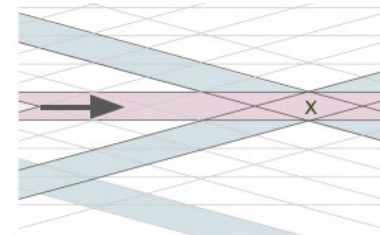
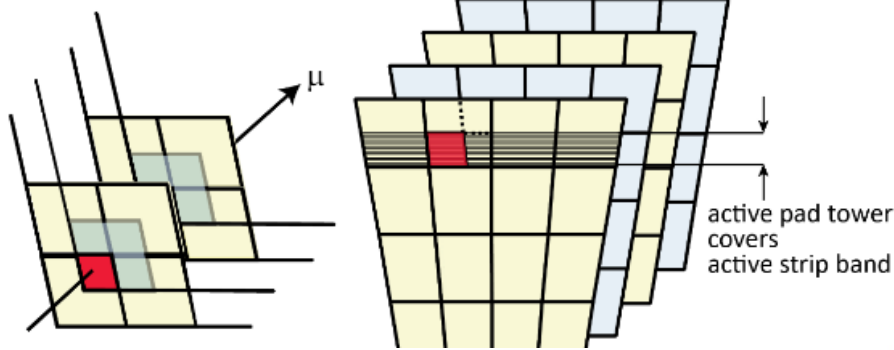
1 MM quadruplet has 2 eta and two stereo layers = X,U,V, X readout

NSW trigger concept

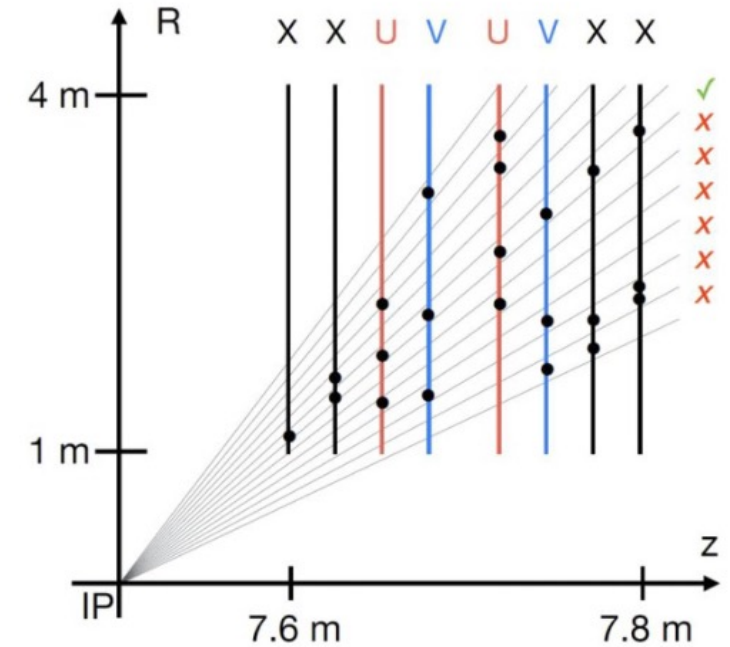
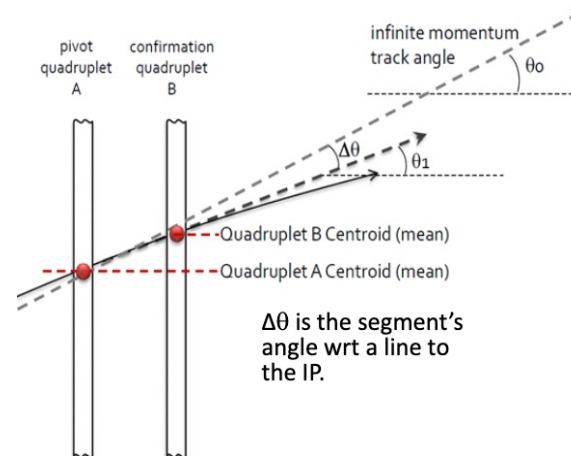
- **STGC**: 2-stage trigger
- **PAD**: coarse trigger sufficient for Run3. sTGC pads are staggered by $\frac{1}{2}$ pad size in both directions --> logical pad size = $\frac{1}{4}$ of pad area
- Acting as pre-trigger to select strips of interest to transmit to the trigger processor. Needed for Hi-Lumi

- **MM**: exploits eta (X) and stereo (U,V) layer hits
- Match of first hit per group of 64 (VMM) among U,V and X layers
- When sufficient hits on an IP pointing road are found, their coordinate are used to fit a track segment

sTGC quadruplet



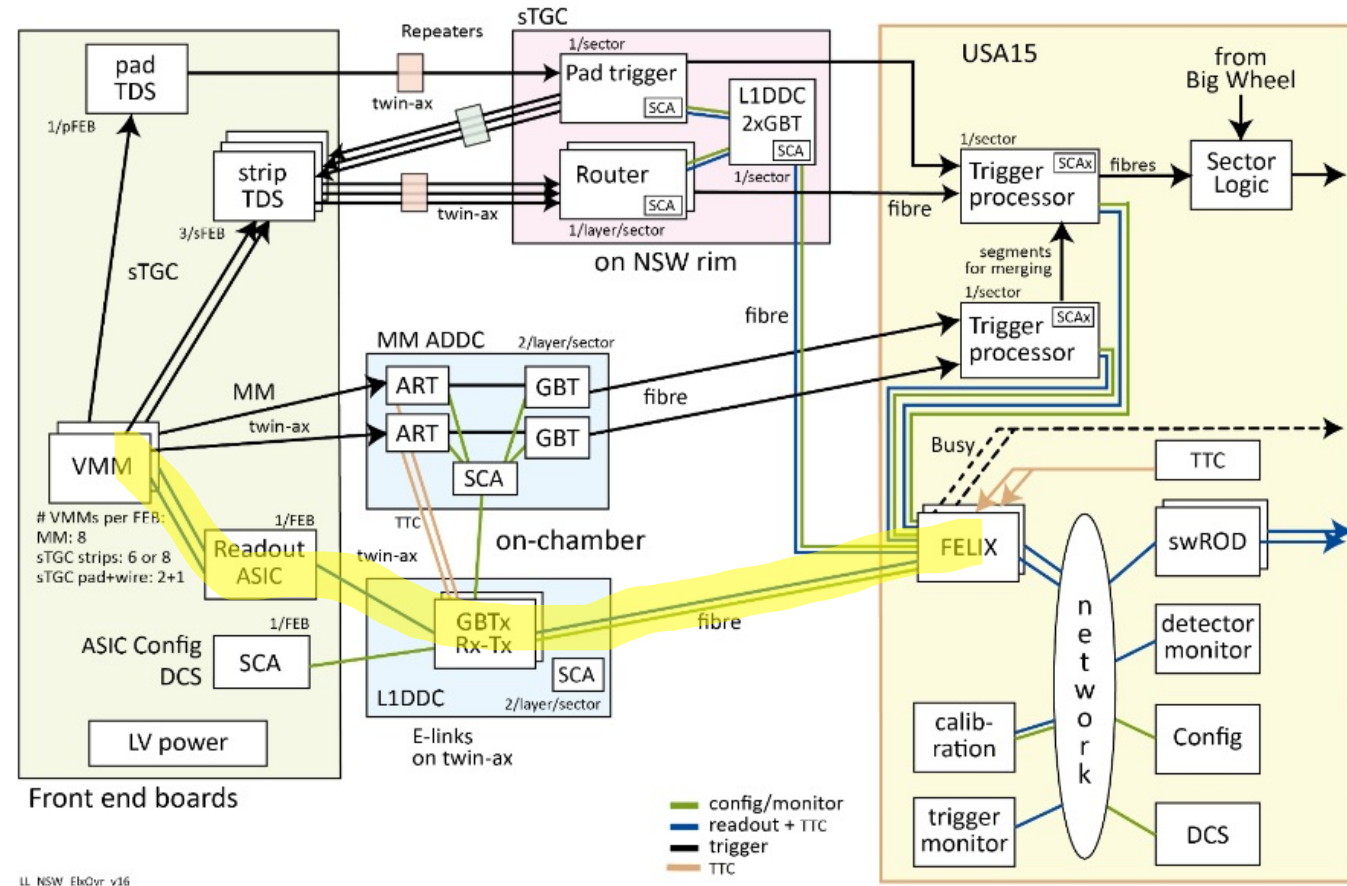
- **STRIP**: charge centroid on each layer combined in a super-point on each quadruplet. Trigger segment calculated from the two super-points of a wedge. Finer granularity than PAD --> better angular resolution



<https://cds.cern.ch/record/2842618/files/ATL-MUON-SLIDE-2022-625.pdf>

Electronics and DAQ chain

- Front-end based on the same versatile custom FE ASIC for both sTGC and MM: VMM
 - rad hard 130 nm 1.2V CMOS
 - 10 million transistors
 - large: 130 mm² silicon
 - 64 chan of charge amplifier, shaper, peak finder
 - 10-bit and 6-bit ADCs, 8-bit TDC
- 53k VMM; >70M config registers
- Calibration is a challenge
 - Charge amplifiers and ADC
 - Baseline, thresholds, charge, time
 - Redout control: internal phases (data decoding and aggregation)
 - Data sampling phase for GBTx data transceivers
 - And many others...
- The readout, configuration and synchronization paths implemented with the GBTx and FELIX

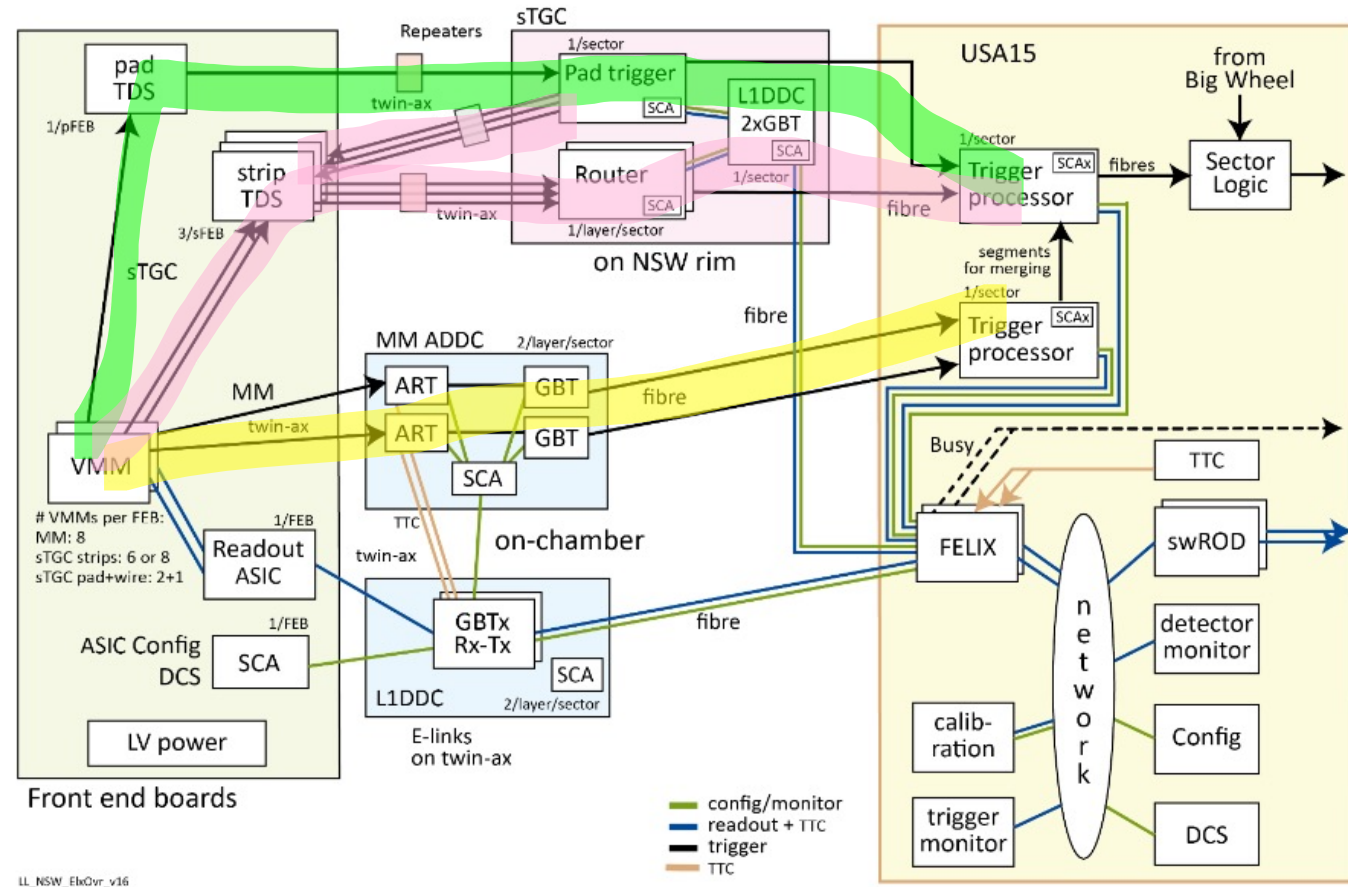


Data path: Digitized readout data from the detector including monitoring and calibration

<https://cds.cern.ch/record/2842618/files/ATL-MUON-SLIDE-2022-625.pdf>

Electronics and DAQ chain: trigger paths

- Digitized data from VMM to Trigger processor
- MM: address in real time (ART, 1st hit per VMM) sent to the MM trigger processor
- PAD: pad Trigger Data Serializer (TDS) sends data to the Pad trigger processor on NSW rim and strip band ID to the strip TDS
- STRIP: Strip TDS reads strip data in the band ID defined by the Pad Trigger and send them to the router
- Up to 8 MM segments and up to 4 sTGC segments are sent to the Trigger processor. Duplication are removed
- Up to 8 segments are sent to the sector logic to confirm trigger from the Big Wheel (middle end-cap station)



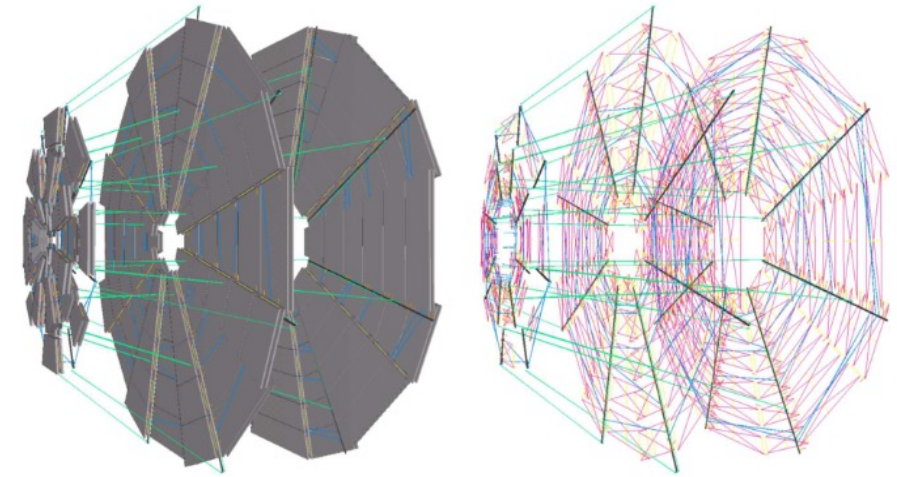
MM trigger path

STGC Pad trigger path

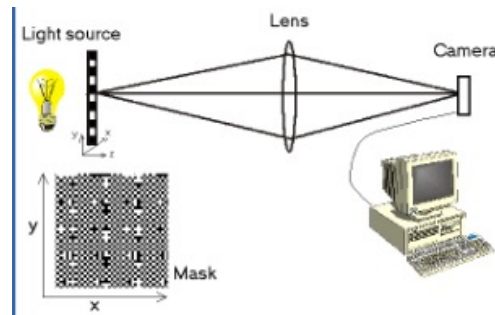
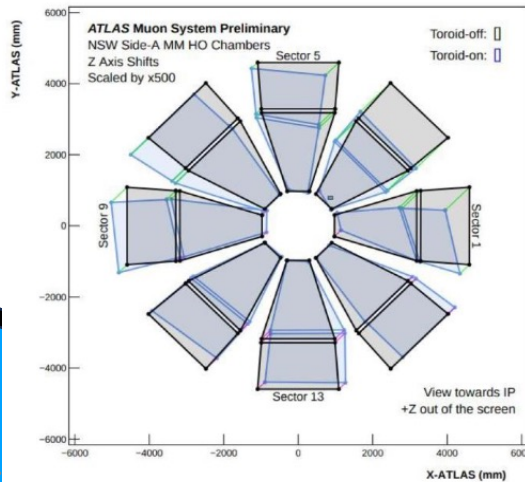
STGC strip trigger path

Alignment

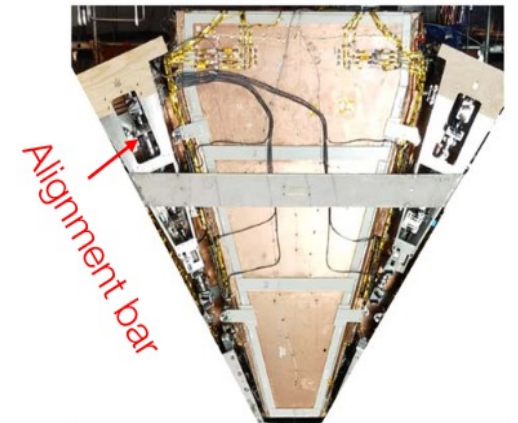
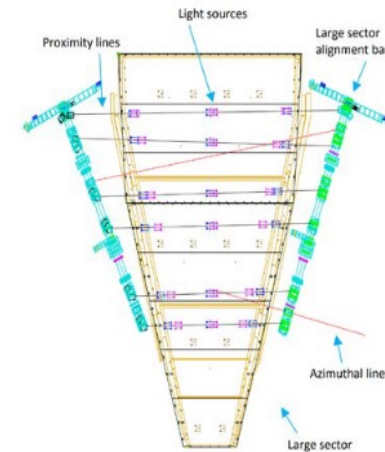
- Muon p_T accuracy of 10% accuracy for 1 TeV muon requires a geometrical alignment better than 100 μm for each detector element
- Alignment of the ATLAS Muon system based on
 - Internal alignment of the detector components ('as-built' parameters) measured during construction
 - An array of optical sensors to continuously monitor position and deformation of the chambers
 - Recalibration of the optical system with straight tracks: special pp collision runs with toroid OFF
- The alignment of the NSW has recently reached the required performance
 - Further improvements possible by fine tuning of the 'as-built'
- NSW tilt up to 2.7 mm when toroid is switched on/off



Layout of the optical alignment system in one end-cap, with and without the detectors visible



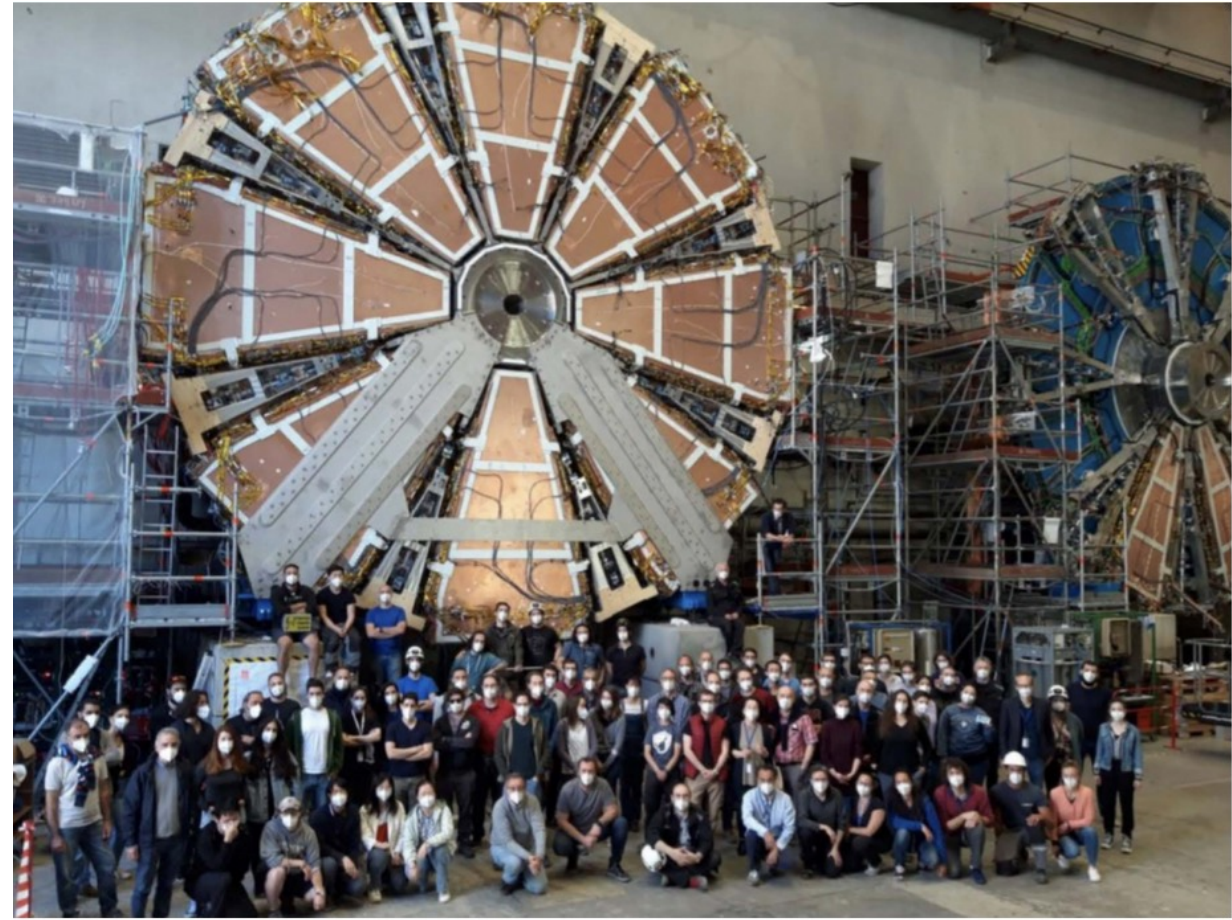
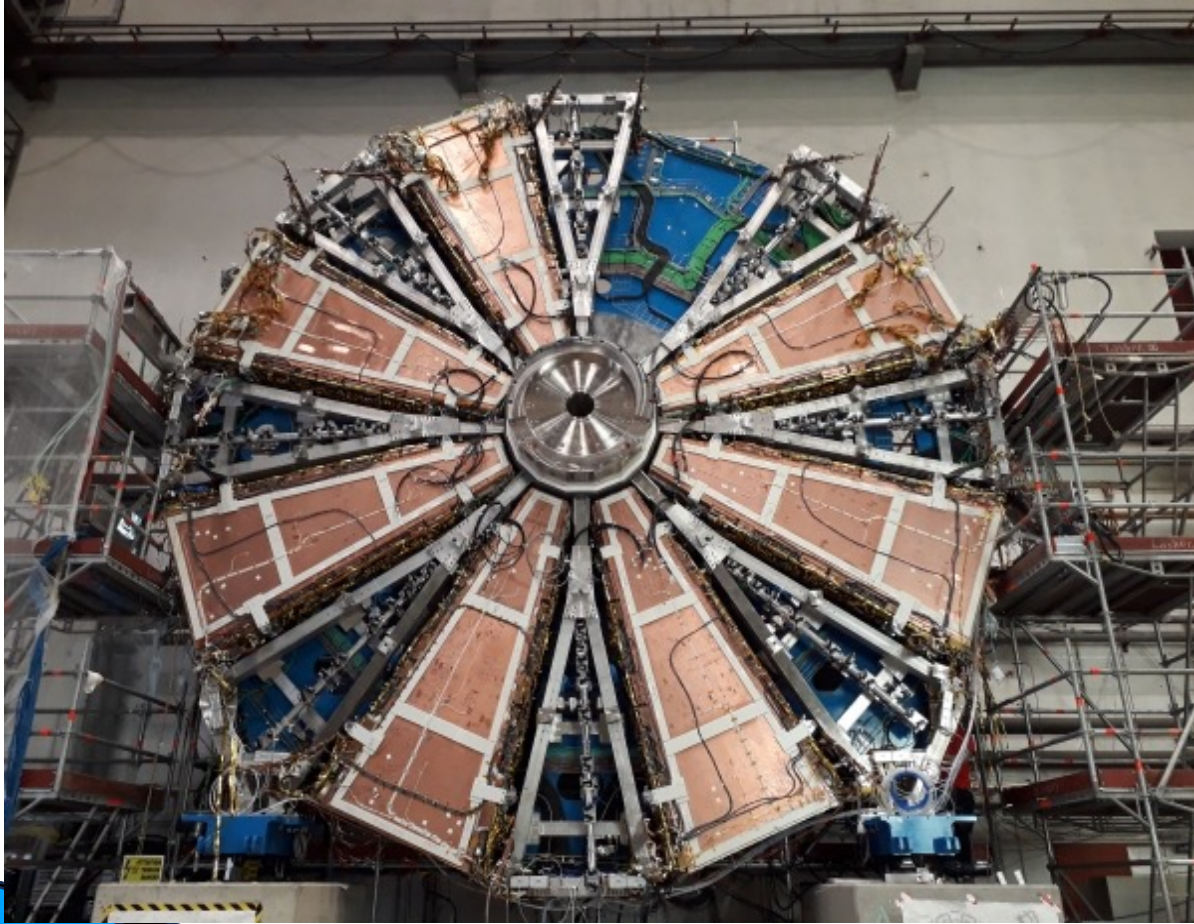
Sketch of the light-mask-lens-camera system



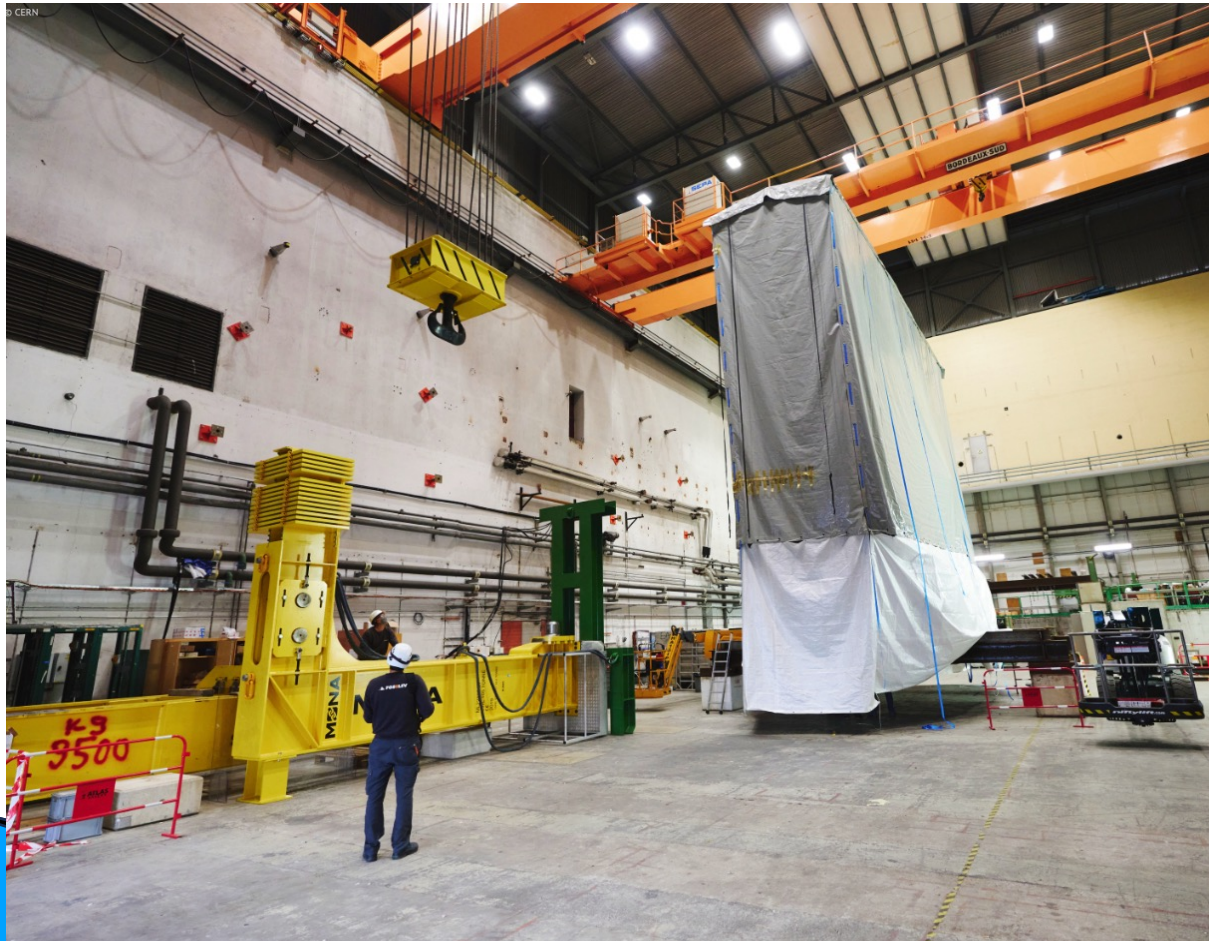
Intermezzo



Intermezzo

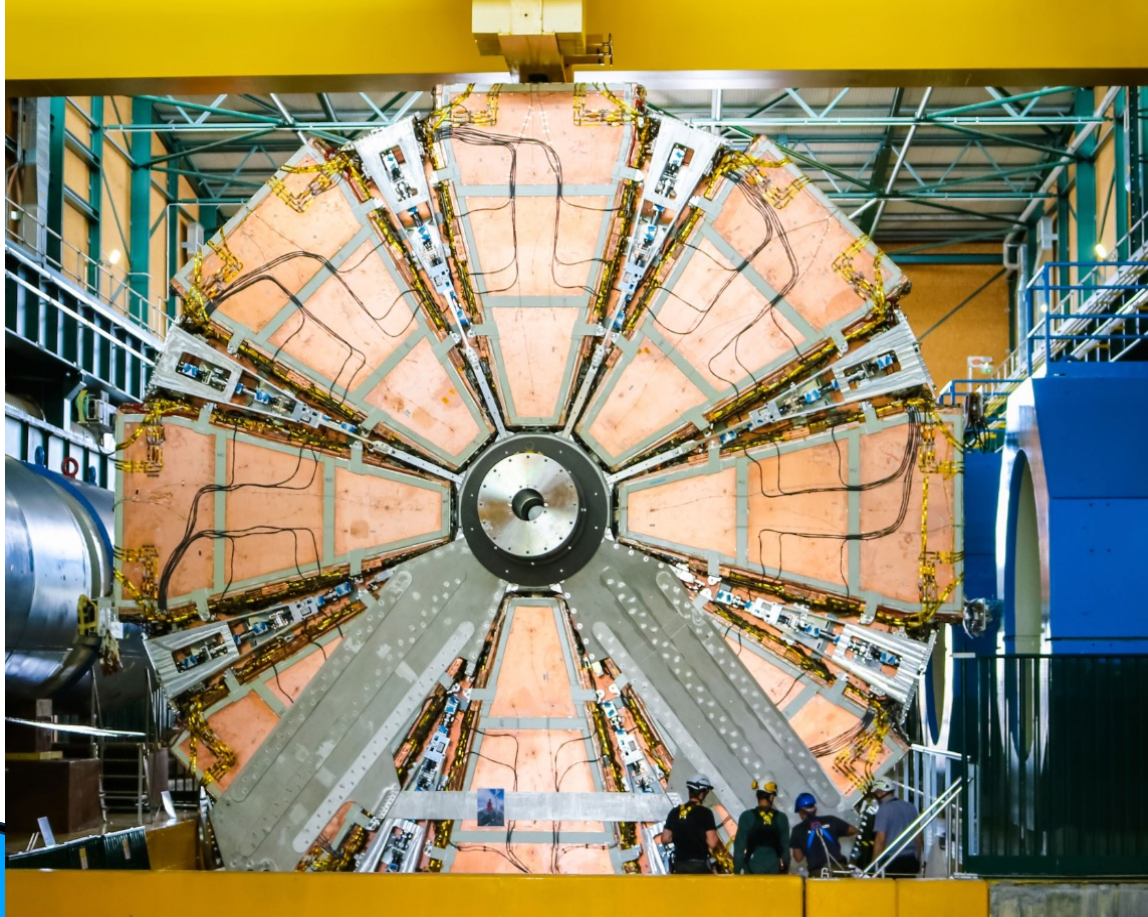


Intermezzo

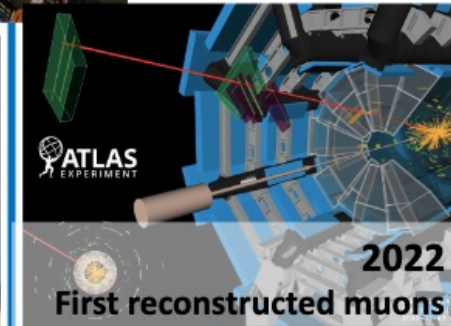
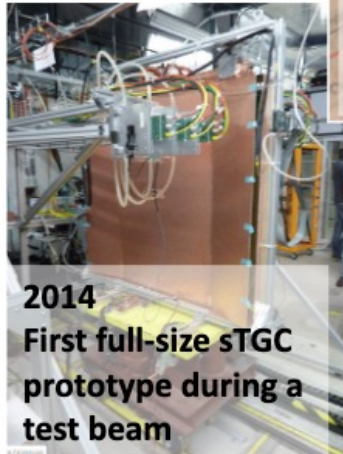
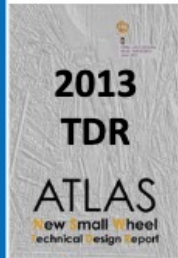
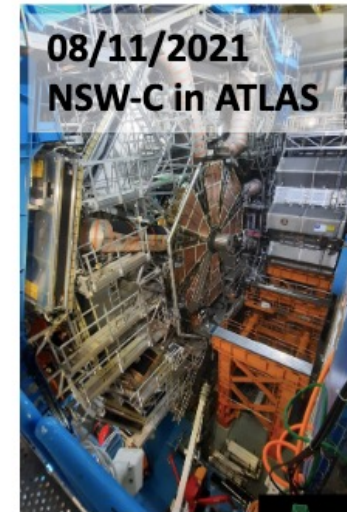
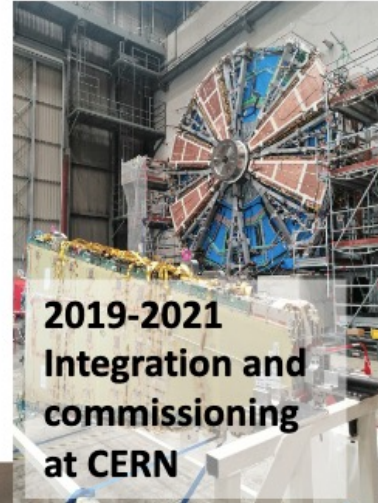
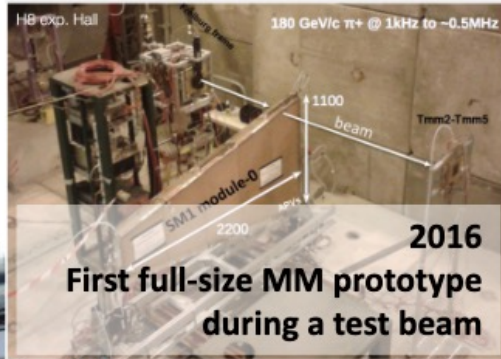
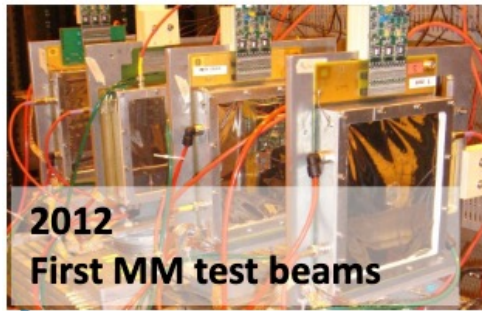


17.05.24

Intermezzo



From concept to reality: from TDR to data taking

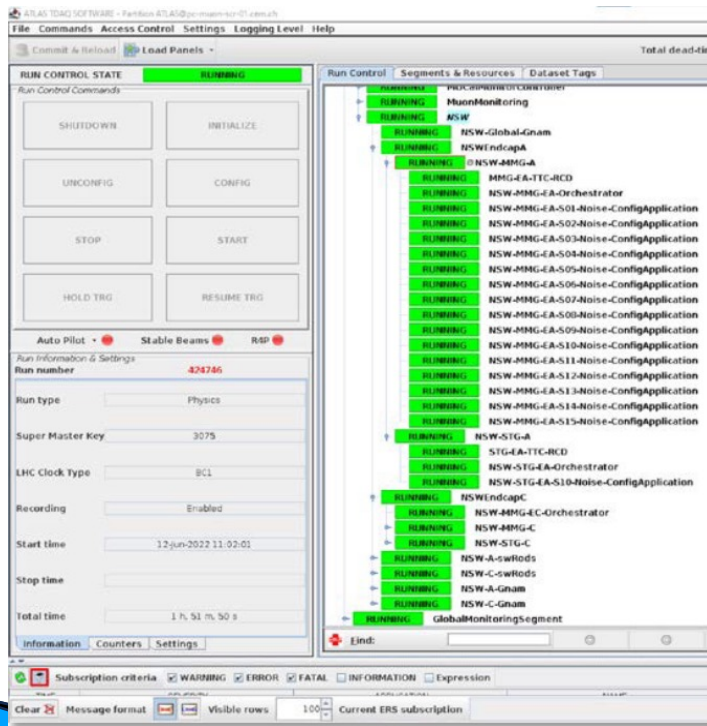


<https://cds.cern.ch/record/2886755/files/ATL-MUON-SLIDE-2023-686.pdf>

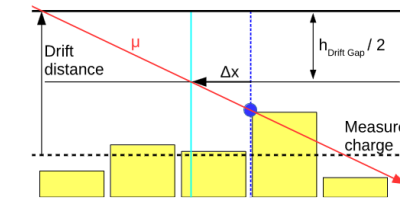
- 10 years from the writing of the TDR to the first recorded events in Run3. R&D on detectors and elx started even earlier

Integration in ATLAS: DAQ, DCS, Muon reconstruction

- NSW integrated into ATLAS systems at start of Run3: DAQ, Detector Control System and ATLAS Muon reconstruction software

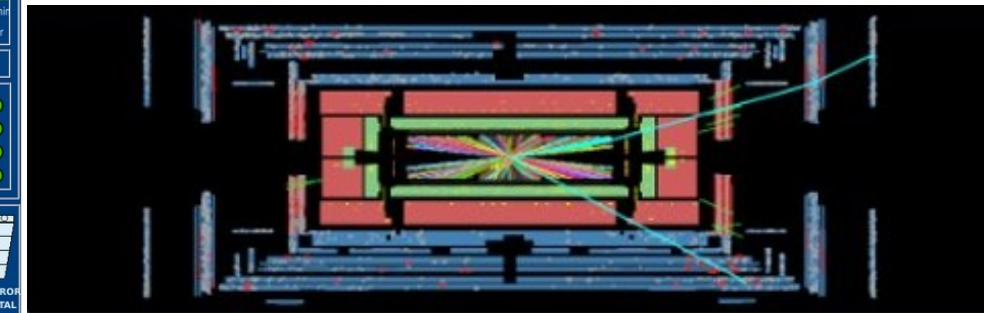
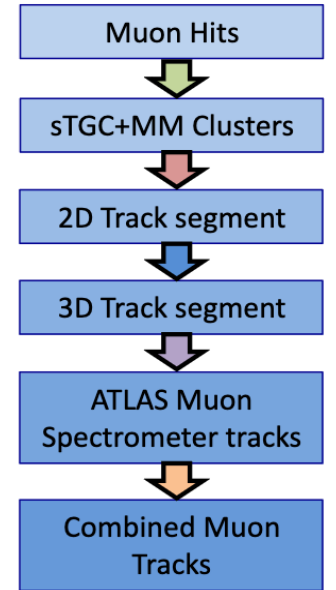


From detector hits to reconstructed muon



Cluster position reconstructed with charge centroid.
Improved methods under development

<https://cds.cern.ch/record/2889022>



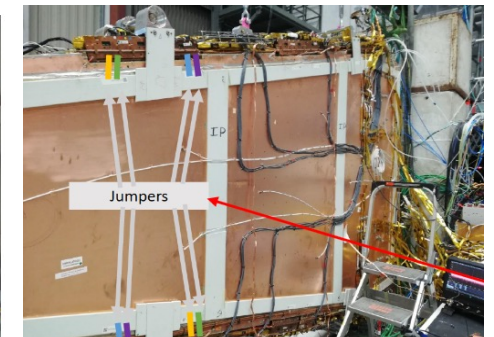
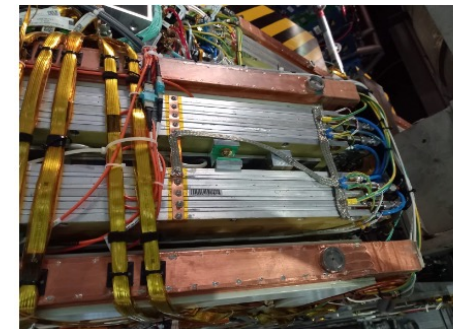
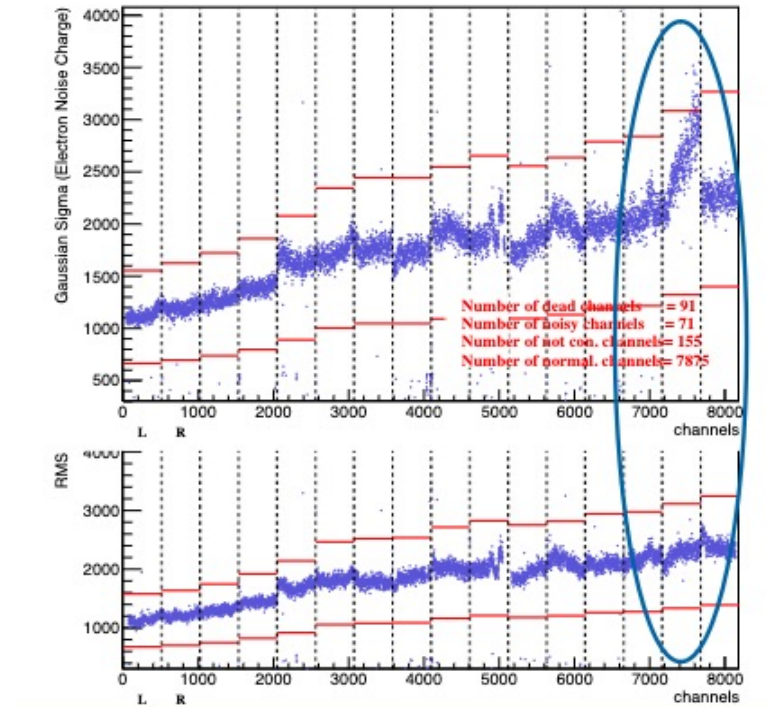
- 2022 commissioning year: understanding the system; discovering problems
- Since 2023 fully contributing to ATLAS trigger and the physics analysis program

Main issues during commissioning and operation

- Large system --> many problems; complex system --> tricky problems
- Selected short-list of issues discovered during NSW commissioning and operations
 - Electronic Noise
 - DAQ instabilities

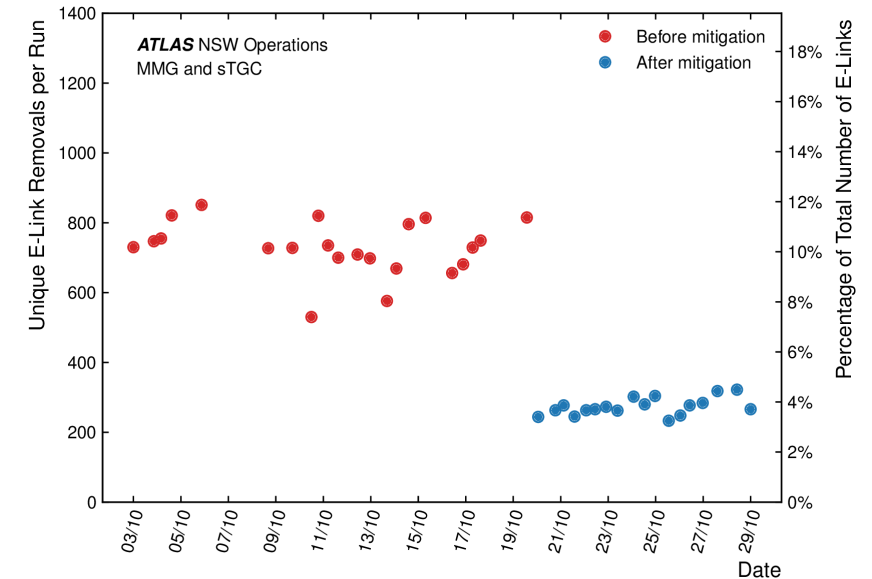
Main issues during commissioning and operation

- Large system --> many problems; complex system --> tricky problems
- Selected short-list of issues discovered during NSW commissioning and operations
 - Increase of electronic noise on both sTGC and MM
 - DAQ instabilities
- Increase of noise observed during test of sectors after mounting on the wheel in 188
- Identified to mostly come from LV power supply and sub-optimal grounding
- Actions taken solved the problem on surface:
 - Refurbishment of LV power supply (additional filters added)
 - Modification of grounding scheme and improvement of detector ground
 - Addition of Faraday cage on elx boards: required the dismounting of A-side Small sectors already mounted in the wheel
- After the installation in ATLAS discovered a remaining high noise level on the longest MM strips, correlated with the magnetic field. Still fighting against it, causing ~% of channels to be masked

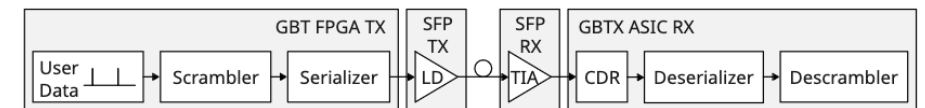


Main issues during commissioning and operation

- Large system --> many problems; complex system --> tricky problems
- Selected short-list of issues discovered during NSW commissioning and operations
 - Electronic Noise
 - **DAQ instabilities**
- Suffered from an instability affecting all the elx boards connected to a single optical link, pointing to GBTx transceiver issue
 - Bit errors in the GBTx data stream anti-correlated with the signal rate sent on the TTC e-links (high data rate --> low error rate)
 - **Added a mechanism to pulse an unused bit in the TTC frame --> successful mitigation implemented in 2023 for MM (200 kHz), in 2024 for sTGC (20 MHz)**
- NSW team worked closely with FELIX team and CERN GBTx group. Fruitful share of information with LHCb that observed similar issues
- NSW providing info and test elx to GBTx team who uncovered a bit in the scrambler (randomizer) logic: under certain conditions it deadlock and sends out all 0s for a certain period
- **Final mitigation: pseudo-random pulsing at 20 MHz of an unused bit (ECOR) in FELIX firmware**
- Remaining marginal instabilities attributed to the known [VTRx ROSA flex outgassing problem](#). Accessible VTRx on NSW replaced in 23/24 YETS

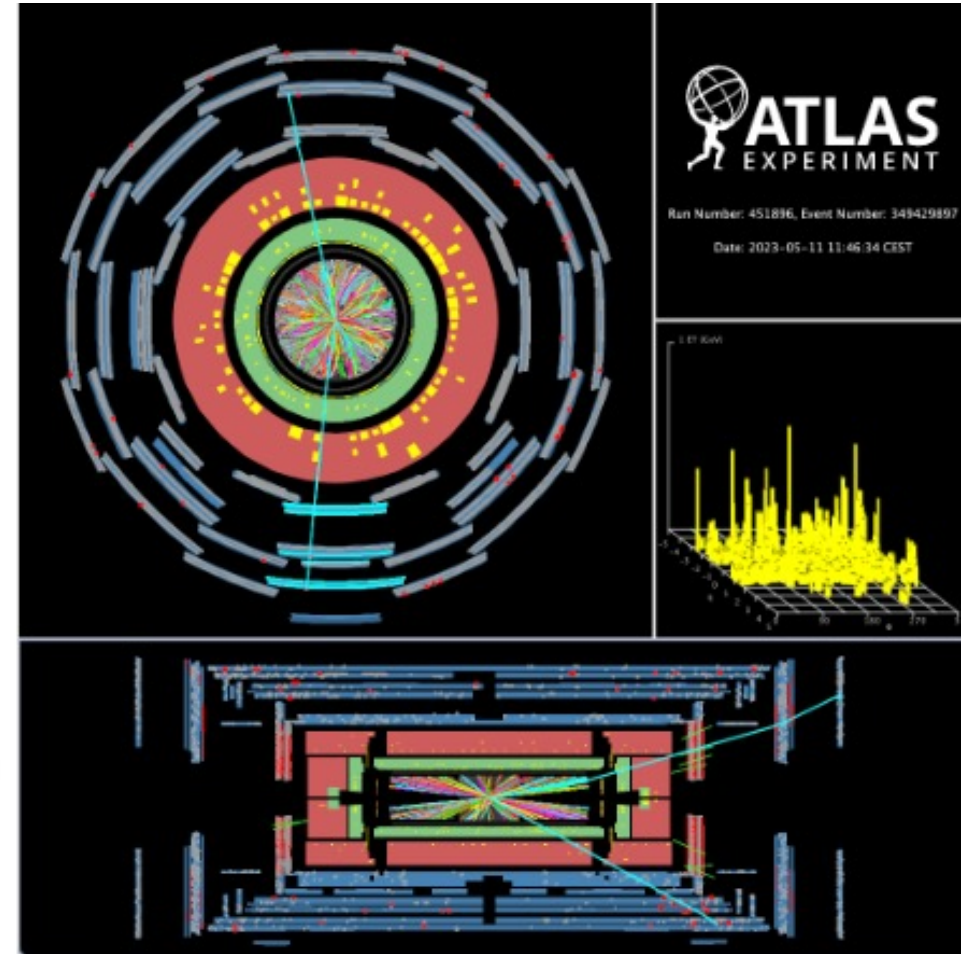
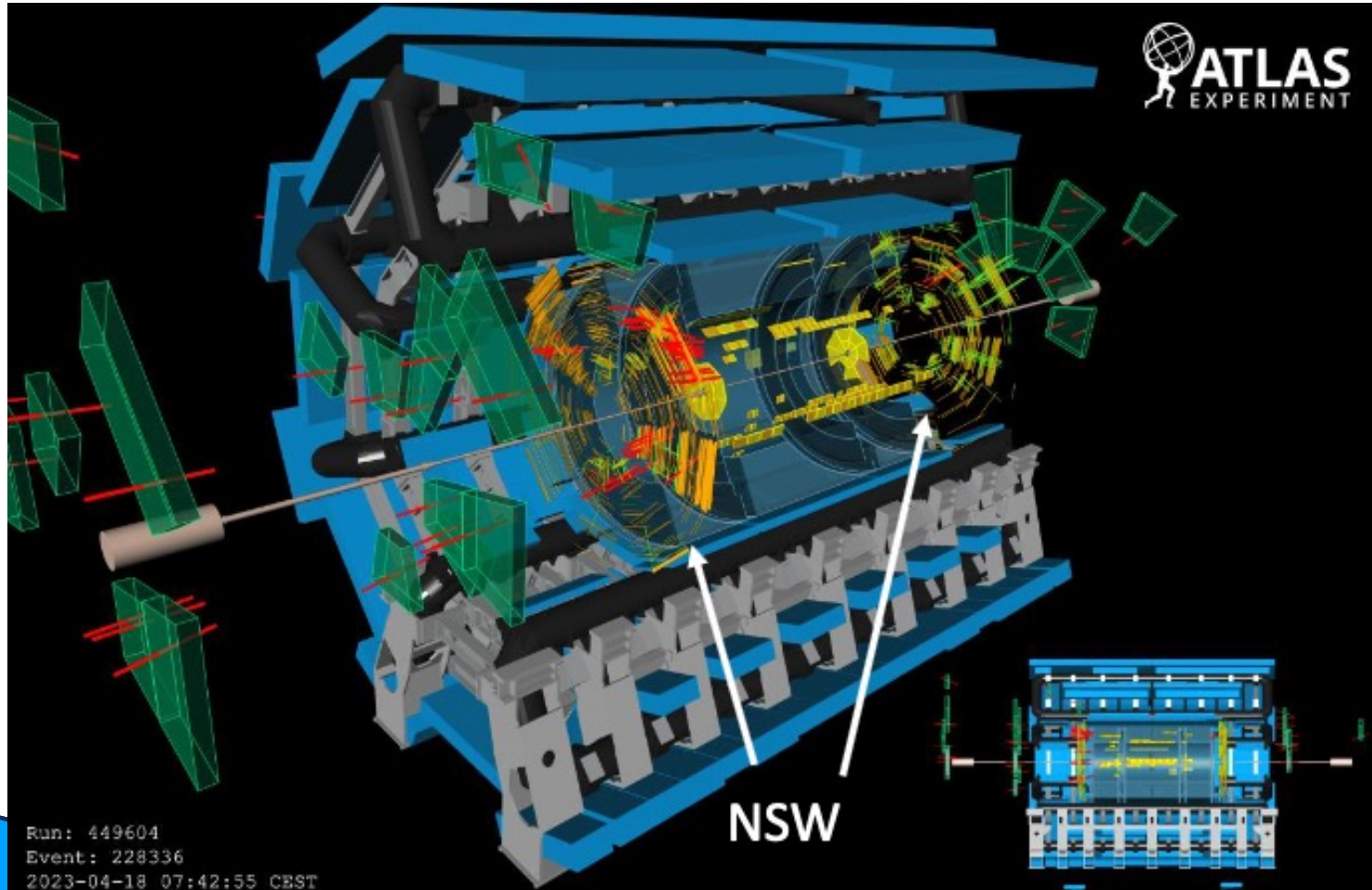


Number of unique E-link removed during runs in October 2023 before (red) and after (blue) the mitigation for MM. Mitigation for sTGC has been implemented in 2024



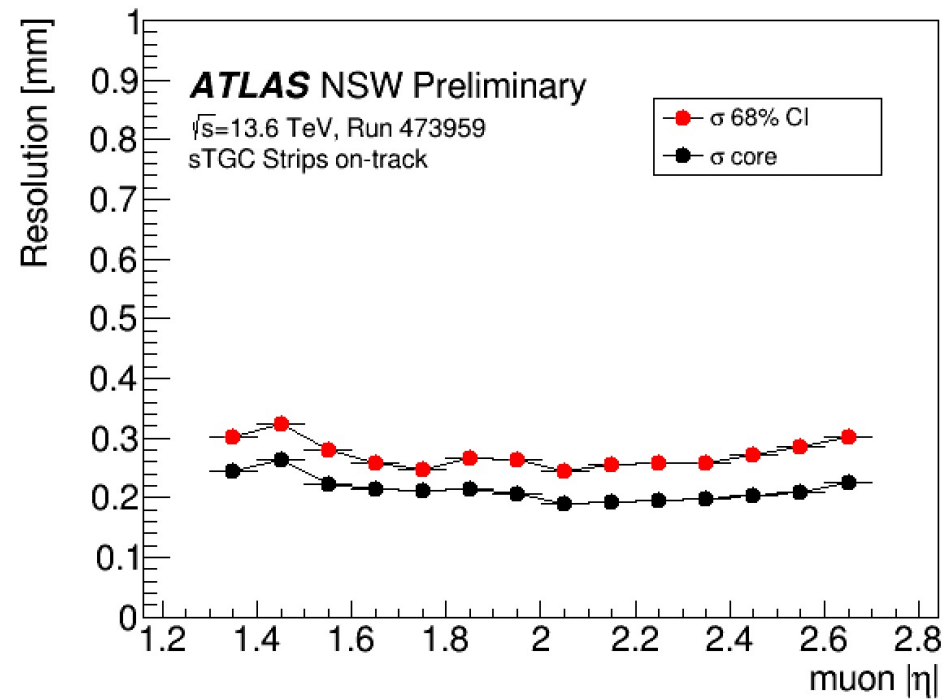
Simplified schematic diagram of the GBTx system component contributing to the issue. Details: [GBTx Scrambles Deadlock Application Note](#)

NSW Performance

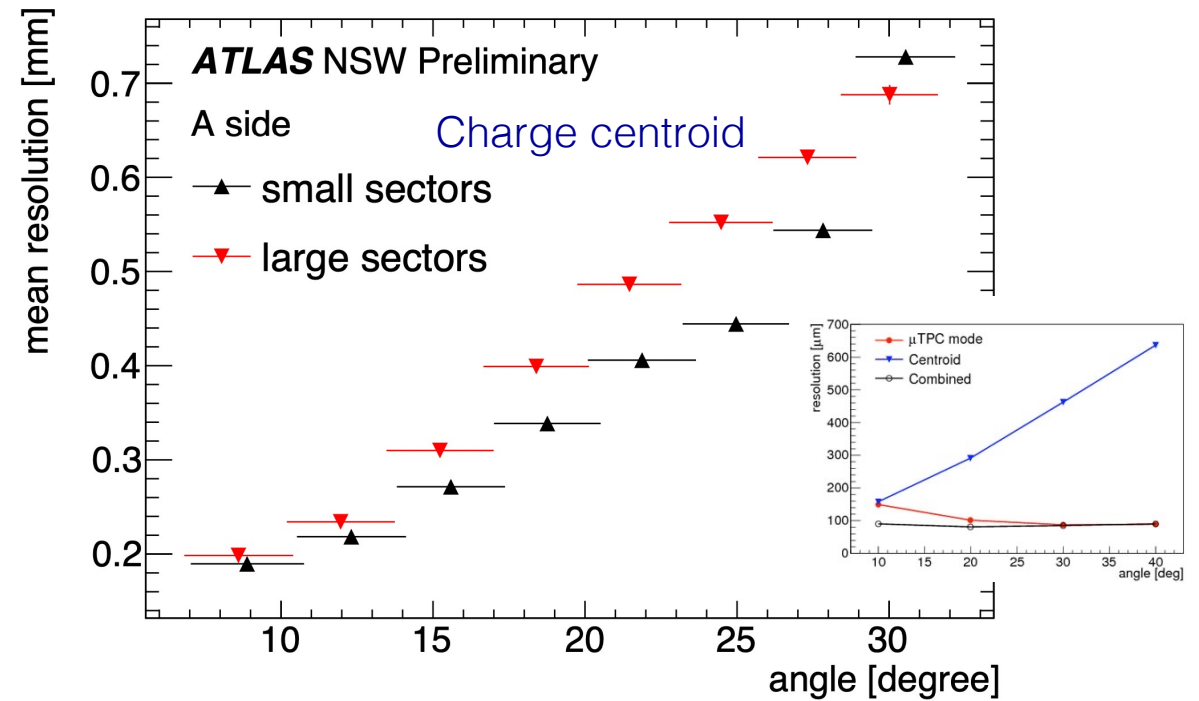


Hit-track residuals

- sTGC



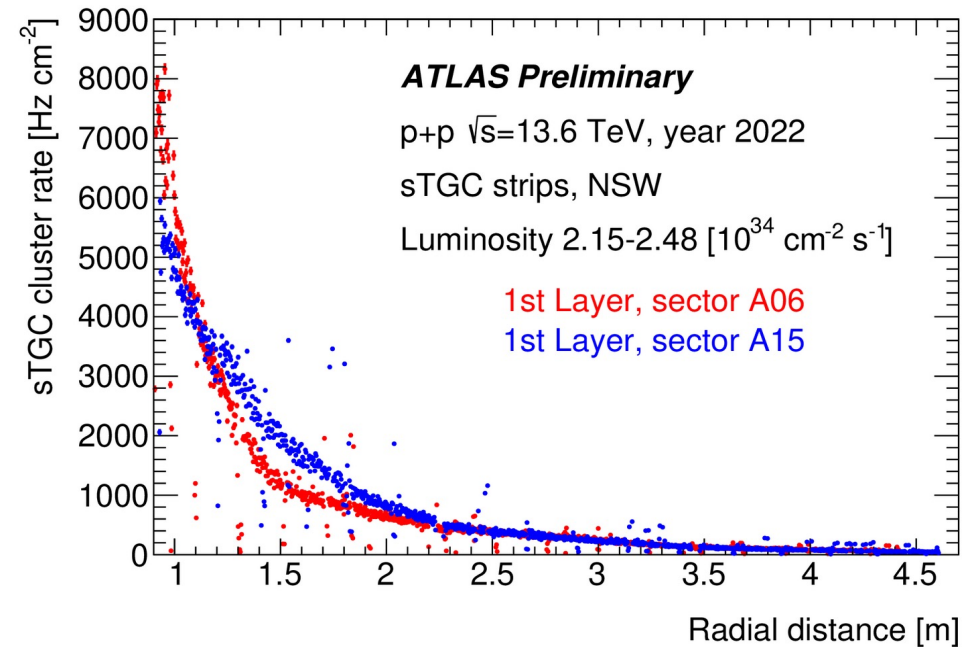
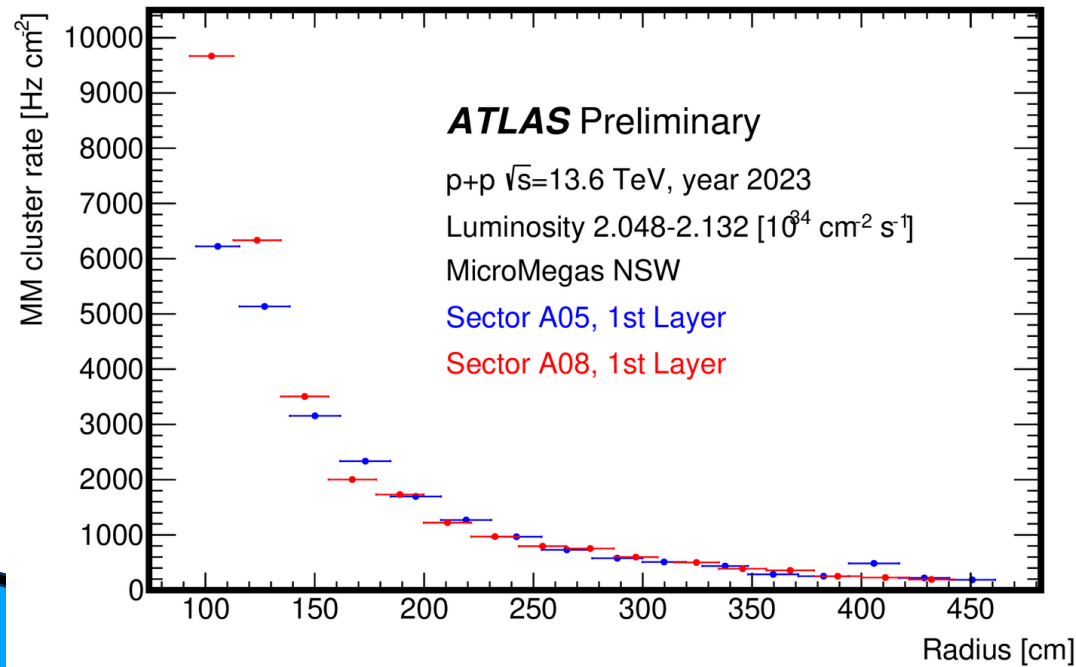
- MMG



Resolution obtained with cluster centroid method. Better algorithm can be used or sTGC;
time information (μ TPC) can be exploited for MM particularly at small $|\eta|$ (large angles)

Rate measurements

- Rate measurement vs distance from beam (radius) in 1st layers (closest to interaction point)
- 6-10 kHz/cm² at L = 2.2 x 10³⁴ cm⁻²s⁻¹, quickly reducing with radius
- At HL-LHC (5 x 10³⁴ cm⁻²s⁻¹) will hit the requirement of 20 kHz/cm² in the most forward strips



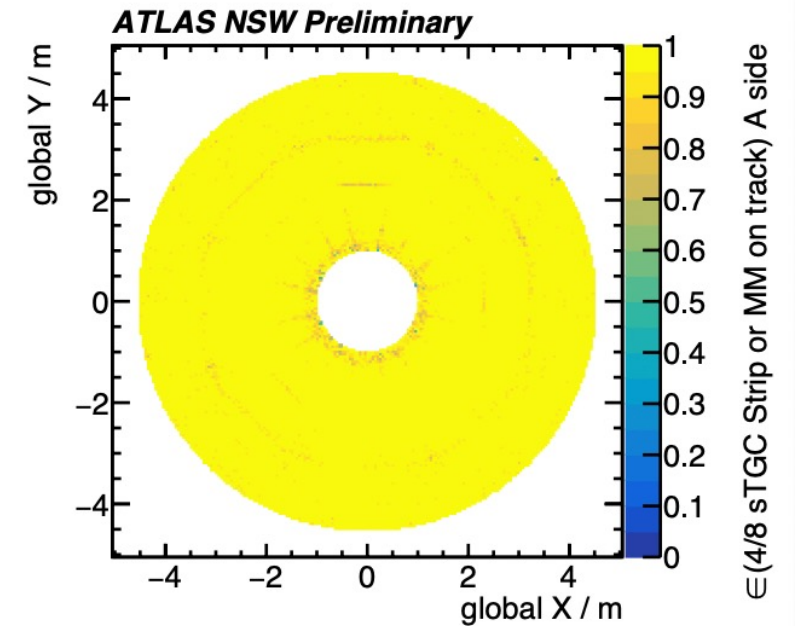
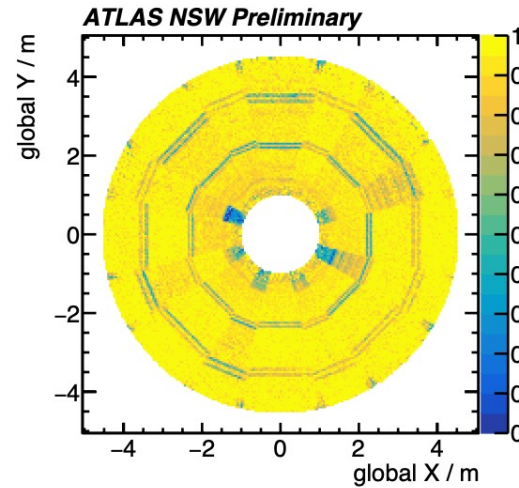
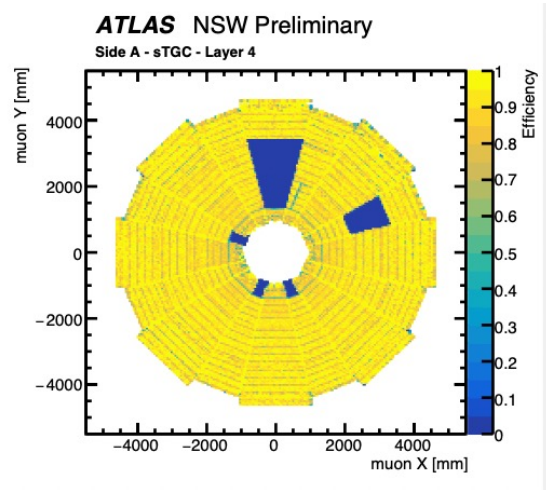
Efficiency: hit-on-track

- Single layer

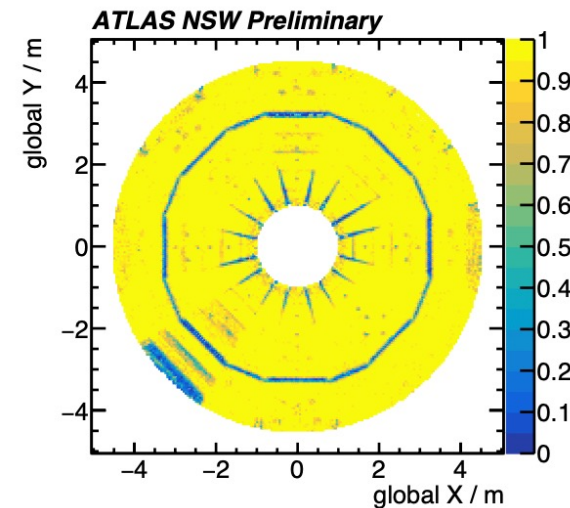
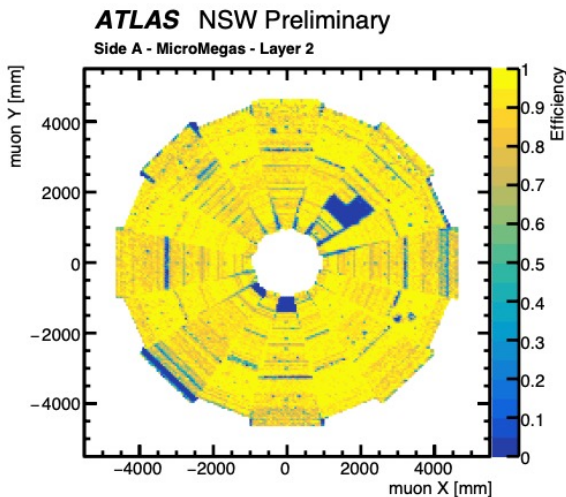
- 4/8 layers

- 4/8 sTGC or MM layers

- sTGC



- MM



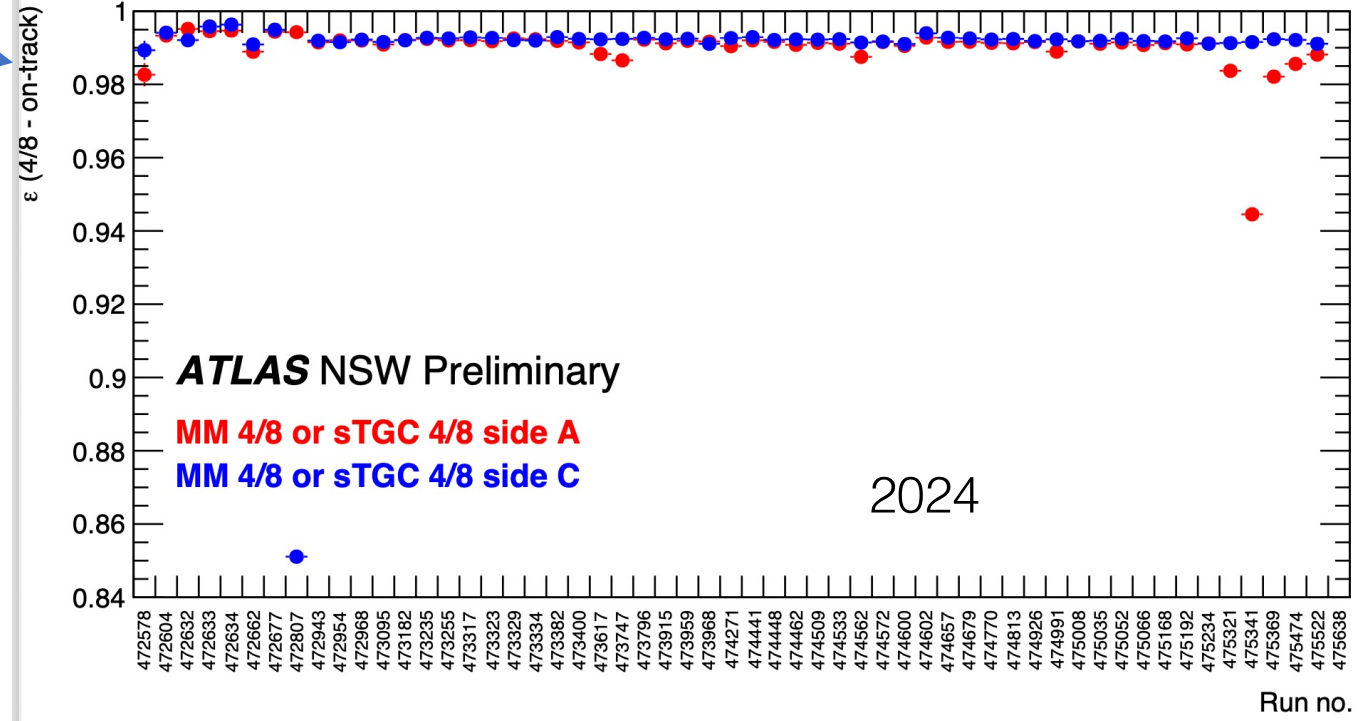
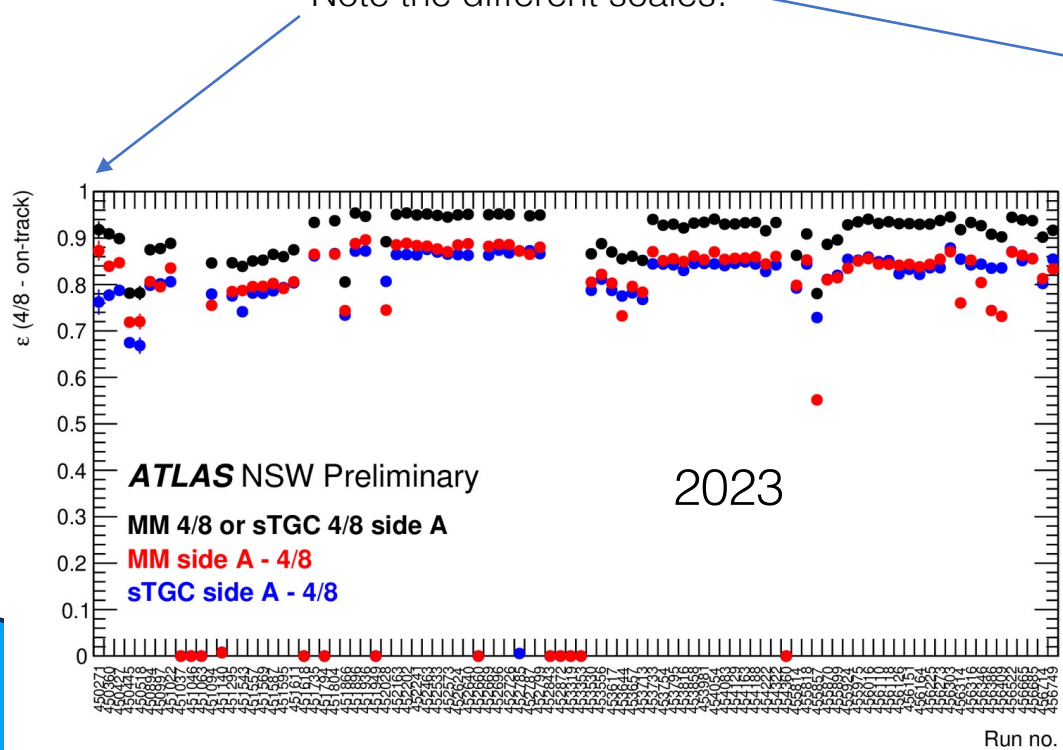
Single layer efficiency affected by hw failures (elx, LV or HV) and by runtime issues (HV trips, DAQ instabilities etc)

The NSW redundancy provides a fully efficient detector system

Efficiency

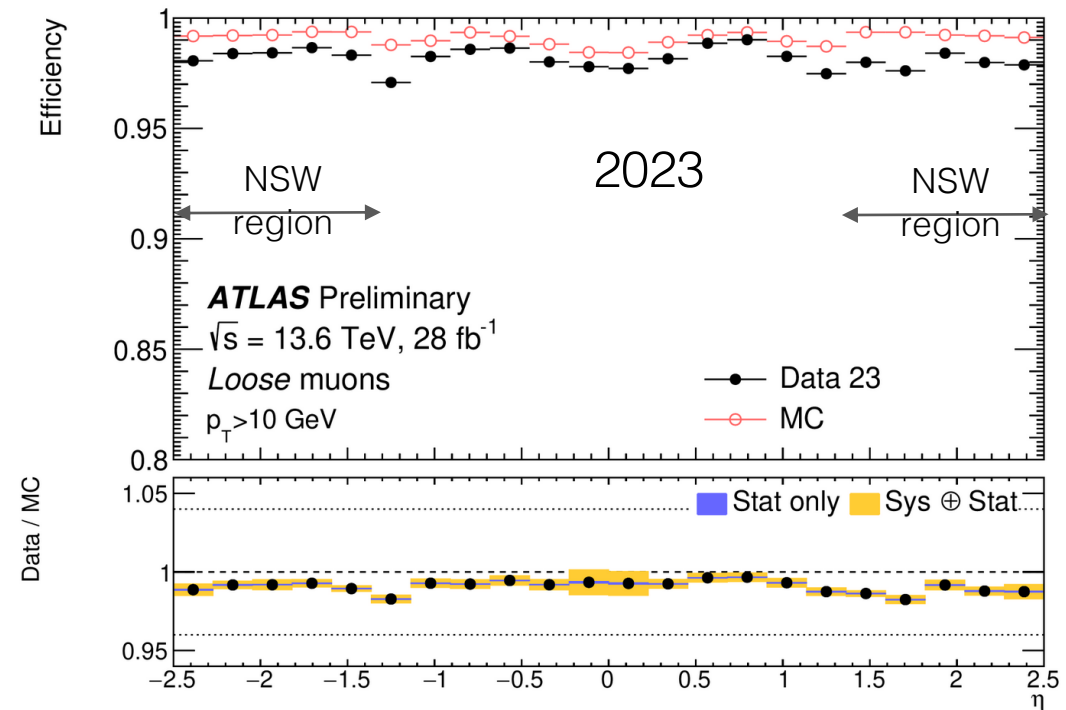
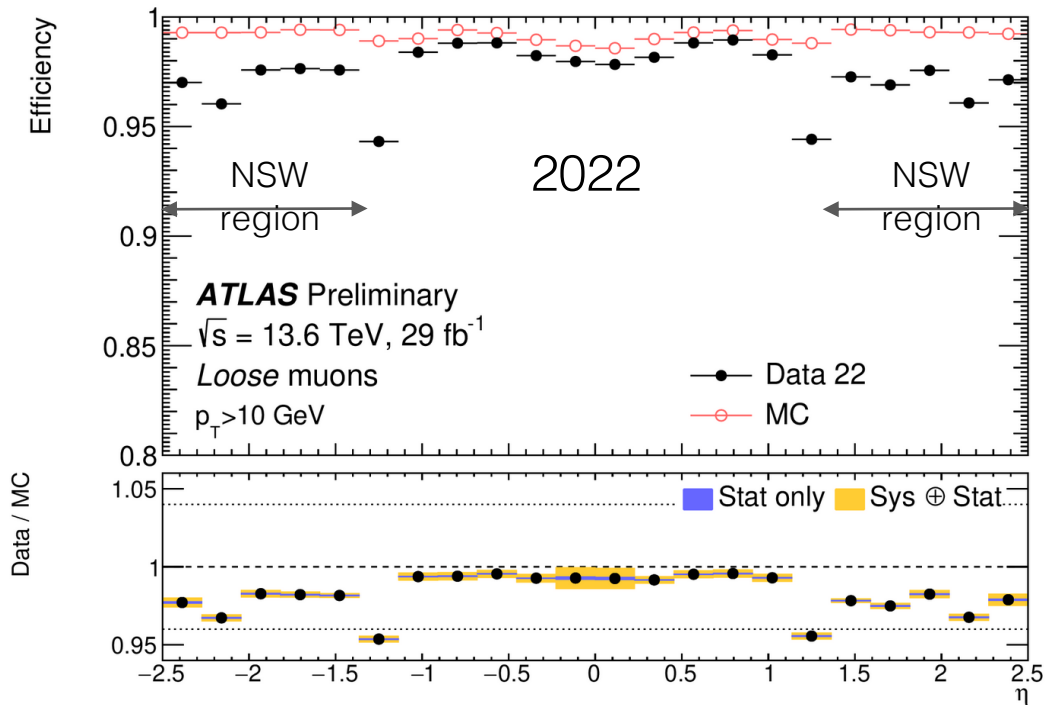
- Efficiency in 2023 improved compared to 2022 but still below expectations
- Issues: hw failures and DAQ instabilities not mitigated yet (only done during Pb-Pb collision runs in fall)
- In 2024 the NSW performance are matching the requirement!

Note the different scales!



Reconstruction

- Big improvement in 2023 muon reco and id efficiency in Z events compared to 2022: >98% in NSW region
- Further improvement expected in 2024 thanks to: better alignment, enhanced system stability



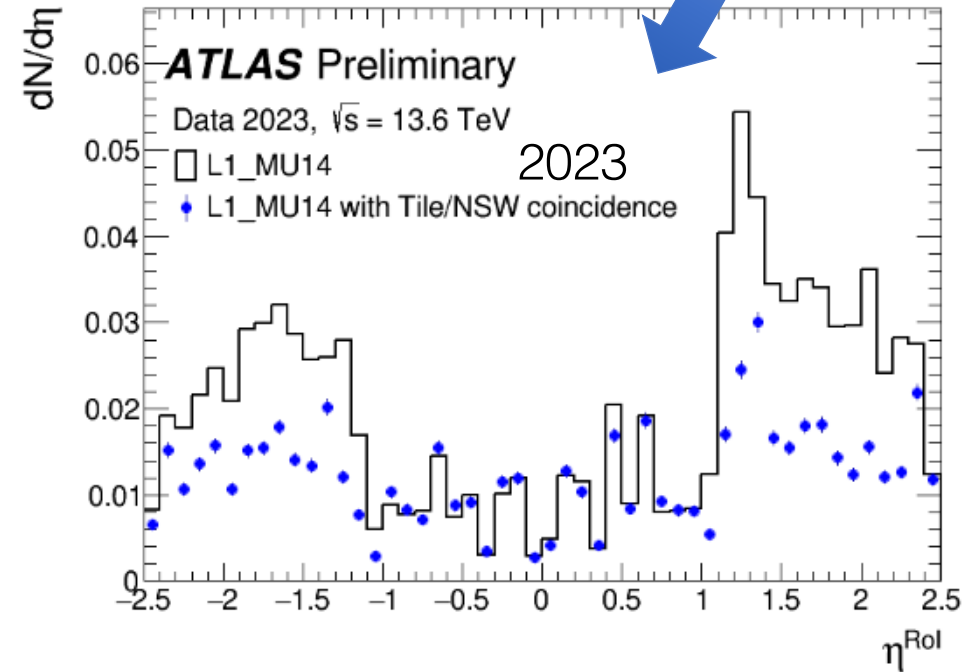
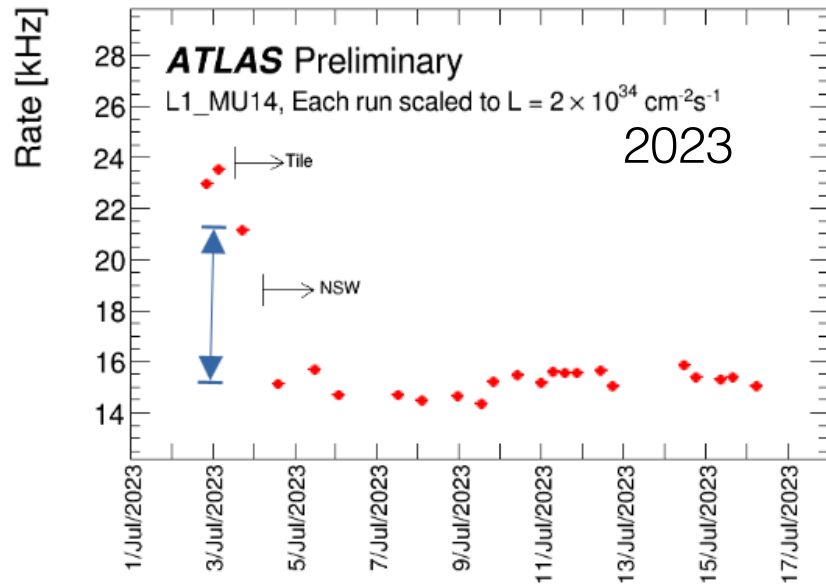
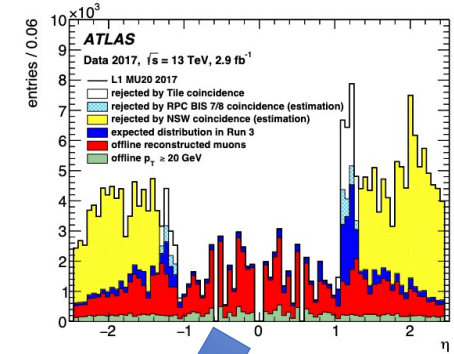
Efficiency for reconstructing and identifying muons with transverse momentum (p_T) above 10 GeV, as a function of the muon pseudorapidity (η). The measurement is based on $Z \rightarrow \mu^+ \mu^-$ candidate events from data collected in 2022 (left) and 2023 (right)

Trigger

- Activation of the NSW sTGC PAD trigger in 2023
- 68% of PAD trigger sectors included: L1_MU14 trigger rate reduced by ~6 kHz

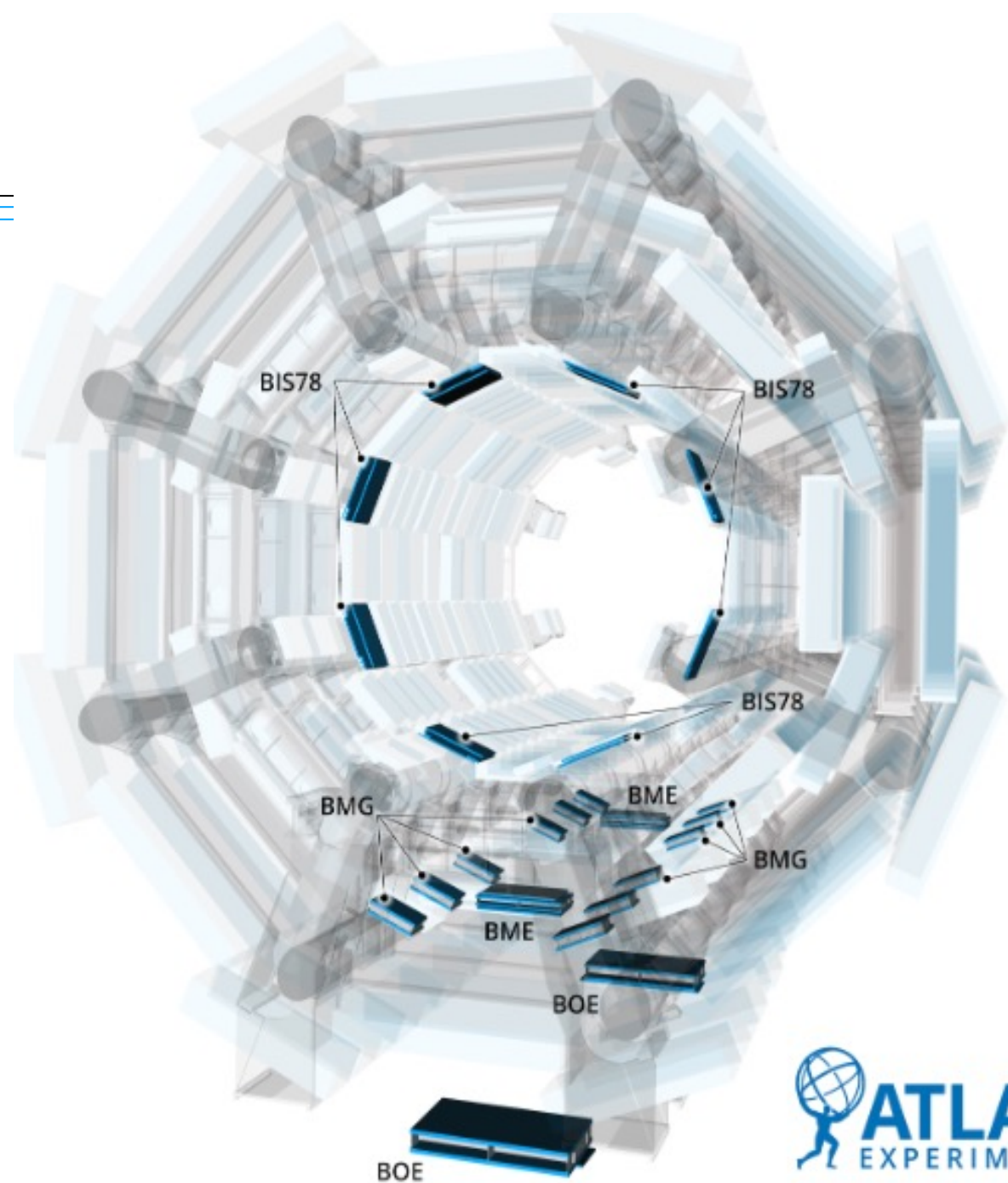
The NSW trigger does the job!

- Additional trigger sectors have been included in 2024 further improving the rejection power
- Goal to reach ~100% of the sTGC PAD trigger sectors and include the MM trigger soon in 2024
- sTGC strip trigger will come later (PhaseII)



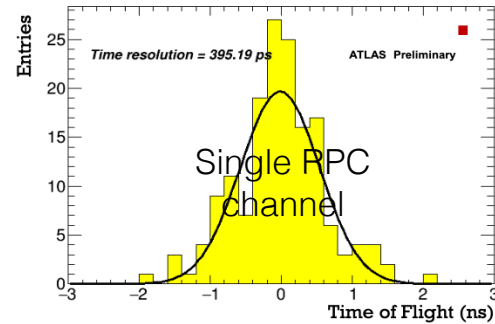
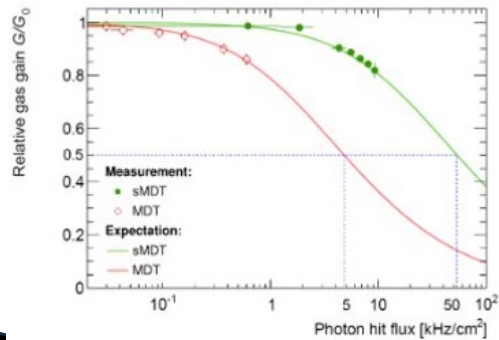
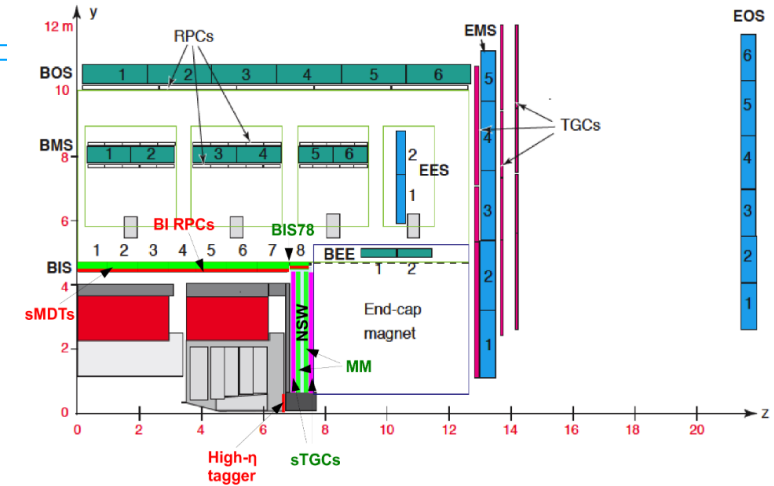
Muon System Phase1 Upgrade

- BIS78 sMDT+RPC

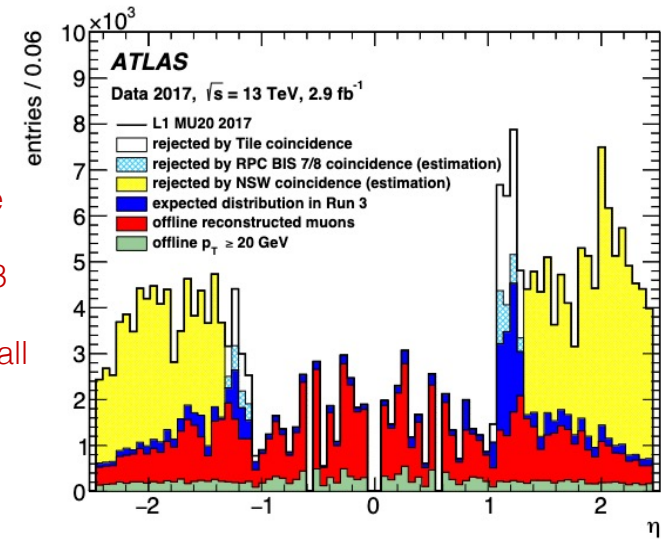


BIS78

- Run3: Replace BIS7&BIS8 MDT on side A with BIS78 sMDT+RPC assembly to improve tracking and provide trigger capability. Pilot project in view of the Phasell Muon barrel upgrade with sMDT and new RPC technology
- Motivation similar to NSW: reduce fake trigger rates in the barrel-endcap transition region $1.1 < |\eta| < 1.27$ for Small sectors
- Small Monitored Drift Tubes (sMDT): smaller tube diameter of ATLAS MDT (15 vs 30 mm)
 - Shorter drift time -> higher rate capability
 - Compact dimension
 - Gas: Ar:CO2 70:30 at 3 bar
- The BIS78 RPC detectors are of a new generation
 - Thinner (1.2 mm) resistive plates; lower resistivity to increase the rate capability
 - Smaller gas gap (1 vs 2 mm) for an improved time response, 3 vs 2 independent gaps
 - Smaller signals: need of a high-amplification, low-noise, fast FE Elx



To limit the large environmental impact of the RPC gas in ATLAS the operating gas has been changed in 2023 from C2H2F4:iC4H10:SF6 (94.7:5:0.3) to C2H2F4:CO2:iC4H10:SF6 (64:30:5:1) for all the ATLAS RPC detectors.



- BIS78-A sMDT fully integrated in ATLAS, while RPC with new FE elx and new DAQ chain oriented to Phasell still under commissioning

A look to Run4

New Inner Tracker (ITk)

All silicon with 9 layers up to $|η|=4$
Less material finer segmentation
Improve vertexing, tracking, b-tagging

Trigger and DAQ Upgrade

Single level Trigger with 1 MHz output (x 10 current)
Improved DAQ system with faster FPGAs

New High Granularity Timing Detector

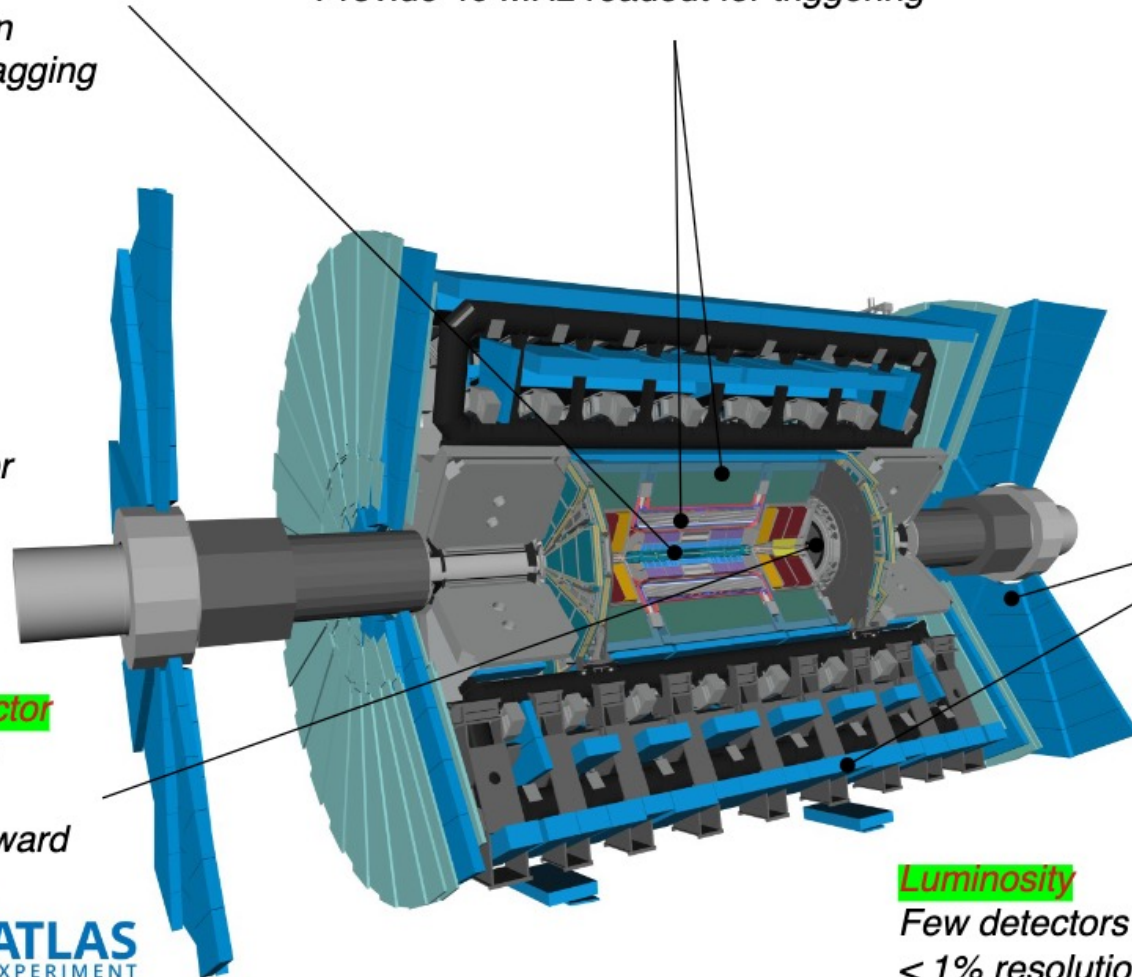
Precision track timing (30 ps) with LGAD in the forward region.
Improve pile-up rejection in the forward region

Calorimeter Electronics

On-detector electronics upgrades of LAr and Tile Calorimeters
Provide 40 MHz readout for triggering

Legacy detectors

New detectors



Muon Detector

Upgrade of the detector electronics for new T/DAQ system
Upgrade of inner barrel chambers with new RPC and sMDT
Improve trigger efficiency and momentum resolution, and reduced fakes

Luminosity

Few detectors devoted to luminosity to get < 1% resolution as ATLAS has in Run2:
LUCID-3, ITk-BCM', HGTD



Conclusions

- New Small Wheel has been a challenging project, with many issues of all kinds found along the way
- Completed right on time to be installed for the start of Run3, it is now successfully contributing to the Physics program of ATLAS
- This success is owed to a fantastic team of physicists, engineers and technicians who dedicated their best energies to the project, for years
- There is still room for improvement to exploit the full NSW potential in the HL-LHC phase
- ATLAS is preparing an even more ambitious upgrade project for Phase II to continue to be a reference for the HEP in the next decades



'We're in hell right now, gentlemen, believe me. And we can stay here, get the shit kicked out of us, or we can fight our way back into the light.'

Al Pacino (alias Tony D'Amato), *Any Given Sunday*

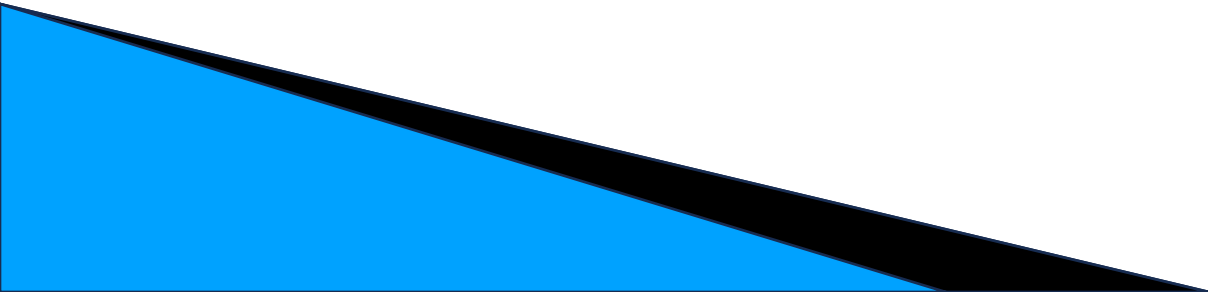
Thank you



- Atsuhiko Ochi (1969-2024)

- In memory of Stephanie, Florian, Guido, Stefano, Atsuhiko who all contributed to the NSW and left too early the large experiment called Earth

BACKUP

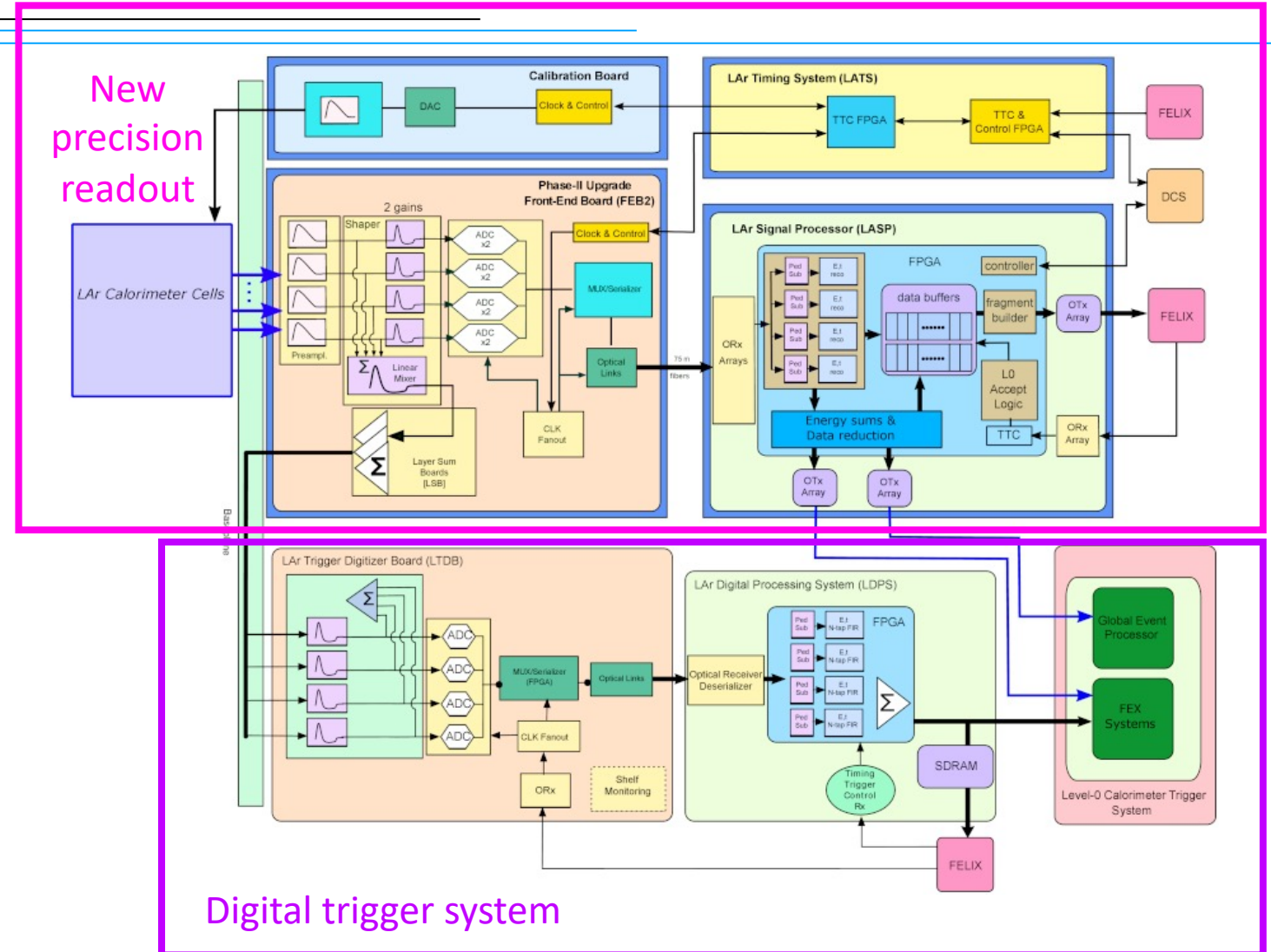


References

- [1] ATLAS Liquid Argon Calorimeter Phase-I Upgrade :
Technical Design Report
<https://cds.cern.ch/record/1602230/files/ATLAS-TDR-022.pdf>
- [2] The Phase-I trigger readout electronics upgrade of the
ATLAS Liquid Argon calorimeters
<https://dx.doi.org/10.1088/1748-0221/17/05/P05024>
- [3] The ATLAS Trigger System for LHC Run 3 and Trigger
performance in 2022
<https://arxiv.org/abs/2401.06630>
- [4] The ATLAS Experiment at the CERN Large Hadron Collider: A
Description of the Detector Configuration for Run 3 :
<https://atlas.web.cern.ch/Atlas/GROUPS/PHYSICS/PAPERS/GENER-2019-02/>

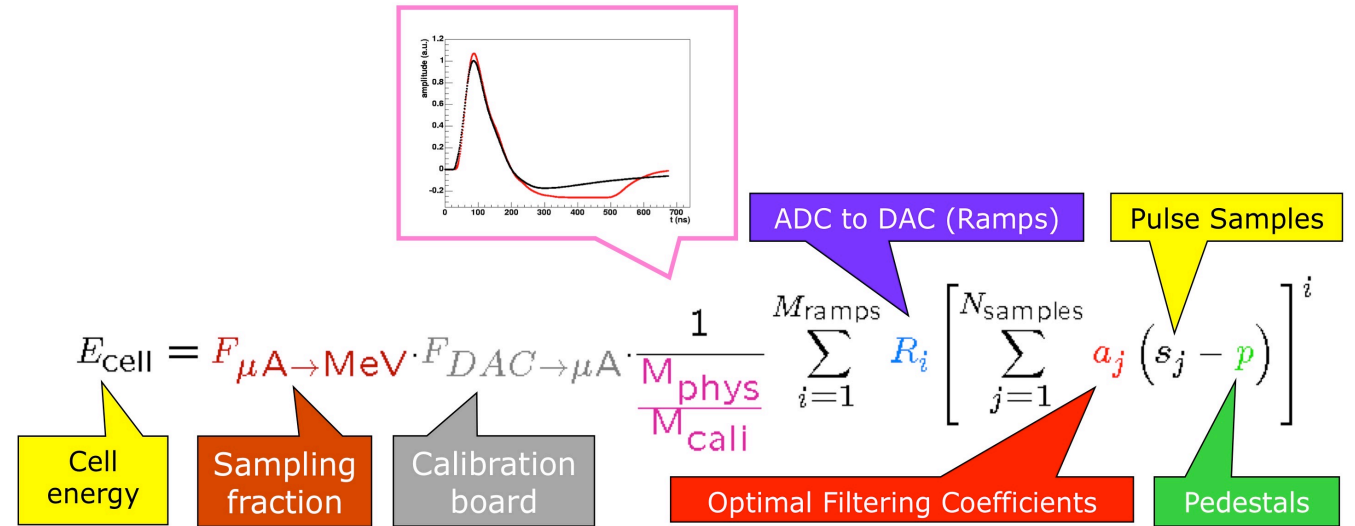
LAr Phase-II upgrade

- Exchange of main readout electronics
 - New FEB2 for digitisations @40MHz and streaming of cell signal
 - New processing board (LASP) to compute cells energies and send to both Global trigger (40MHz) and DAQ (1MHz)
 - New timing and calibration system
- Digital Trigger system shall be adapted to new data taking conditions
 - 1 MHz of L0-Accept
 - New powering schema of Front-End electronics



Energy reconstruction

- Using 4 samples since Run 2 in the Main readout and in the LATOME
- Optimal Filtering Coefficients (OFCs) are derived from the ideal pulse shape & noise autocorrelation
=> Measure regularly in calibration



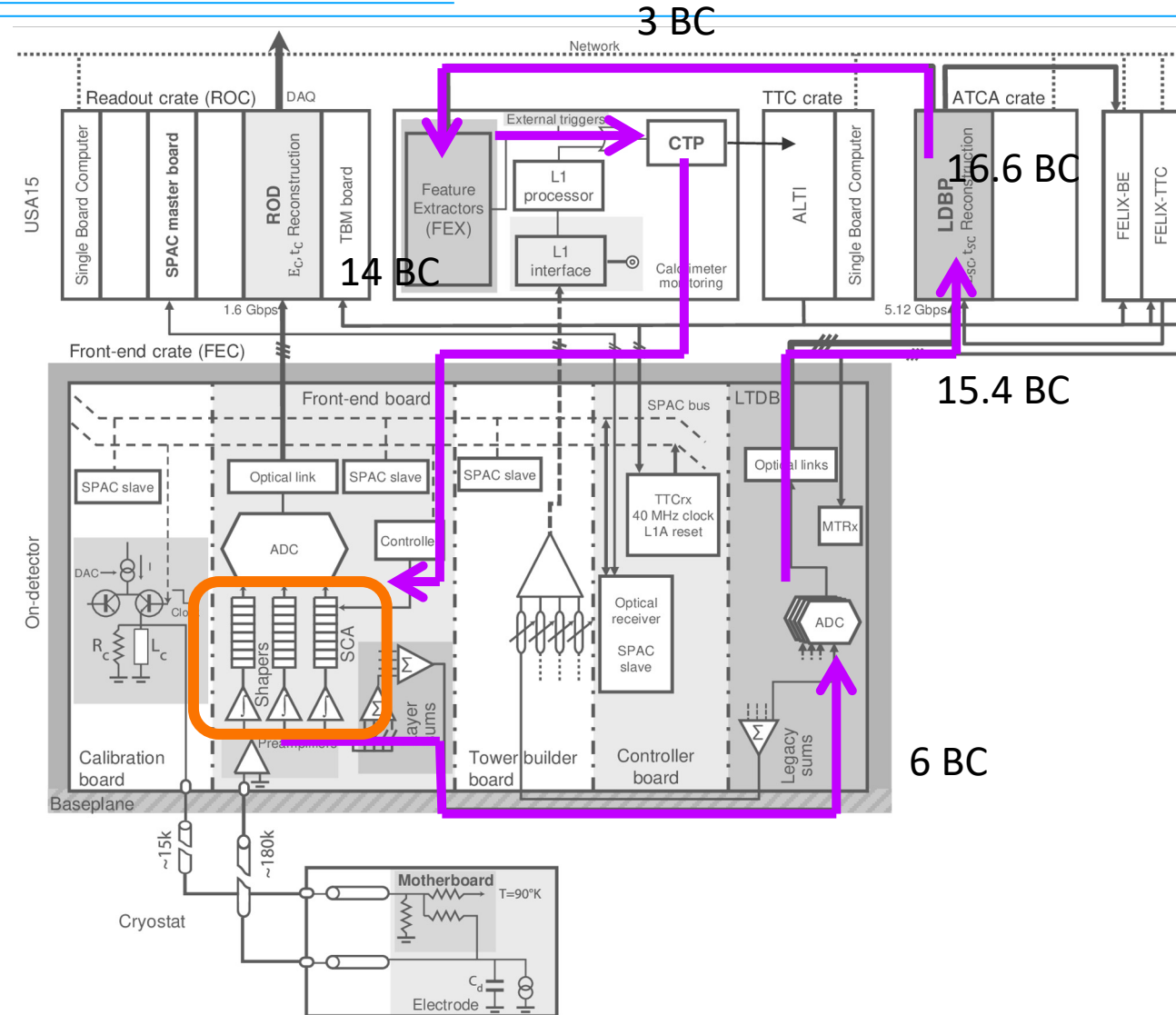
The above formula describes the LAr electronic calibration chain (from the signal ADC samples to the raw energy in the cell). Note that this version of the formula uses the general M_{ramps} -order polynomial fit of the ramps. We use a linear fit as the electronics are very linear, and we only want to apply a linear gain in the DSP in order to be able to undo it offline, and apply a more refined calibration. In this case, the formula is simply:

$$E_{\text{cell}} = F_{\mu\text{A} \rightarrow \text{MeV}} \cdot F_{\text{DAC} \rightarrow \mu\text{A}} \cdot \frac{1}{\frac{M_{\text{phys}}}{M_{\text{call}}}} \cdot R \left[\sum_{j=1}^{N_{\text{samples}}} a_j (s_j - p) \right]$$

Latency

| | Latency | | Sub-total [BCs] | Total [BCs] |
|---|---------|-------|-----------------|-------------|
| | [ns] | [BCs] | | |
| Time-of-flight at $\eta = 2$ | 15.0 | 0.6 | | |
| Cable to pulse preamplifier | 30.0 | 1.2 | | |
| Preamplifier, shaper, and linear mixer | 21.6 | 0.9 | 2.7 | 2.7 |
| LTDB | 153.7 | 6.1 | 6.1 | 8.8 |
| Optical fiber cable (77 m) LTDB to LDPB | 385.0 | 15.4 | 15.4 | 24.2 |
| Deserializing and descrambling | 81.1 | 3.2 | | |
| BCID aligning | 28.2 | 1.1 | | |
| Channel remapping | 67.7 | 2.7 | | |
| Optimal filtering | 108.2 | 4.3 | | |
| Encoding and summing | 94.6 | 3.8 | | |
| Serializing | 35.7 | 1.4 | 16.6 | 40.8 |
| Optical fiber cable (15 m) LDPB to FEX | 75.0 | 3.0 | 3.0 | 43.8 |

MAX Latency $2.5\mu\text{s} = 100\text{BC}$

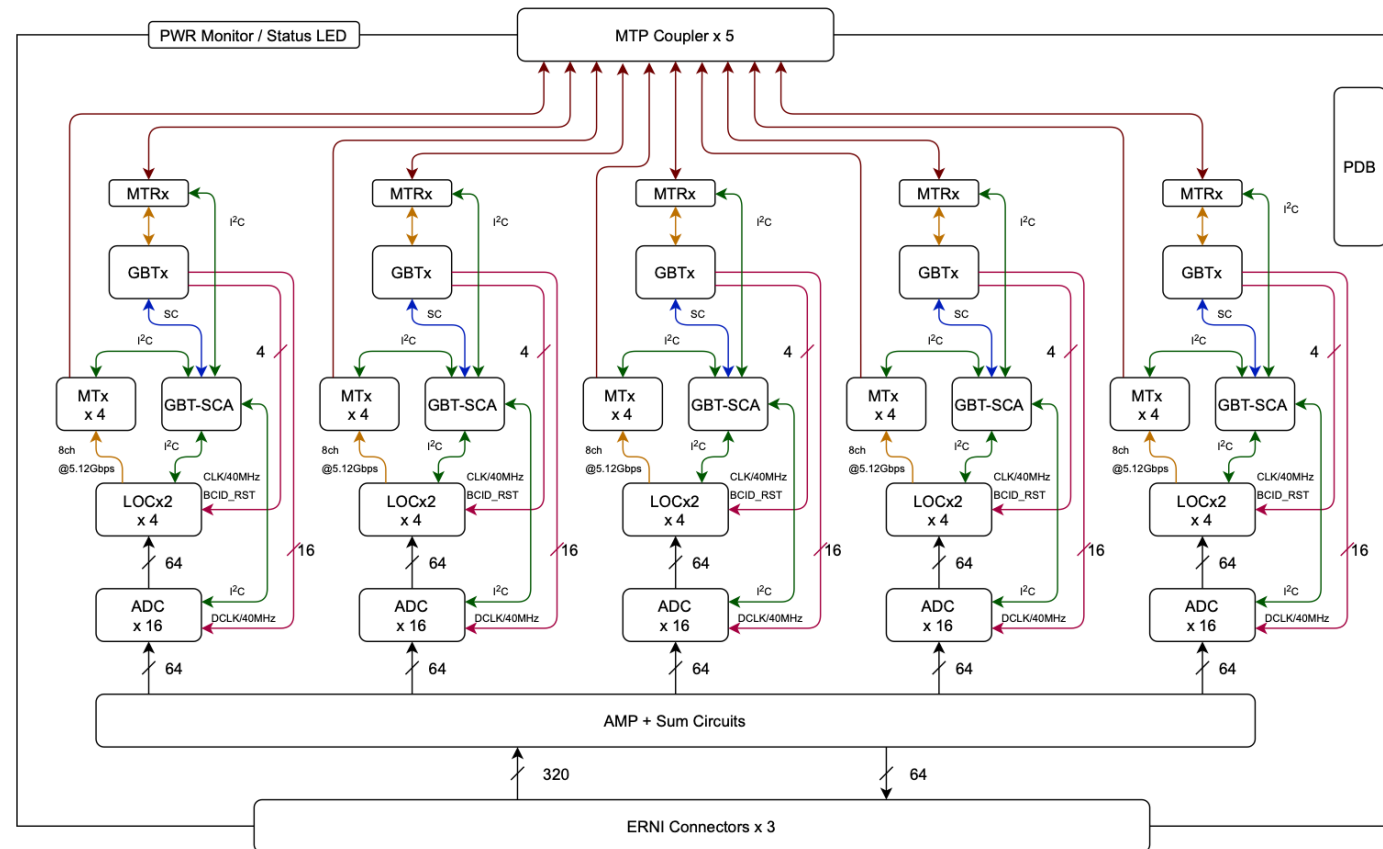


LTDB architecture in details

LTDB has a 5 fold structure

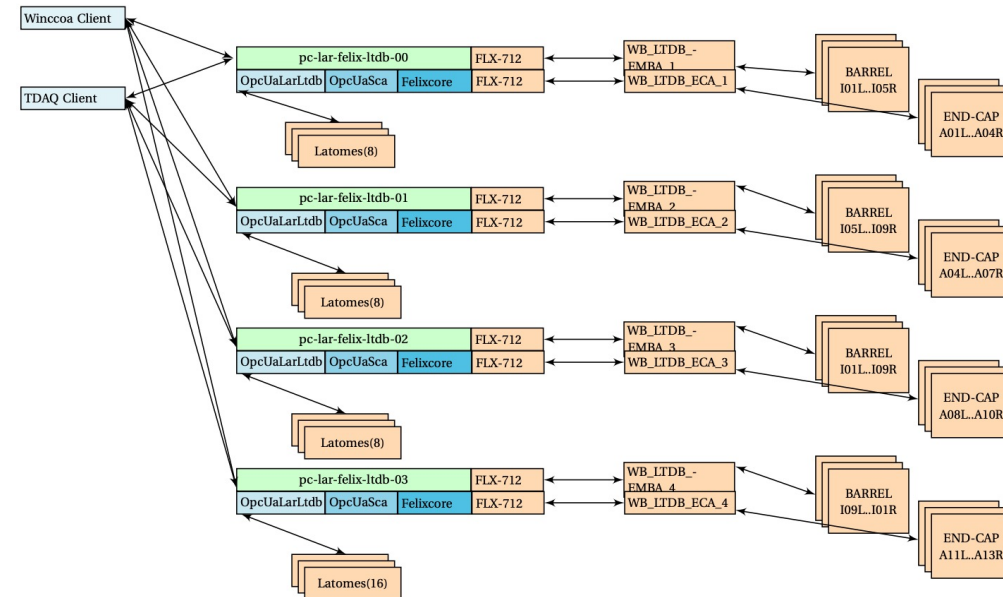
Each slice readout 64 super cells and contains :

- 16 12bADCs
- 4 serializer (locx2)
- 1 GBT-SCA controller
- 1 GBTx receiver
- 4 Data transmitter (MTx)
- 1 Control Transceiver (MTRx)



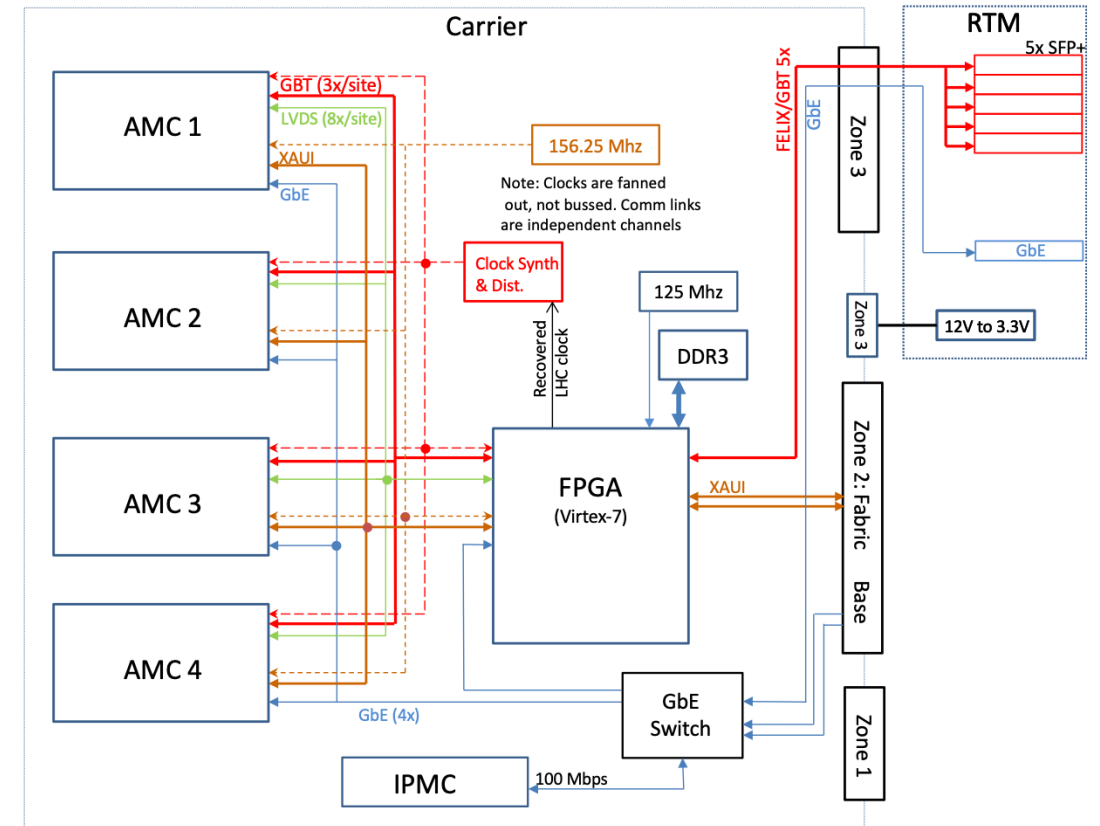
LTDB configuration

- LTDB are configured via dedicated FELIX servers
- Running OPCA server for communication with GBT-SCA
- Communicate via GBT to the LTDBs



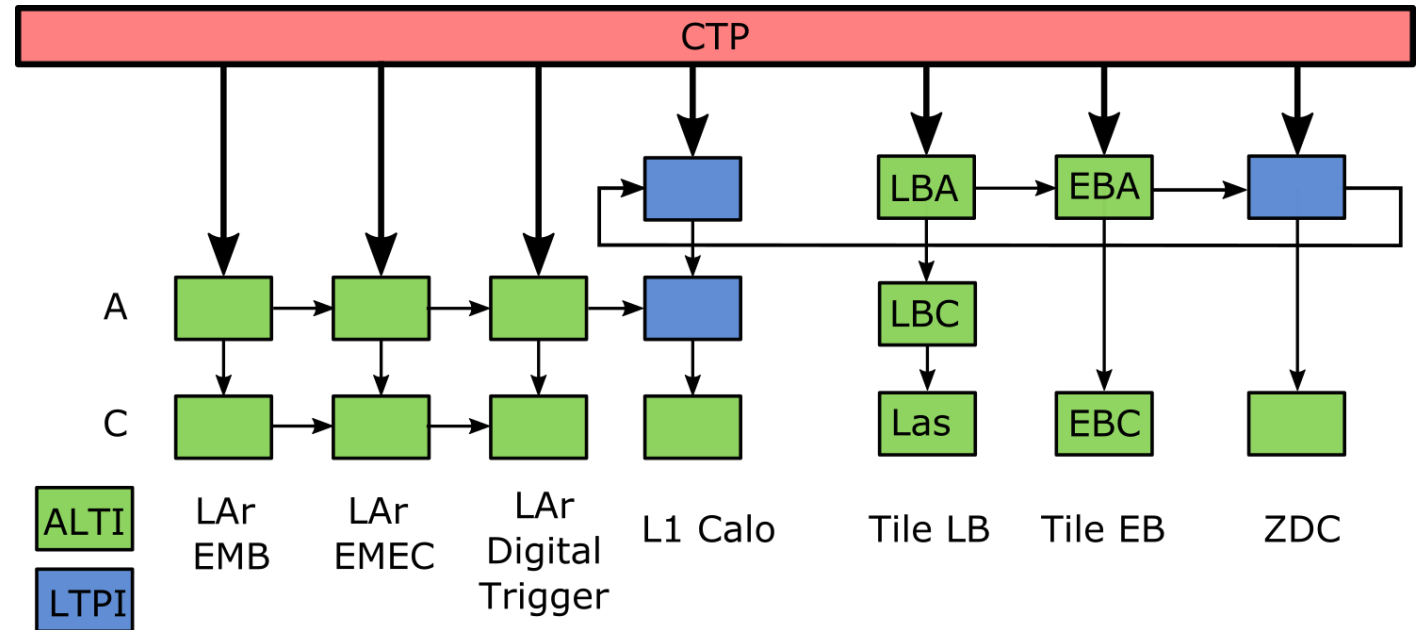
LAr Carrier

- Carrier fan out TTC signal to the LATOME
- Collect data for the readout path before sending to FELIX
- Contain network architecture for 1GbE control and monitoring of the blade
- Host IPMC managing hardware level sensor monitoring and power sequencing

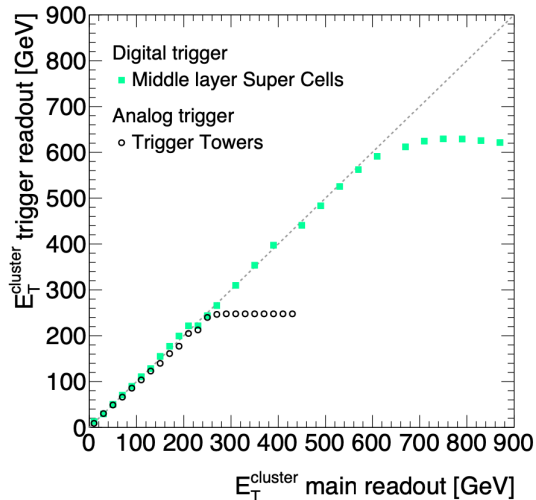
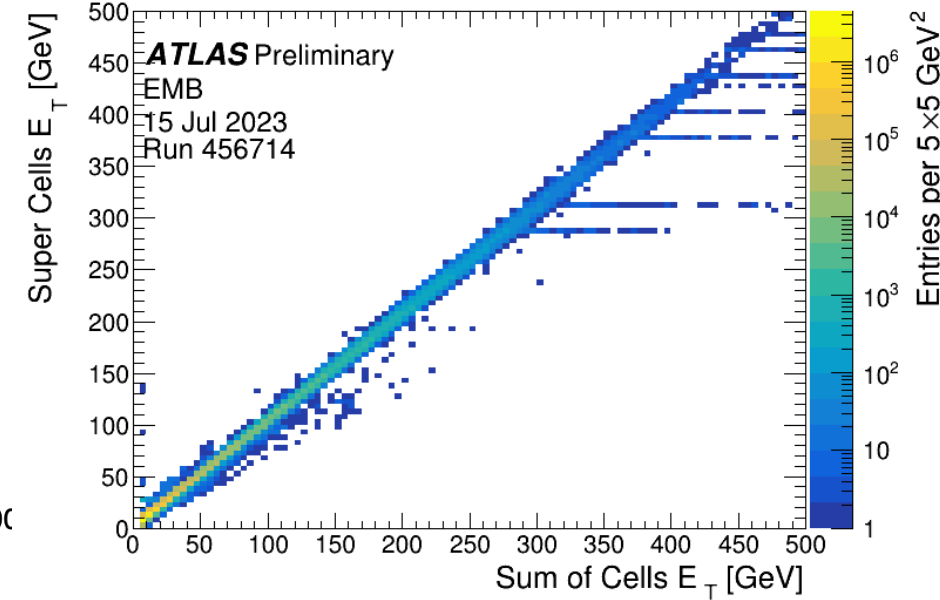
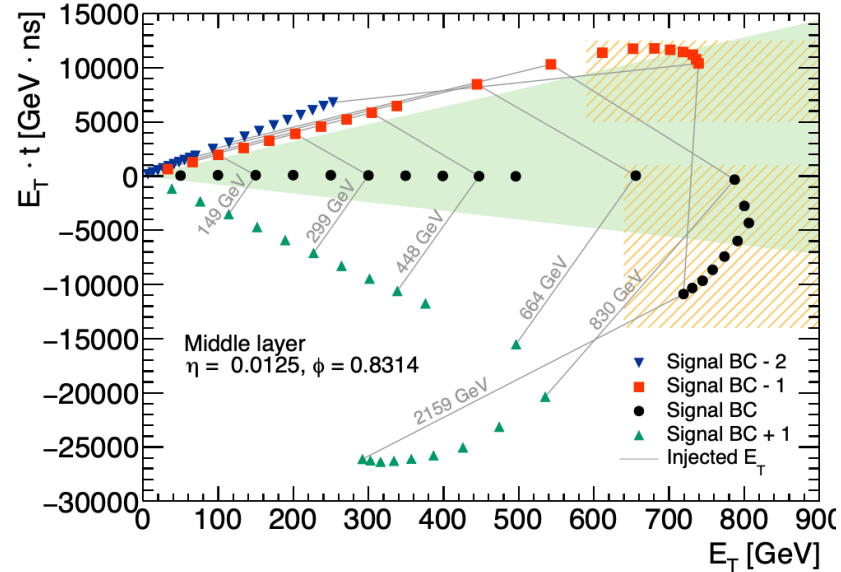
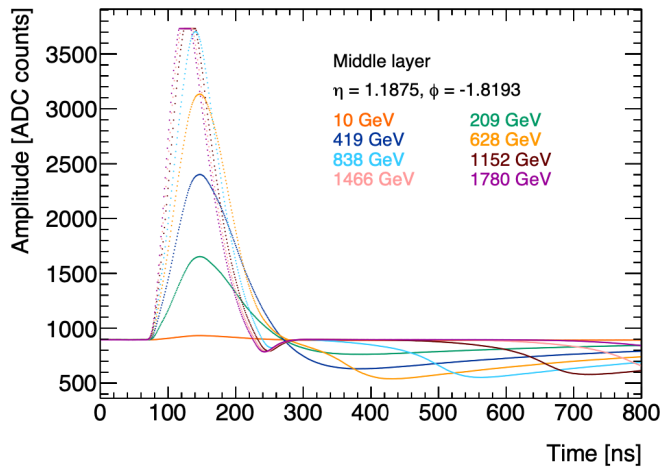


Time Trigger and Control Architecture (TTC)

- L1 Trigger accept is fan out to the detectors via TTC system
- Custom electronic board to either
 - operate all ATLAS subdetector together
 - Run the system independently (Calibration)
- New ALTI boards were installed that either retransmit signal from CTP, or can generate them in standalone running



Saturation



- Use only 1 gain on LTDB -> Saturation may occurs for high energy pulse
- More complicated to assign proper energy to the Correct BCID
- Saturation detection mechanism in place on the LATOME firmware

- Expected fluence

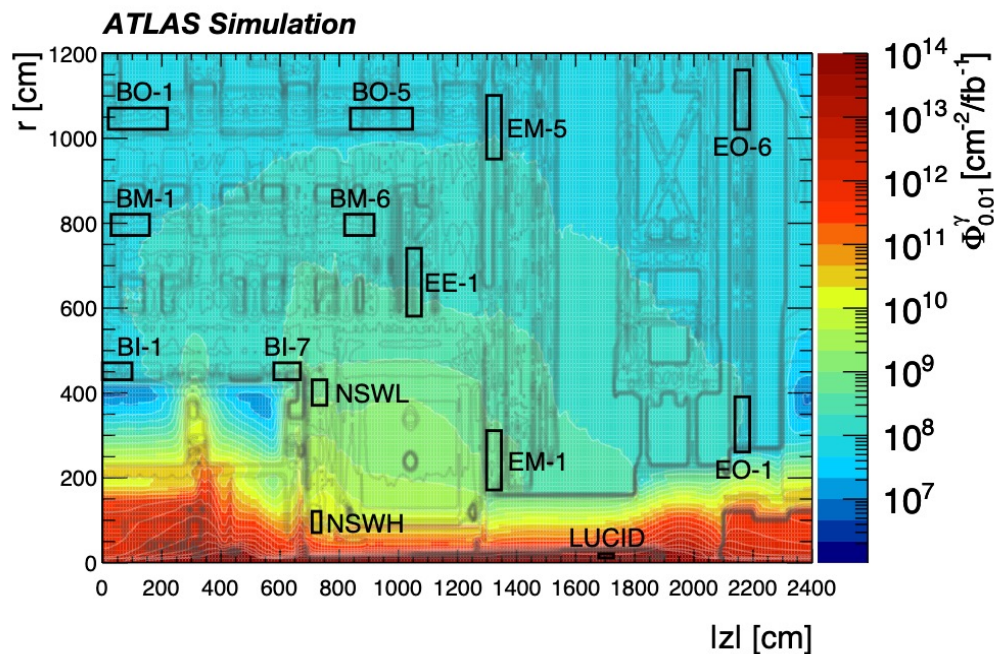
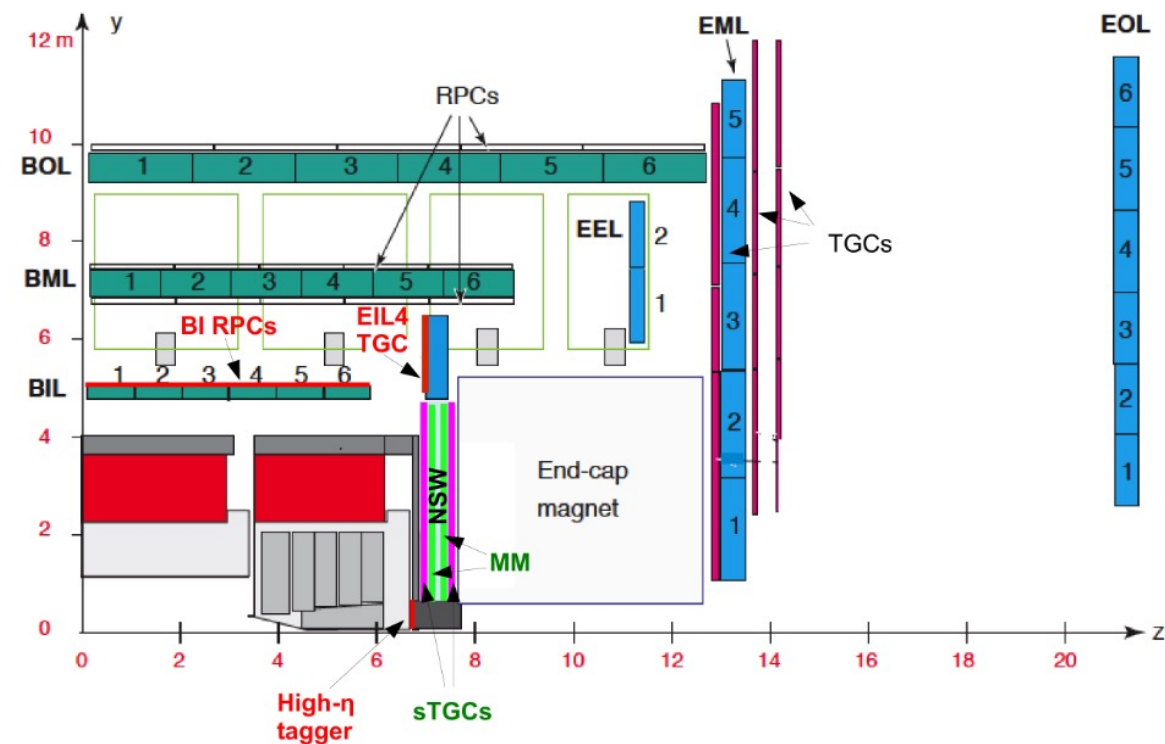
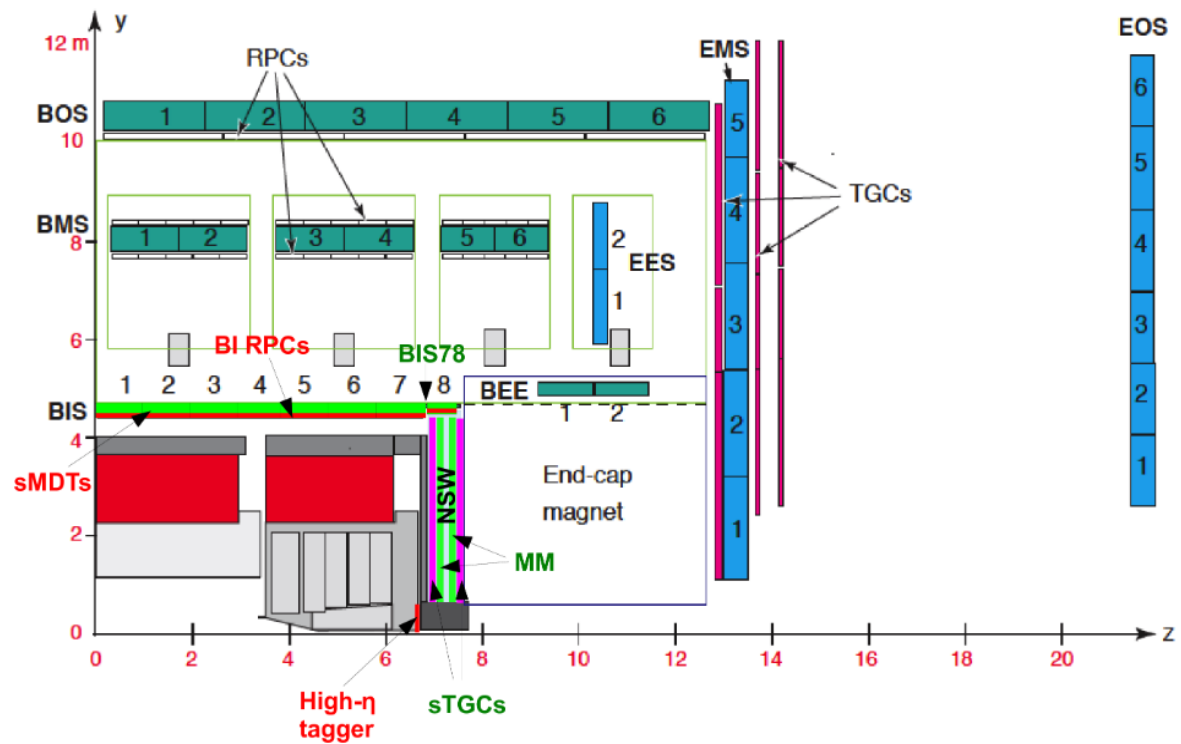


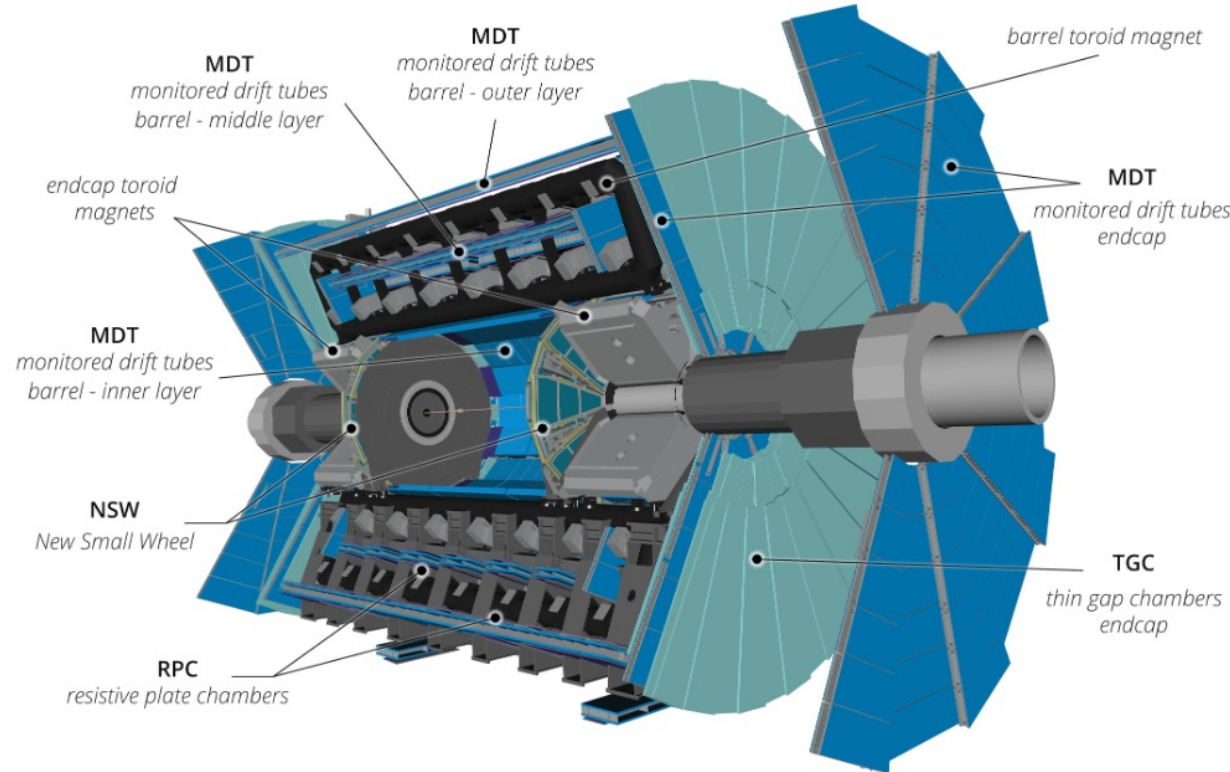
Table 2.3: TID and $\Phi_{\text{neq}}^{\text{Si}}$ obtained from GEANT4 simulations in the ATLAS cavern and muon spectrometer as averages over the volumes indicated in Figure 2.7. The rightmost column gives the fluence of photons with $E > 10$ keV ($\Phi_{0.01}^{\gamma}$). r and $|z|$ refer to the centre of the given region. The statistical uncertainty is in the last digit given, or smaller.

| Region | $ z $ [cm] | r [cm] | TID [Gy/fb ⁻¹] | $\Phi_{\text{neq}}^{\text{Si}}$ [cm ⁻² /fb ⁻¹] | Φ_{20}^{had} [cm ⁻² /fb ⁻¹] | $\Phi_{0.01}^{\gamma}$ [cm ⁻² /fb ⁻¹] |
|--------|------------|----------|----------------------------|---|--|--|
| LUCID | 1705 | 15 | 2.91×10^{-3} | 2.57×10^{12} | 4.83×10^{11} | 5.78×10^{13} |
| NSWH | 725 | 95 | 4.40×10^{-1} | 1.79×10^{10} | 1.86×10^9 | 3.09×10^{10} |
| EM-1 | 1325 | 240 | 7.6×10^{-3} | 3.03×10^8 | 6.45×10^7 | 6.17×10^8 |
| NSWL | 735 | 400 | 6.9×10^{-3} | 2.02×10^8 | 4.81×10^7 | 9.03×10^8 |
| BI-7 | 625 | 450 | 4.4×10^{-3} | 9.05×10^7 | 1.13×10^7 | 3.42×10^8 |
| EE-1 | 1055 | 660 | 2.43×10^{-3} | 1.10×10^8 | 2.30×10^7 | 2.05×10^8 |
| BM-6 | 870 | 795 | 1.63×10^{-3} | 4.63×10^7 | 1.13×10^7 | 1.56×10^8 |
| EO-1 | 2165 | 325 | 1.3×10^{-3} | 3.19×10^7 | 3.99×10^6 | 9.58×10^7 |
| EM-5 | 1325 | 1025 | 1.15×10^{-3} | 3.21×10^7 | 8.34×10^6 | 9.32×10^7 |
| BO-5 | 945 | 1045 | 1.07×10^{-3} | 2.36×10^7 | 6.94×10^6 | 7.98×10^7 |
| BM-1 | 95 | 795 | 8.1×10^{-4} | 1.52×10^7 | 2.43×10^6 | 8.87×10^7 |
| BI-1 | 50 | 450 | 7.3×10^{-4} | 2.70×10^7 | 7.0×10^5 | 8.55×10^7 |
| BO-1 | 120 | 1045 | 6.4×10^{-4} | 1.03×10^7 | 2.59×10^6 | 5.69×10^7 |
| EO-6 | 2165 | 1090 | 5.9×10^{-4} | 1.36×10^7 | 3.23×10^6 | 5.82×10^7 |

Figure 2.7: Contours of constant fluence for photons with $E > 10$ keV ($\Phi_{0.01}^{\gamma}$) in the ATLAS cavern and muon spectrometer regions. The black boxes indicate regions over which the main radiation quantities given in Table 2.3 are averaged. More detailed explanations of the detectors in these regions can be found in Section 5. The faint grey lines are density contours from the GEANT4 geometry model and only serve to give an indication of the detector geometry.



ATLAS Muon spectrometer for Run3

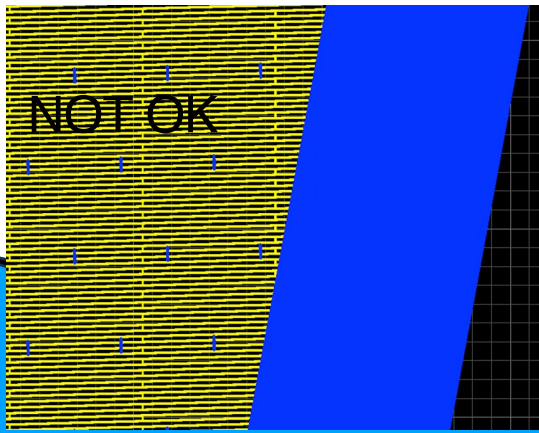
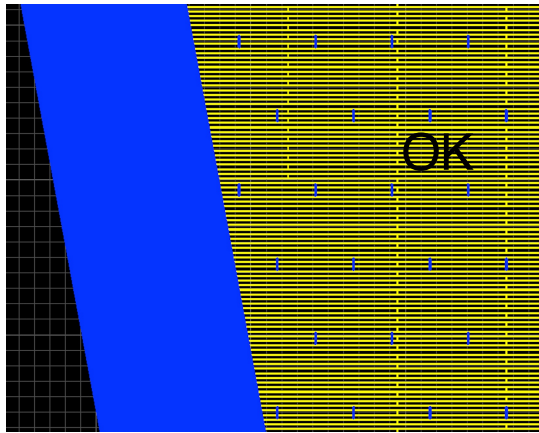


| MDT | |
|-----------------------|---|
| η coverage | $ \eta < 2.7$ (innermost layer: $ \eta < 1.3$) |
| Number of modules | 1098 |
| Number of channels | 355k |
| Function | Precision tracking |
| sTGC | |
| η coverage | $1.3 < \eta < 2.7$ (2.4 for trigger) |
| Number of quadruplets | 192 |
| Number of gas volumes | 768 |
| Number of channels | 357k |
| Function | Trigger, precision tracking, 2nd coordinate |
| Micromegas | |
| η coverage | $1.3 < \eta < 2.7$ (2.4 for trigger) |
| Number of quadruplets | 128 |
| Number of gas volumes | 512 |
| Number of channels | 2.05M |
| Function | Precision tracking, trigger, 2nd coordinate |
| RPC | |
| η coverage | $-1.05 < \eta < 1.3$ |
| Number of modules | 652 |
| Number of channels | 389k |
| Function | Trigger, 2nd coordinate |
| TGC | |
| η coverage | $1.05 < \eta < 2.7$ (2.4 for trigger) |
| Number of modules | 1530 |
| Number of gas volumes | 3492 |
| Number of channels | 312k |
| Function | Trigger, 2nd coordinate |

MM 'hot' topic

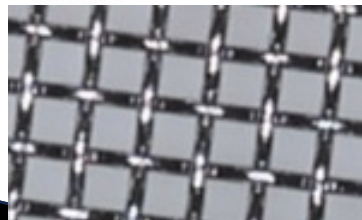
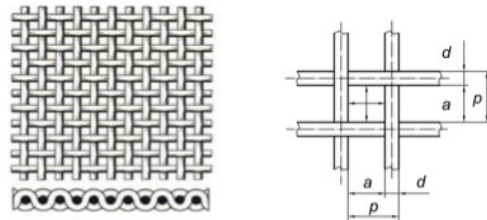
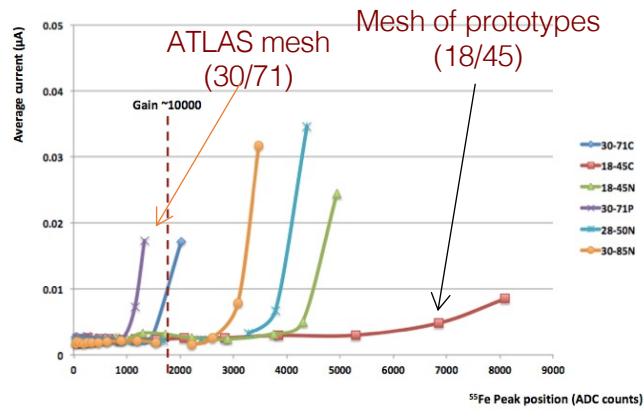
- Design issue

Resistive interconnections extending to the edge: reduce R_{min} → Passivation



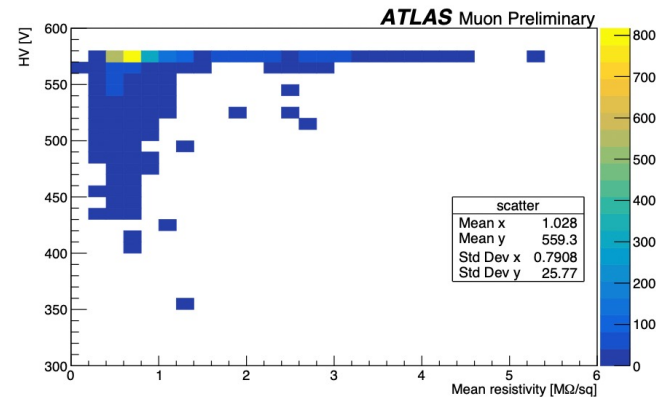
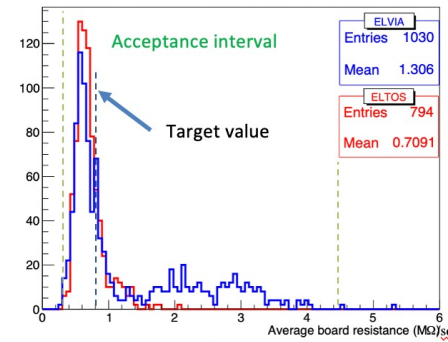
Mesh selection

The mesh used for ATLAS is the less performing for HV stability



Resistivity

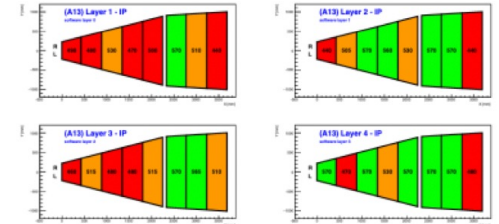
Target value too low (optimised on small bulk prototypes with 18/45 mesh). Min resistance not enough to quench discharged close to the edge → Process optimisation (when possible) + passivation



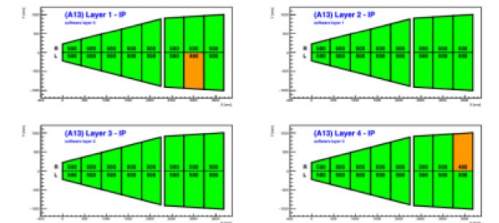
Gas mixture

Baseline gas mixture Ar:CO₂ 93:7 ok for prototypes not for final detectors. Big improvement by adding 2% of iC₄H₁₀ → Gas changed

Ar:CO₂ 93:7



Ar:CO₂iC₄H₁₀ 93:5:2

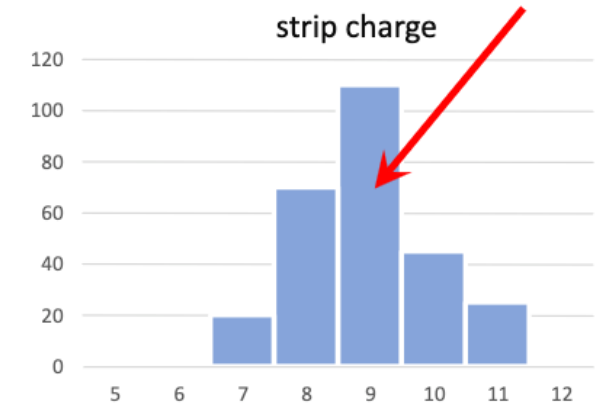


Signal processing

Signals to be electronically processed:

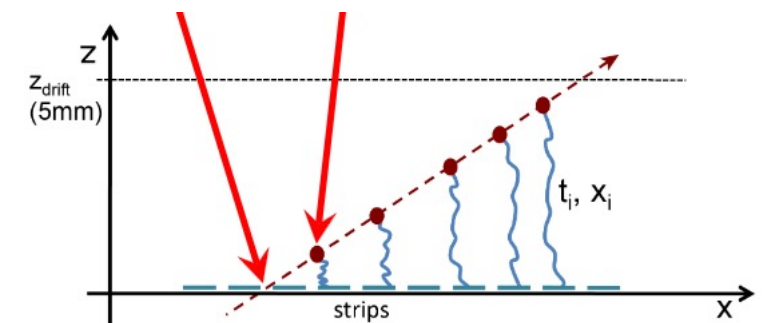
- sTGC strips: charge centroids
 - Strip width: 3.2 mm; avg 1 pC charge per strip, 50 ns peaking time,
 - Readout: per channel 10-bit ADC,
 - Trigger: per channel 6-bit ADC
- sTGC pads: charge and time
 - 3 pC charge per pad (tails to 50 pC!), 25 or 50 ns peaking time
 - Readout: per channel 10-bit ADC and 8-bit TDC for timing calibration
 - Trigger: per channel pulse at peak
- MM strips
 - Strip width: 0.4 mm; max 0.25 pC charge/strip, 100 or 200 ns peaking time,
 - 10-bit ADC and 8-bit TDC
 - Readout: both charge centroid mode and μ TPC mode
 - Trigger: The hit coord is the channel number of 1st strip hit in a bunch crossing. This channel is usually the closest to the intercept with the strip plane. (Requires a window of a few BC's)
- Phasel1 requirement to be met already with Phasel1 elx

sTGC & MM: coordinate from charge distribution centroid



MM: μ TPC mode for tracking

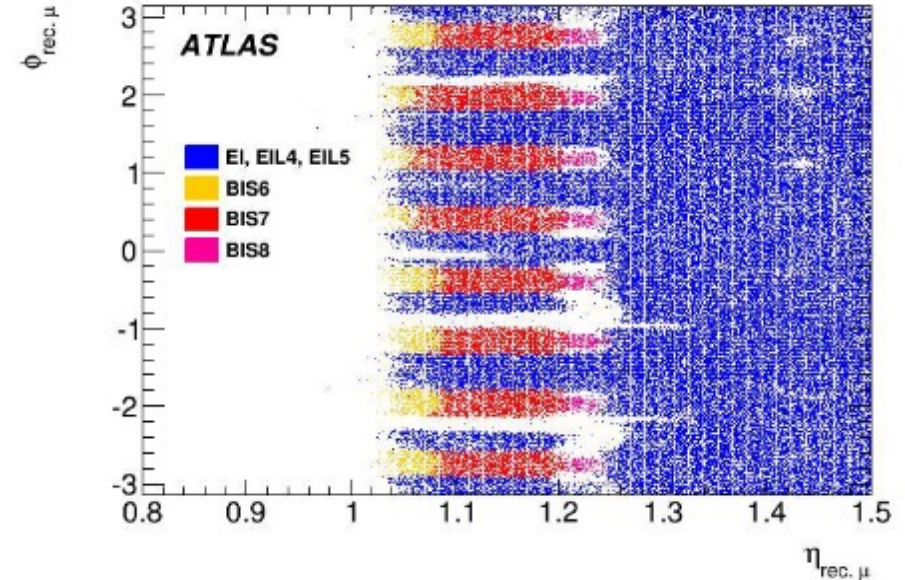
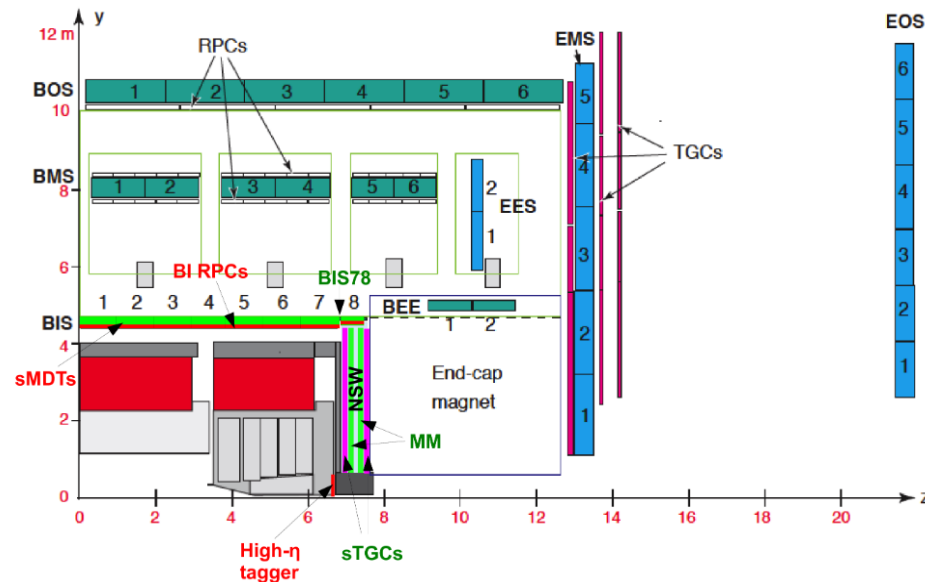
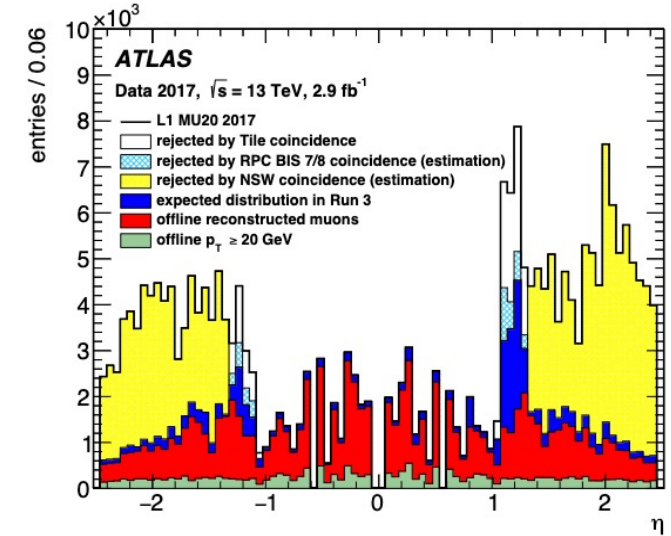
Channel of first arrival charge for trigger



<https://cds.cern.ch/record/2842618/files/ATL-MUON-SLIDE-2022-625.pdf>

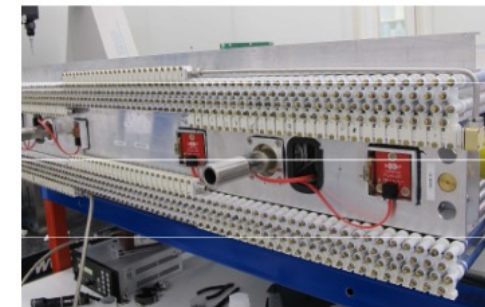
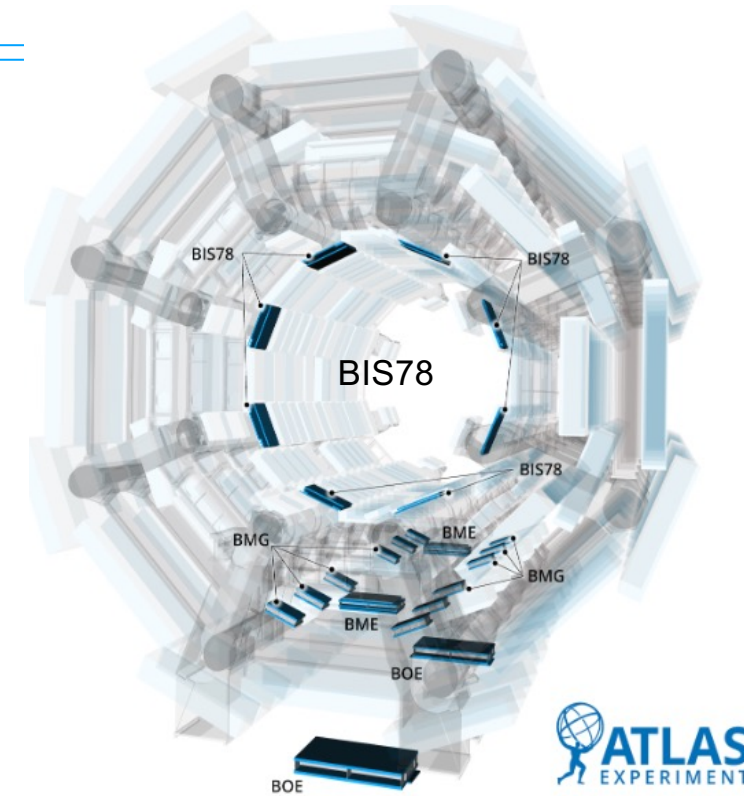
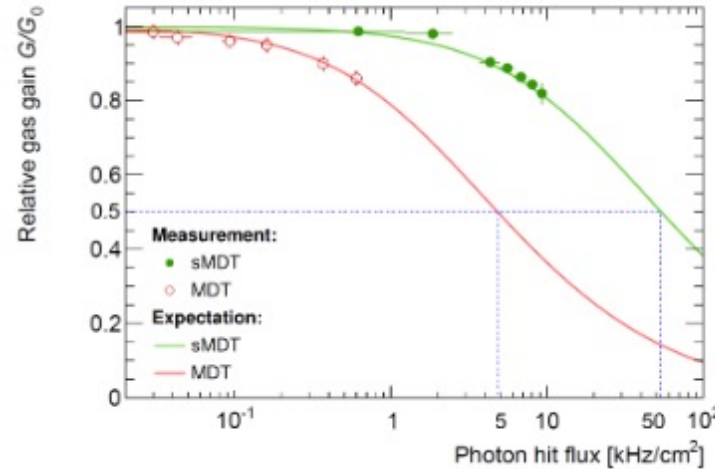
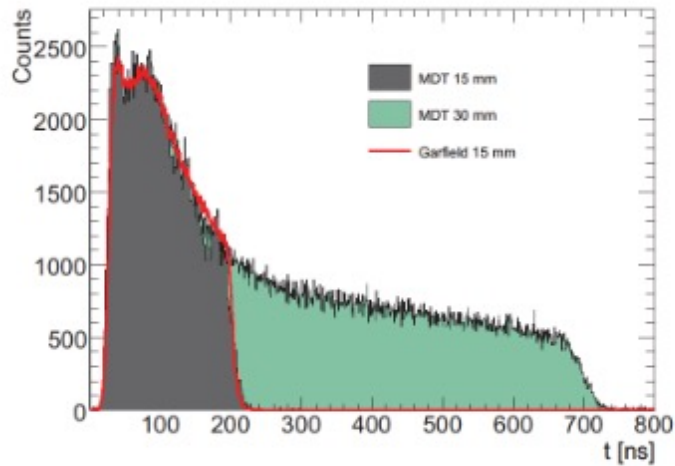
BIS78

- Motivation similar to NSW: to reduce fake trigger rates in the Barrel-End-cap transition region $1.1 < |\eta| < 1.27$ for Small sectors
- In Run1 and Run2 BIS7 and BIS8 Muon stations equipped with MDT tracking detectors only: no trigger capability. Limited space for BIS8 MDT: only single multilayer
- Run3: Replace BIS7&BIS8 MDT on side A with BIS78 sMDT+RPC assembly to improve tracking and provide trigger capability
- Pilot project in view of the massive upgrade based on sMDT+RPC for Phase II



BIS78: sMDT

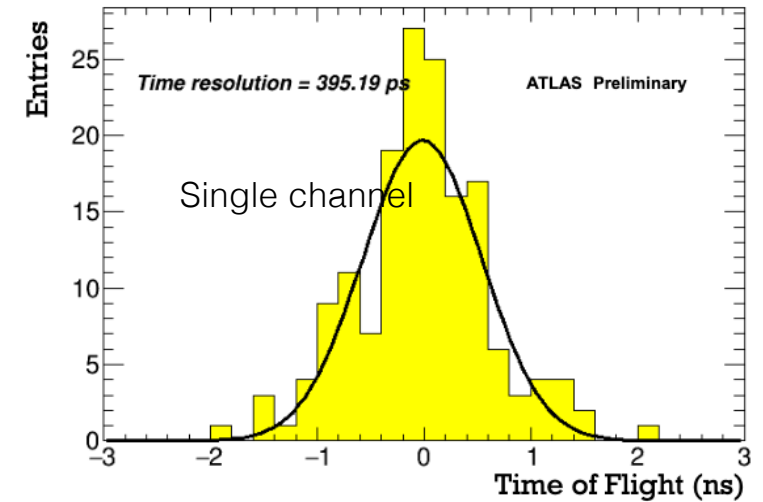
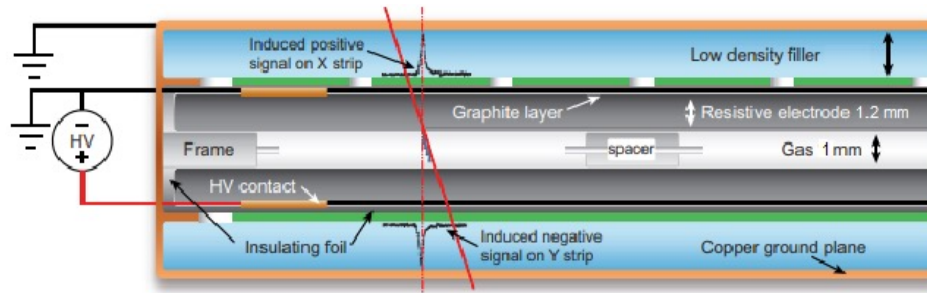
- Small Monitored Drift Tubes (sMDT) have smaller tube diameter compared to legacy ATLAS MDT (15 vs 30 mm)
 - Shorter drift time -> higher rate capability
 - More compact dimension: the limited space of BIS8 can host 2 sMDT multilayers and an RPC detector
 - Gas: Ar:CO₂ 70:30 at 3 bar



- sMDT BIS78 Side-A detector chambers have been installed in LS3 and integrated into the ATLAS data taking
- Elx and DAQ chain mostly based on legacy system except a new version of the FE TDC (HPTDC, 0.25 μm CMOS technology), that allowed a flowless integration into ATLAS

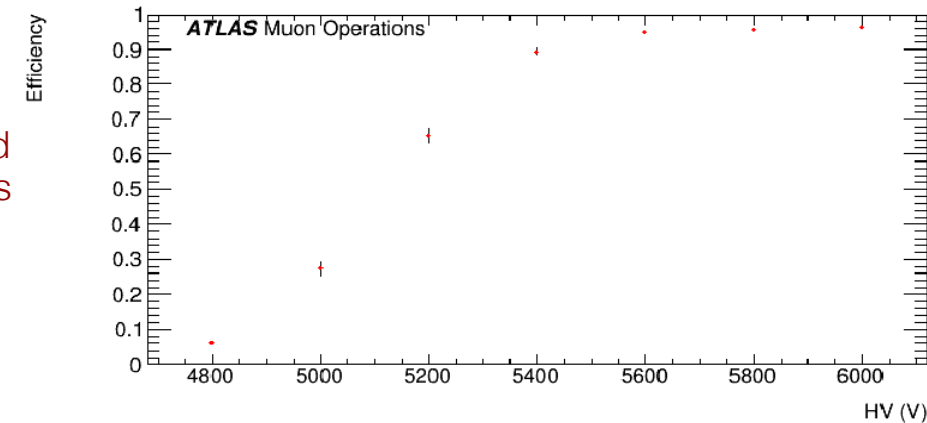
BIS78: RPC

- The BIS78 RPC detectors are of a new generation developed for Phasell upgrade
 - Thinner (1.2 mm) resistive plates; lower resistivity to increase the rate capability
 - Smaller gas gap (1 vs 2 mm) for an improved time response
 - Smaller signals: need of a high-amplification, low-noise, fast FE Elx
- Gap of 1 mm: max efficiency limited by fluctuations in generation of primary cluster: new RPC chambers have 3 independent gas gaps (vs 2 of legacy detectors)



- Good efficiency and excellent time performance confirmed with collision data

- Standard ATLAS RPC gas initially considered: $C_2H_2F_4:iC_4H_{10}:SF_6$ (94.7:5:0.3) To limit the large environmental impact of the RPC gas in ATLAS (legacy system suffering of large gas leak) the operating gas has been changed in 2023 to $C_2H_2F_4:CO_2:iC_4H_{10}:SF_6$ (64:30:5:1) for all the ATLAS RPC detectors Performance ~unchanged after modifying the HV working point
- BIS78-A RPC new FE elx and new DAQ chain oriented to Phasell (using FELIX, like LAr L1Calo and NSW) still under commissioning --> detector not yet fully integrated in ATLAS



STGC and MM construction and operating parameters

- sTGC

| Item/Parameter | Characteristics | Value |
|--|---|---------------------------|
| Readout strip pitch | | 3.2 mm |
| Readout strip width | | 2.7 mm |
| Total number of strips | | 282×10^3 |
| Typical pad azimuth | Inner / Outer Quadruplets | $5^\circ / 7.5^\circ$ |
| Typical pad radial height | | 80 mm |
| Range of "full" pad areas | | 61 to 519 cm ² |
| Total number of pads | | 46 656 |
| Anode-cathode gap | | 1.4 mm |
| Wire pitch | | 1.8 mm |
| Wire diameter | Gold-plated tungsten | 50 μ m |
| Total number of wires | Ganged in groups of 20, group boundaries offset by 5 wires between layers | 6 390 296 |
| Number of wire groups | Total / Read out | 31 776 / 28 704 |
| HV on wires | Positive polarity | 2.8 kV |
| Cathode resistivity | Inner / Outer Quadruplets | 150 / 200 k Ω /□ |
| Pre-preg thickness between readout and cathode | Inner / Outer Quadruplets | 150 / 200 μ m |
| Gas | n-pentane:CO ₂ | 45:55 |
| Bending Coordinate Resolution | single-plane η from strips | 100 to 200 μ m |
| Azimuthal Resolution | single-plane $r\phi$ (from wire groups) | 2.6 mm |
| NSW-TP Bending Coordinate Res. | L1 η from centroid fit to strips in band | < 1 mrad |
| Pad Trigger Azimuthal Res. | ϕ at L1 from pad towers (Inner/Outer) | 7 mrad / 10 mrad |
| | $r\phi$ (at L1 from pad towers) | 7 to 38 mm |

- MM

| Item/Parameter | Characteristics | Value |
|-------------------------------|---|---------------------------|
| Micro-mesh | Stainless steel; mesh separate from readout board | |
| Micro-mesh | Wire diameter | 30 μ m |
| Micro-mesh | Gap between wires | 71 μ m |
| | Micro-mesh is separate from readout board. | |
| Amplification gap | | 120 to 130 μ m |
| Drift/conversion gap | | 5 mm |
| Resistive strips | Interconnected | R=10 to 20 M Ω /cm |
| Readout strip width | | 0.3 mm |
| Readout strip pitch | Inner / Outer Modules | 0.425 / 0.45 mm |
| Stereo angle | one + and one - slope layer per quadruplet | $\pm 1.5^\circ$ |
| Total number of strips | | 2.1M |
| Baseline Gas | Ar:CO ₂ :iC ₄ H ₁₀ | 93:5:2 |
| Backup Gas | Ar:CO ₂ | 93:7 |
| HV on resistive strips | Baseline gas | 500 V |
| HV on resistive strips | Backup gas | 570 V |
| HV on drift panel | | -240 V |
| Amplification field | | ~ 40 kV/cm |
| Drift field | | 480 V/cm |
| Bending Coordinate Resolution | single-plane, η -strips centroid fit | 100 to 200 μ m |
| Second Coordinate Resolution | ϕ , single-plane, stereo strips centroid fit | 2.7 mm |
| NSW-TP Bending Coord. Res. | from NSW-TP fitter | 300 μ m |
| NSW-TP Second Coord. Res. | $r\phi$, from NSW-TP fitter | 11 to 12 mm |